

CENTRAL RESEARCH LIBRARY

ORNL-TM-4330

OAK RIDGE NATIONAL LABORATORY LIBRARIES



3 4456 0550196 2

cy.1

# CALCIUM SULFATE SCALING IN REVERSE OSMOSIS (HYPERFILTRATION) OF BRACKISH WATERS BY HOLLOW-FIBER AND SPIRAL-WOUND MODULES

Robert E. Minturn

OAK RIDGE NATIONAL LABORATORY  
CENTRAL RESEARCH LIBRARY  
DOCUMENT COLLECTION

**LIBRARY LOAN COPY**

DO NOT TRANSFER TO ANOTHER PERSON

If you wish someone else to see this  
document, send in name with document  
and the library will arrange a loan.

UCN-7969  
(3 3-67)



## OAK RIDGE NATIONAL LABORATORY

OPERATED BY UNION CARBIDE CORPORATION • FOR THE U.S. ATOMIC ENERGY COMMISSION

This report was prepared as an account of work sponsored by the United States Government. Neither the United States nor the United States Atomic Energy Commission, nor any of their employees, nor any of their contractors, subcontractors, or their employees, makes any warranty, express or implied, or assumes any legal liability or responsibility for the accuracy, completeness or usefulness of any information, apparatus, product or process disclosed, or represents that its use would not infringe privately owned rights.

CALCIUM SULFATE SCALING IN REVERSE OSMOSIS (HYPERFILTRATION) OF  
BRACKISH WATERS BY HOLLOW-FIBER AND SPIRAL-WOUND MODULES

by

Robert E. Minturn

Final Report to the Office of Saline Water, Membrane Division,  
U. S. Department of the Interior

F. E. Witmer, Program Monitor.

Work Order No. 30, Agreement No. 14-30-2535

July 1973

Water Research Program  
Oak Ridge National Laboratory  
Oak Ridge, Tennessee

J. S. Johnson, Jr., Director

OAK RIDGE NATIONAL LABORATORY  
Oak Ridge, Tennessee 37830  
operated by  
UNION CARBIDE CORPORATION  
for the  
U.S. ATOMIC ENERGY COMMISSION

OAK RIDGE NATIONAL LABORATORY LIBRARIES



3 4456 0550196 2



CONTENTS

	<u>Page</u>
FOREWORD . . . . .	viii
I. INTRODUCTION. . . . .	1
II. REVERSE OSMOSIS TESTS WITH BRACKISH WATERS. . . . .	1
A. Experimental. . . . .	1
B. Visual observation of $\text{CaSO}_4 \cdot 2\text{H}_2\text{O}$ precipitates . . . . .	5
1. Effect of velocity and feed concentration . . . . .	7
2. Effect of polymetaphosphate . . . . .	9
3. Effect of pH. . . . .	11
4. Possible degradation of polymetaphosphate . . . . .	12
C. Tests with commercial modules . . . . .	17
1. Tests with simulated Webster Water. . . . .	17
a. Incremental increases in salt concentration . . . . .	17
b. Attempts to achieve steady state. . . . .	21
c. Long-term run at high, single-pass recovery rates . . . . .	21
d. Periodic replacement of depleted salts. . . . .	24
e. Depletion as a function of recovery rate. . . . .	27
f. Simulated second-section feed concentrates. . . . .	29
g. Analyses of solid deposits. . . . .	35
h. Tests with GESCO module only. . . . .	39
i. Comparison of runs with fresh and with. reconstituted feeds . . . . .	41
j. Pretreatment to increase recovery . . . . .	41
(1) Cross-flow pretreatments . . . . .	42
(2) Reverse osmosis of pretreated feed . . . . .	43
2. Tests with simulated Wellton-Mohawk canal water . . . . .	47
a. First section simulation. . . . .	47
b. Second section simulation . . . . .	47
3. Tests with simulated Foss Reservoir water . . . . .	50
4. Discussion and recommendations . . . . .	55
III. OSMOTIC PRESSURES OF SALINE WATERS. . . . .	62
IV. CONCENTRATION POLARIZATION IN HYPERFILTRATION OF $\text{NaCl}$ SOLUTIONS CONTAINING TRACE AMOUNTS OF $\text{Ca(II)}$ and $\text{SO}_4^{2-}$ , by Lawrence Dresner . . . . .	95
ABSTRACT. . . . .	95
A. Introduction . . . . .	95
B. Basic equations . . . . .	97

CONTENTS (cont'd)

	<u>Page</u>
(IV.) C. Small concentration polarization--laminar flow . . . . .	99
D. Fully developed concentration profile--laminar flow. . . . .	102
E. Turbulent flow . . . . .	108
F. Constant activity coefficients . . . . .	109
G. Activity coefficients not constant . . . . .	112
H. Numerical results for trace $\text{CaSO}_4$ in NaCl Solutions in laminar flow . . . . .	113
I. Effect of common ion and of non-ideality of solutions. . . . .	116
REFERENCES. . . . .	121
APPENDIX. . . . .	123

LIST OF FIGURES

	<u>Page</u>
1. Schematic of Experimental Apparatus. . . . .	2
2. Fluid Flow Patterns as a Function of Flow Velocity . . . . .	6
3. Precipitation of CaSO <sub>4</sub> on Cellulose Acetate Membranes. . . . .	8
4. Effect of Decrease of Circulation Velocity on Flux and Rejection in Hyperfiltration of CaSO <sub>4</sub> -NaCl Solutions with Cellulose Acetate Membranes. . . . .	13
5. Effect of Decrease of Circulation Velocity on Flux and Rejection in Hyperfiltration of CaSO <sub>4</sub> -NaCl Solutions with Cellulose Acetate Membranes. . . . .	14
6. Effect of Decrease of Circulation Velocity on Flux and Rejection in Hyperfiltration of CaSO <sub>4</sub> -NaCl Solutions with Cellulose Acetate Membranes. . . . .	15
7. Flux and Rejection as a Function of Calcium Concentration; Du Pont and GESCO Modules . . . . .	19
8. Limits on Recovery in Simulated Webster Water from Solubility Products of CaSO <sub>4</sub> . . . . .	20
9. Flux and Rejection as a Function of Calcium Concentration in Webster Water. . . . .	22
10. Flux-Time in R.O. of Webster Water . . . . .	23
11. Effect of Replenishing Calcium in R.O. of Webster Water. . . . .	26
12. Effect of Time and Water Recovery on Product of Calcium and Sulfate Concentration, Webster Water with and without Calgon . . .	28
13. Depletion of Ca(II) Concentration with Time from Webster Water . .	31
14. Depletion of Ca(II) Concentration with Time from Webster Water . .	32
15. Calcium Depletion from Webster Water with Time; Comparison of GESCO and Du Pont Modules . . . . .	34
16. Deposits on End Plates and on Fiber Bundles in Du Pont Module. . .	38
17. Normalized Ca(II) Concentration Versus Time. GESCO Module with Webster Water Concentrates . . . . .	40
18. Effect of Pretreatment on Maximum Water Recovery with Webster Water. . . . .	44
19. Decrease in Ion Concentrations in Feed with Time at Two Water Recovery Levels. . . . .	45

LIST OF FIGURES (cont'd.)

	<u>Page</u>
20. Limits on Recovery with Wellton-Mohawk Water from Calcium Sulfate Solubility. . . . .	48
21. $[Ca(II)] \times [SO_4^{=}]$ Versus Time. Wellton-Mohawk Feed Treated by Du Pont and GESCO Modules in Parallel. . . . .	49
22. Calcium and Sulfate Concentration in Feed Versus Time. Wellton-Mohawk Feed Treated by Du Pont and GESCO Modules in Parallel. . . . .	49
23. Calcium and Sulfate Concentration in Feed as a Function of Time, Wellton-Mohawk Water. . . . .	51
24. Calcium and Sulfate Product in Feed Versus Time, Wellton-Mohawk Water. . . . .	51
25. Time Dependence of Ion Concentrations and Ion Concentration Product, Foss Water . . . . .	52
26. Ion Concentrations and Ion Concentration Product Versus Time, Foss Water. . . . .	54
27. Molarity-Molality Relationships for Single-Salt Solutions . . . . .	65
28. Equivalent Molality Versus ppm. . . . .	67
29. Hyperfiltration Channel between Plane Parallel Membranes. . . . .	103
30. Concentration Polarization of Trace $CaSO_4$ in NaCl Solutions--Laminar Flow. . . . .	114

LIST OF TABLES

	<u>Page</u>
I. Compositions of Simulated Brackish Waters. . . . .	4
II. Effect of Calgon Concentrations on the Time for $\text{CaSO}_4 \cdot 2\text{H}_2\text{O}$ Crystals to Form on Cellulose Acetate Membranes under Laminar Flow Conditions. . . . .	10
III. Effect of pH and Calgon on Precipitation of Calcium Sulfate on Cellulose Acetate Membranes. . . . .	16
IV. Properties of Reject Stream at Ends of Runs. . . . .	29
V. Silica and Bicarbonate Concentrations in Nominal Webster Water and in Initial Feeds for Three Runs with Simulated Webster Water . .	35
VI. Ratio of Solubility Product Quotients in Reject Streams to $[\text{Ca}(\text{II})][\text{SO}_4^-]$ Concentration Product . . . . .	36
VII. Ca(II) Depletion, Normalized, at 180 Minutes into a Number of Runs for Fresh and Reconstituted 2X Webster Water. . . . .	42
VIII. Calcium Sulfate Ion Products at Ends of Three Runs . . . . .	53
IX. Reproducibility of Sulfate Analyses. . . . .	55
X. $\text{RT}/(55.51 \bar{V}_1)$ for a Number of Temperatures . . . . .	63
XI. Osmotic Coefficients, $\phi$ , as a Function of Total Equivalent Concentrations and Equivalent Fractions of Several Common Ions . . .	72-94
XII. Concentration Polarization in Laminar Flow with a Fully Developed Concentration Profile . . . . .	118
XIII. Concentration Polarization in Laminar Flow in Early Entrance Region. . . . .	118

## FOREWORD

This is Part II of the final report satisfying the requirements of Work Order No. 30 under Agreement No. 14-30-2533 between the Department of the Interior and the Atomic Energy Commission entitled "The Solubility of Calcium Sulfate Dihydrate in Brackish Water Concentrates." The first part of this report,<sup>1</sup> entitled "Solubilities of Calcium Sulfate Dihydrate in Brackish Waters and Their Concentrates," by LeRoy B. Yeatts, Paul M. Lantz, and William L. Marshall, has been submitted to the Office of Saline Water Membrane Division and also is to be issued as ORNL 4914.

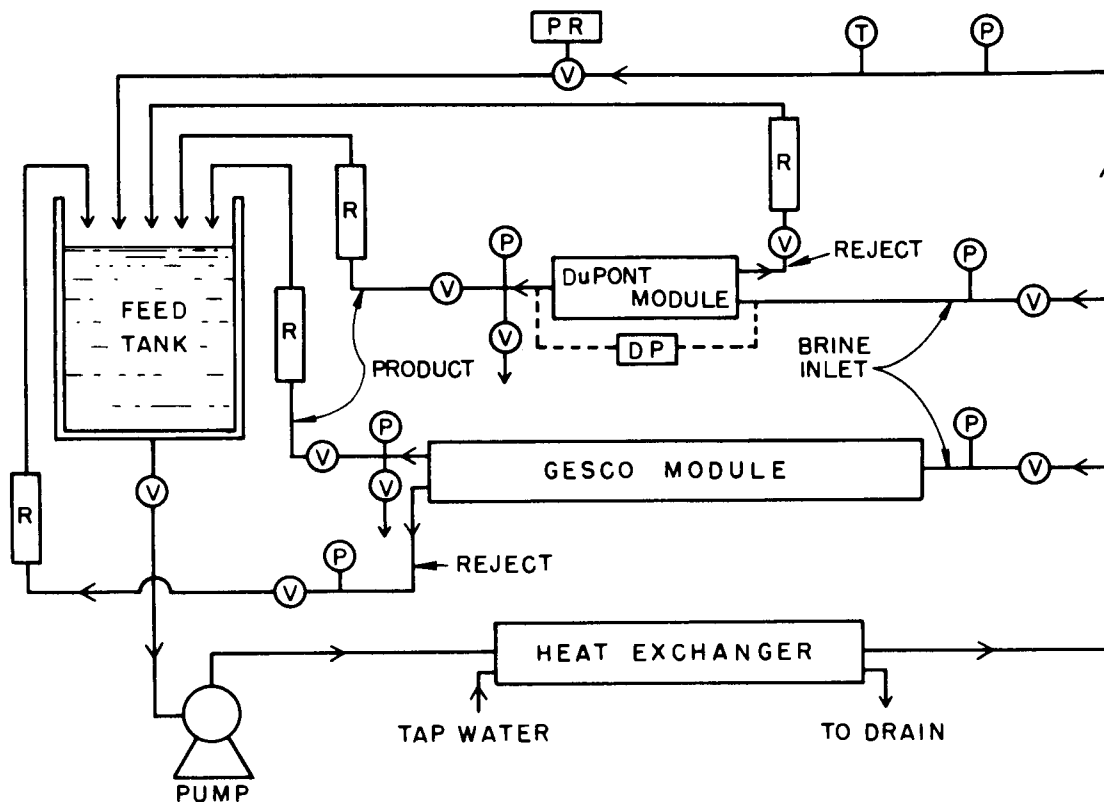
## I. INTRODUCTION

The main objective of this part of Work Order No. 30 was to operate hollow-fiber and spiral-wound modules in reverse osmosis of synthetic waters specified by OSW in order to establish a correlation between the practical solubility limits as a function of operating conditions and the equilibrium solubility limits that were determined in the concurrent work by Yeatts, et. al.<sup>1</sup> A subsidiary objective was to organize existing literature data on the free energies of solutions of electrolytes common in natural waters in a manner allowing convenient estimation of osmotic pressures. The results of the experimental program directed to reverse osmosis tests of commercial modules are given in Section II of this report, thermodynamic data and procedures for its use are presented in Section III, and a theoretical discussion of concentration polarization in multicomponent systems is presented in Section IV.

## II. REVERSE OSMOSIS TESTS WITH BRACKISH WATERS

### A. Experimental:

Figure 1 is a schematic diagram of the experimental reverse osmosis (RO) loop used for most of the experiments in this study. Except for the two RO units and the pump, the apparatus is a modification of equipment on hand at the start of this program. The equipment is designed so that the RO units could be operated independently or in parallel; usually they were operated in parallel. Brine pressure was sensed at the common inlet manifold, and the pressure was regulated to 400 psig by the pneumatic valve in the pressure regulator. Flow rates through, and pressure drops across, the RO units were adjusted with the proper valves; the pressure drop across the DuPont module was monitored by a DP cell. Temperature was sensed in the high pressure manifold and regulated automatically by changes in the flow of cooling water to the heat exchanger. Originally, the feed tank was a 200-liter polyethylene tank; this was later replaced by a 200-gallon stainless steel tank. Reject and product flow rates were measured by calibrated rotameters. Product streams could be directed either to the



SCHEMATIC DIAGRAM OF EXPERIMENTAL APPARATUS FOR RO TREATMENT OF SIMULATED BRACKISH WATERS WITH COMMERCIAL MODULES. DP: Differential Pressure Gauge ; P: Pressure Gauge ; PR: Pressure Regulator ; R: Rotameter ; T: Temperature Gauge ; V: Valve.

Fig. 1

drain or back to the feed tank to maintain constant feed volume. All product and reject streams could be sampled.

The DuPont RO unit, hereinafter referred to as the DuPont module, was a B-9 "Permasep" Permeator, Serial 4619, containing 1958 ft<sup>2</sup> of aromatic polyamide polymer asymmetric hollow fibers, and was rated at 2000 gallons per day (gpd) at 400 psig by the manufacturers. The GESCO unit, hereinafter referred to as the GESCO module, was an assembly of three Model 4100 ROGA spiral wound modified cellulose acetate membrane modules. Total membrane area in this unit was about 195 ft<sup>2</sup>, and the unit was rated at 2100 gpd, also at 400 psig. The pump used was a Goulds Model 3933, size MB13500, with 316 stainless steel wetted parts. This is a 65-stage centrifugal pump with a capacity of 13 gallons per minute (gpm) at 500 psig.

Several naturally occurring brackish waters were simulated. The compositions of natural waters vary considerably from time to time at a given site, and the compositions we used, given in Table I, are meant to be representative. Chemicals were laboratory grade or better and were used without further purification. On occasion a simulated water was made up to contain a multiple of the concentration of dissolved salts listed in Table I. Such concentrated waters were meant to represent second or third section reject streams, and are hereinafter referred to as 2X or 2.5X Webster Water, etc.

During the experimental runs, divalent cation concentrations were determined by titration with EDTA, using Calcon as an indicator for Ca(II) and Eriochrome Black T as an indicator for Mg(II). Total cations were exchanged on Dowex 50X12 in the hydrogen form, and the acid eluted was titrated with standard base, using a Sargent Model D recording titrator. Chloride ion concentrations were determined with a Buchler-Cotlove Chloridometer, and pH's were measured with a Beckman expanded scale pH meter. Other ions were analyzed with the help of a Hach DR-EL "Engineer's Laboratory;" sulfate by using the turbidimetric method, silicate by using the heteropoly blue method, and Al(III) by using the Erochrome Cyanine R method.

TABLE I.  
COMPOSITIONS OF SIMULATED BRACKISH WATERS USED IN THIS STUDY.

Ion	WEBSTER WATER		WELLTON-MOHAWK		FOSS RESERVOIR	
	<u>M</u>	ppm	<u>M</u>	ppm	<u>M</u>	ppm
Na	0.0088	200	0.0413	945	0.0032	74
K	0.0004	16	0.0004	16	--	--
Ca	0.0035	140	0.0061	244	0.0051	204
Mg	0.0043	105	0.0036	88	0.0051	124
Fe	$5 \times 10^{-6}$	0.3	--	--	--	--
B	--	--	0.00016	1.7	--	--
HCO <sub>3</sub>	0.0049	300	0.0058	355	0.0026	159
Cl	0.0003	10	0.0343	1210	0.0014	50
SO <sub>4</sub>	0.0088	845	0.0102	982	0.0098	980
NO <sub>3</sub>	--	--	0.00013	8	--	--
F	--	--	0.00011	2	--	--
SiO <sub>2</sub>	0.0005	30	0.00047	28	--	--
PO <sub>4</sub>	--	--	0.00003	3	--	--

In reporting experiments carried out at negligible water recovery levels, we have customarily utilized an "observed" rejection,

$$R_{\text{obs}} \equiv \frac{c_f - c_w}{c_f},$$

where  $f$  stands for the feed and  $w$  for the effluent or product.  $R_{\text{obs}}$  differs from the actual "intrinsic" rejection of the membrane,

$$R \equiv \frac{c_\alpha - c_w}{c_\alpha},$$

where  $\alpha$  refers to concentration at the membrane-brine interface, in that  $c_\alpha$  is greater than the feed concentration because of concentration polarization.

In the experiments carried out with modules here, water recoveries are substantial, and the proper concentration to insert for  $c_f$  in the definition for  $R_{\text{obs}}$  would be that in the turbulent core (or the "cup-mixing" concentration, if flow is laminar), which varies through the system.

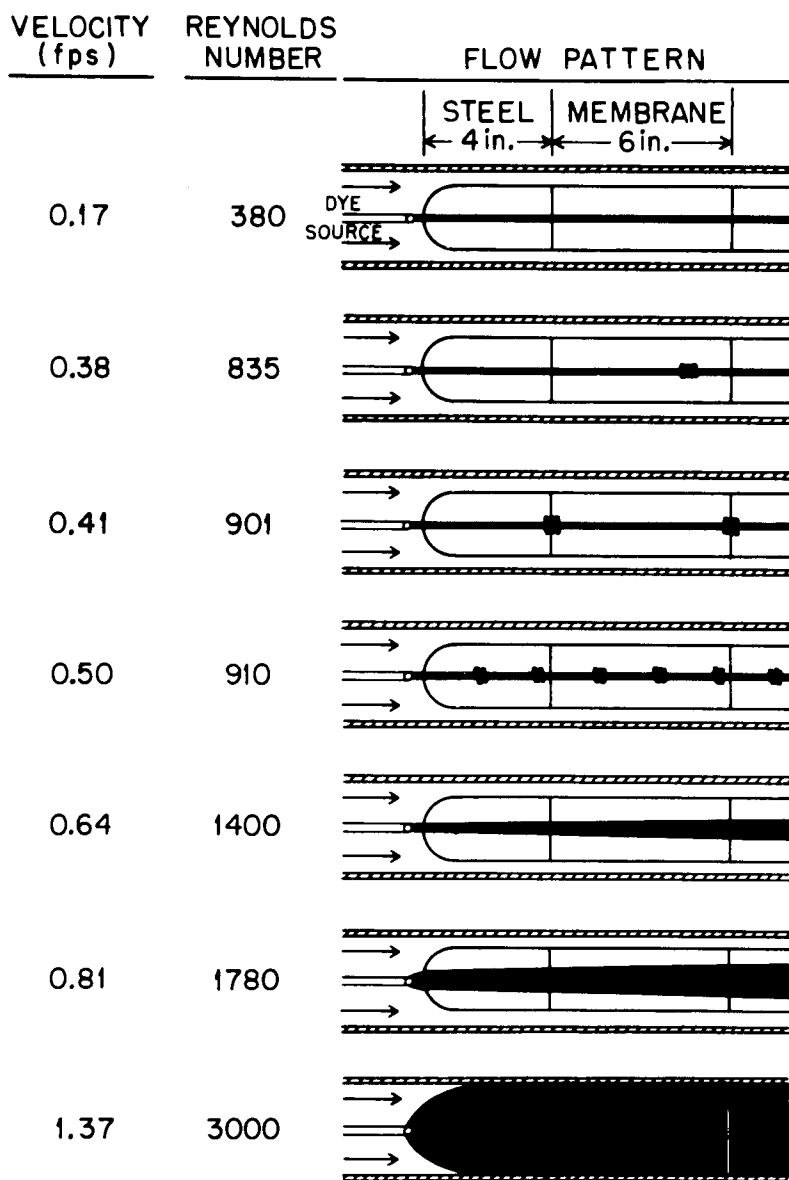
However, we shall, in this report, utilize  $R_{\text{obs}}$  to designate the rather complex average rejection implied by the definition previously stated, obtained by comparing the concentration in the feed tank with that in the effluent.

Some preliminary experiments on the precipitation of  $\text{CaSO}_4 \cdot 2\text{H}_2\text{O}$  at the membrane-feed interface under supersaturated conditions caused by concentration polarization were carried out in one of our standard hyperfiltration loops. This loop has been described previously.<sup>2</sup>

B. Visual observation of  $\text{CaSO}_4 \cdot 2\text{H}_2\text{O}$  precipitates:

We carried out a series of experiments in which we induced precipitation of calcium sulfate dihydrate by causing supersaturation by concentration polarization under well-defined conditions. In these experiments, we wrapped commercially available cast film membranes around two 5/8 in. porous stainless steel fingers, and inserted the fingers into transparent jackets<sup>3</sup> in one of our standard hyperfiltration test loops. Circulation velocities of the  $\text{CaSO}_4$  brine past the two membranes were independently variable from zero to greater than 40 feet per second (fps), and we could thus compare performances under conditions of laminar, transition, and turbulent flow. We established the flow regimes in our test sections by observing, in a preliminary experiment, the flow patterns of a dye introduced from a point source just upstream of the membrane surface. The results of this experiment are sketched in Fig. 2. It can be seen that the flow remains reasonably laminar up to velocities including 0.5 fps ( $N_{\text{Re}} = 910$ ), and is completely turbulent at 1.37 fps ( $N_{\text{Re}} = 3000$ ). The small turbulences at 0.38, 0.41, and 0.5 fps were stationary in the tube under a given set of conditions, giving the appearance of standing waves. Flows of 0.64 fps and 0.81 fps appear to be in the transition region between laminar and turbulent flow.

The transparent jackets used in these experiments allowed us to observe visually changes at the membrane surface, e.g., formation of crystals, and thus to correlate these changes with changes in the measured properties, such as rejection and flux. We could also follow removal of fouling layers by raising circulation velocity.



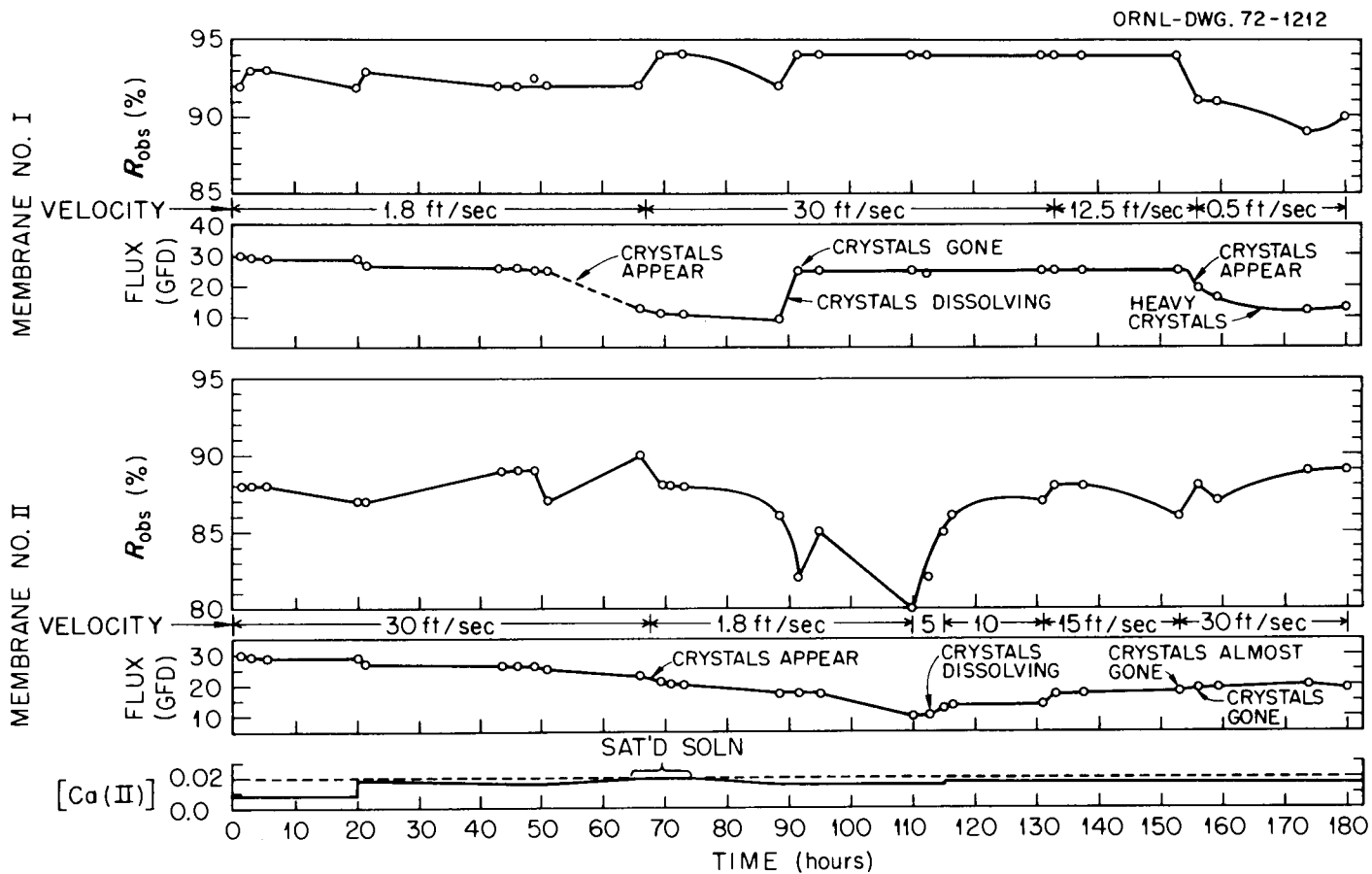
FLUID FLOW PATTERNS AS FUNCTION OF FLOW VELOCITY IN TRANSPARENT TEST SECTION WITH MEMBRANE SUPPORT IN PLACE. Finger OD: 0.625 in. ; Jacket ID: 1.3125 in. ; Dye Source OD: 0.047 in. , Displaced ~0.56 in. from Tube Axis. Flux ~ 0gfd.

Fig. 2

1. Effect of velocity and feed concentration: A chronological history of the first experiment is given in Fig. 3. The feed solution was 0.05 M NaCl containing CaSO<sub>4</sub> at the concentrations indicated at the bottom of the figure. Velocities are indicated between the flux and rejection plots for each membrane, and they were varied at different times from 0.5 fps, where flow was presumably laminar ( $N_{Re} \sim 900$ ), to 30 fps, a velocity at which one can be assured that concentration polarization is negligible, with  $N_{Re} \sim 70,000$ . The membranes were Aerojet 6% cellulose acetate, each with an area of 25 cm<sup>2</sup>.

During the initial part of the experiment, one velocity was set at 1.8 fps,  $N_{Re} \sim 4350$ , while the control was held at 30 fps. Under these conditions, no crystallization was observed on either membrane with a CaSO<sub>4</sub> concentration of 0.0088 M ( $\sim 45\%$  of the saturated value).<sup>4</sup> When the concentration was increased to 0.0176 M ( $\sim 90\%$  of saturated), fluxes through both membranes decreased slightly, but there was no discernible change in their surface appearance. After 50 hours, concentration of the solutions was begun by discarding the product, and at about 55 hours crystals of CaSO<sub>4</sub>·2H<sub>2</sub>O began to appear on the membrane with flow at 1.8 fps. The solution became saturated in calcium sulfate at about 63 hours, but the high circulation velocity past Membrane II prevented massive crystal deposition from appearing. However, when the velocity past Membrane II was dropped to 1.8 fps at 67.5 hours, crystals began to form almost immediately. The velocity past Membrane I was increased to 30 fps at the same time, but the crystals which had formed there at the lower velocity were not removed. These crystals did disappear, however, when the solution was diluted with distilled water to bring the calcium sulfate concentration below the saturation limit, although those on Membrane II, running at the lower velocity, remained intact.

At 110 hours, the velocity past Membrane II was increased to 5 fps. Almost immediately the rejection began to improve, and within a few hours it became apparent that the crystals had begun to dissolve. The flux began to improve slowly, and continued to do so until the last of the crystals disappeared at about 156 hours. The velocity was increased to 10, to 15, and 30 fps, and each increase resulted in small improvements in flux and rejection by Membrane II.



HYPERFILTRATION OF  $\text{CaSO}_4$  IN 0.05M NaCl SOLUTIONS BY AEROJET 6% CA MEMBRANES  
(500 psig, 25°C)

Fig. 3

At 156 hours, when the  $\text{CaSO}_4$  concentration in the feed solution was 0.0172 M, about 88% of saturation, the velocity past Membrane I was reduced to 0.5 fps, and crystals began to form within a few minutes. Both the flux and rejections decreased concurrently, and remained depressed throughout the remainder of the run. The crystals which did form adhered only loosely to the CA membrane, and sloughed off when the finger was removed from the test section. A rough calculation of concentration polarization for this case indicated that the concentration of  $\text{CaSO}_4$  about half way along the membrane exceeded the solubility limit by about a factor of 3.

2. Effect of polymetaphosphate: In the second experiment, we studied the effect that different concentrations of poly(hexametaphosphate) had on the time it took for crystals to appear on the membrane surface under non-turbulent flow conditions. The polyphosphate we used was Calgon. Again two porous stainless steel fingers were wrapped with Aerojet 6% cellulose acetate membrane, and inserted into two parallel test sections. A solution of  $\text{CaSO}_4$ , nominally 0.0176 M, in 0.05 M NaCl was made up in the feed tank, and this solution was then circulated past the membrane surfaces at 30 fps. We then decreased the flow velocity in one of the test sections to 0.5 fps; the velocity in the other section was maintained at 30 fps in order to detect changes in membrane characteristics due to factors other than those we were attempting to study. The time from reduction of velocity to appearance of crystals was recorded.

Once crystals did appear, the velocity was returned to 30 fps in both test sections, and the loop was rinsed under pressure with distilled water until the crystals disappeared and the fluxes returned to normal values. The experiment was then repeated, but with a given concentration of Calgon added to the  $\text{CaSO}_4$ -NaCl solution. Rejections were monitored by conductivity measurements, and flux values were recorded often during each run.

The results are presented in Table II. The time of appearance of some of the crystals was not determined exactly because they formed during the night or over weekends when the experiment was not being monitored. It is apparent, however, that as little as 5 ppm Calgon exerts a definite effect on the rate of membrane fouling by  $\text{CaSO}_4 \cdot 2\text{H}_2\text{O}$

TABLE II

THE EFFECT OF CALGON CONCENTRATIONS ON THE TIME FOR  $\text{CaSO}_4 \cdot 2\text{H}_2\text{O}$  CRYSTALS TO FORM ON CELLULOSE ACETATE MEMBRANES UNDER LAMINAR FLOW CONDITIONS.

(500 psig, 0.5 fps, 25°C)

Calgon (ppm)	[Ca(II)] in feed		Time to see visible crystals (hours:minutes)
	M	% Sat'd*	
0	0.015	77	0:15
0	0.0164	84	0:45
5	0.0129	66	1:45
5	0.0164	84	4:45
5	0.0166	86	> 3:30 but < 17:00
5	0.0143	74	> 3:50 but < 18:00
10	0.015	77	> 3:00 but < 65:00
15	0.0192	99	> 23:00 but < 38:00

\* Based on solubility of  $\text{CaSO}_4$  in 0.05 M NaCl as given by W. L. Marshall and R. Slusher, reference (4) in text.

under the conditions of these experiments. Moreover, increasing the concentration of additive to 10 and to 15 ppm caused a further increase in the average time to see visible signs of crystal growth. Declines in rejections and fluxes can be established only qualitatively with crystal formation, since they varied widely in individual cases. In general, however, rejections, as measured by conductivity changes, declined almost immediately from about 90% to about 80-85% when the velocity was lowered from 30 to 0.5 fps. This is caused by the increase in salt concentration at the membrane from concentration polarization. Fluxes generally decreased more gradually, but became very pronounced when an appreciable fraction of the surface became covered with thin crystals.

In one run, we tested the possibility of removing crystals after they were formed by adding Calgon to the feed solution. We adjusted the velocity through a test section to 0.5 fps without any Calgon additive in the  $\text{CaSO}_4$ -NaCl solution until crystals were clearly deposited on the membrane surface. We then added 5 ppm Calgon, but detected no change in

crystal appearance or membrane performance over the next 20 hours of operation. An increase to 10 ppm Calgon produced no changes in an additional 7 hours, and, likewise, an increase to 20 ppm was ineffective over another seven hour increment. Calgon appears to be much more effective in preventing, or delaying, crystal growth than it is in removing crystals already formed.

In another test, we added 15 ppm Calgon but also added an equivalent amount of Mg(II). We reasoned that the Mg(II), which should complex with the Calgon about as effectively as does the Ca(II), might tie up enough of the polyphosphate to reduce its effectiveness in preventing crystal formation. However, in this particular run, we were unable to perceive crystal formation even after fifty hours of operation.

3. Effect of pH: The next experiments in this series were run, at the suggestion of Dr. Fred Witmer of OSW, to investigate the importance of pH in fouling by  $\text{CaSO}_4 \cdot 2\text{H}_2\text{O}$ . We selected two fingers each containing two porous stainless steel sections, and one section of each tube was wrapped with Eastman KP 90 cellulose acetate membrane while the other section was wrapped with some experimental samples of a Chemstrand polyamide film, kindly supplied to us by Dr. Ray McKinney. The polyamide we obtained was evidently very sensitive to exposure to air, and we were not able, by the techniques we use, to obtain satisfactory performance with it. However, with the CA membrane, we ran the following tests.

We placed the two fingers into transparent test sections so that we could observe the surfaces of the membranes during the course of the experiments. A solution of 0.0176 M  $\text{CaSO}_4$  in 0.05 M  $\text{NaCl}$  was added to the loop and circulated at 30 fps past the membranes. pH was adjusted to one of two values, 5.5 or 8.5, and in certain cases, 5 ppm of poly-metaphosphate (Calgon) was added. The flow velocity was then dropped to 0.5 fps in one of the test sections, (the other was maintained at 30 fps to act as a control), and the flux, rejection, and appearance of the membrane was recorded as a function of time. At the end of a given experiment,  $\text{CaSO}_4$  deposits, if any, were removed by increasing the circulation velocity to 30 fps, and by, in some cases, replacing the salt solution by distilled water.

Ten different runs were made, and the results are shown in part in Figs. 4 through 6. Figure 4 indicates the rejection, determined from conductivity measurements, and flux as a function of time for solutions at two different pH values, 5.5 and 8.5, and with and without Calgon present. There was apparently little difference in flux at the different pH values over the length of time of these runs, but the rejection appeared to be appreciably worse, on the average, for the low pH cases.

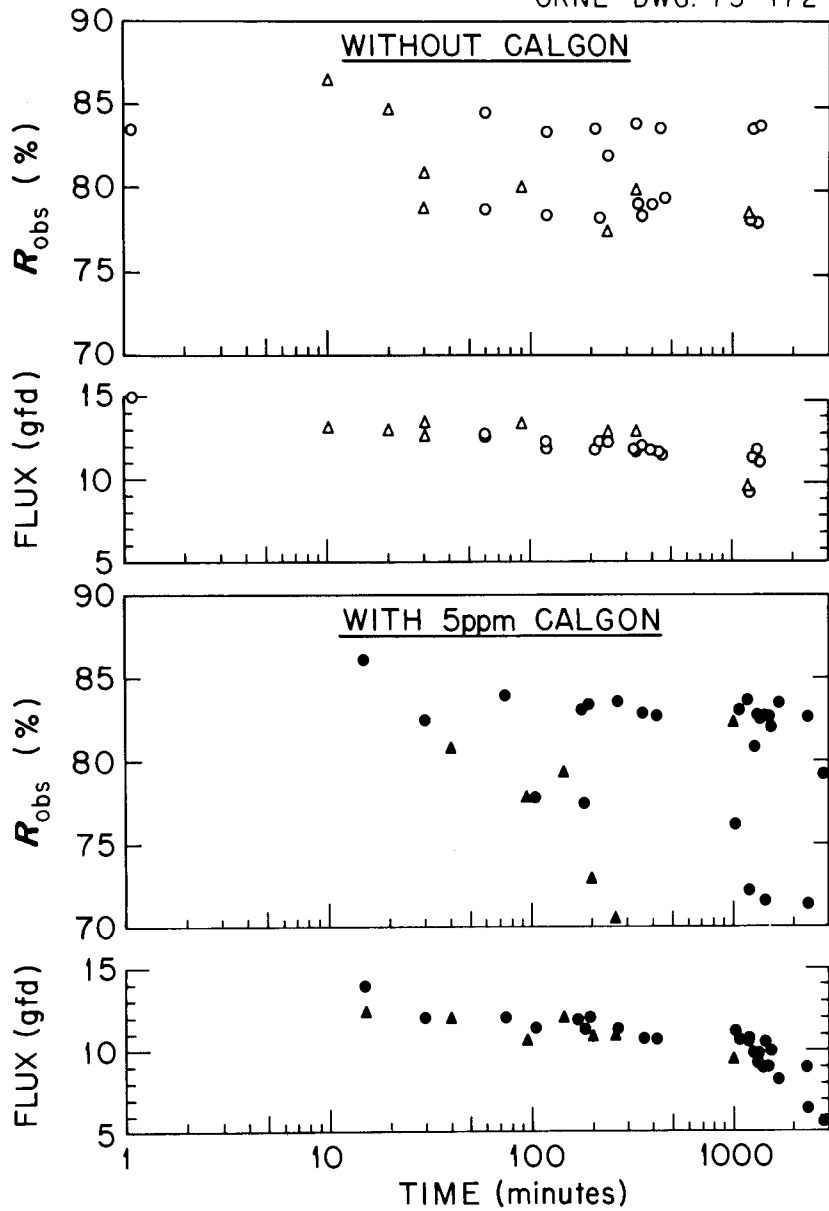
Figure 5 contains all of the data of both halves of Fig. 4, and indicates that fluxes tend to be somewhat lower in the presence of Calgon (solid symbols) than in its absence (open symbols). After longer times, rejections in the presence of Calgon seemed to deteriorate somewhat more rapidly than they did if no Calgon was present. There is a considerable scatter, and any conclusions are tentative.

Figure 6 shows the results of two consecutive runs, at pH 8.5, with and without Calgon. No crystals were obvious during the course of the run in which Calgon was present (solid symbols), but in the run without Calgon, crystals appeared sometime between 440 minutes and 1300 minutes. However, the performance after crystal appearance without Calgon was better in both flux and rejection than that at corresponding times in the run containing Calgon. It might be that precipitated  $\text{CaSO}_4$  was actually present in both cases, but that in the case with Calgon it was in a form affecting performance more seriously.

Table III gives a summary of this set of runs as far as crystal appearance is concerned. Solution pH appears to be a much more important factor than Calgon, at least at the concentration here used, in determining whether or not visible crystals will form and how rapidly they will form. At pH 8.5, with Calgon present, no crystals were observed visually up to times as long as 2800 minutes, about 47 hours. At the lower pH, without Calgon, many crystals became apparent early in the run.

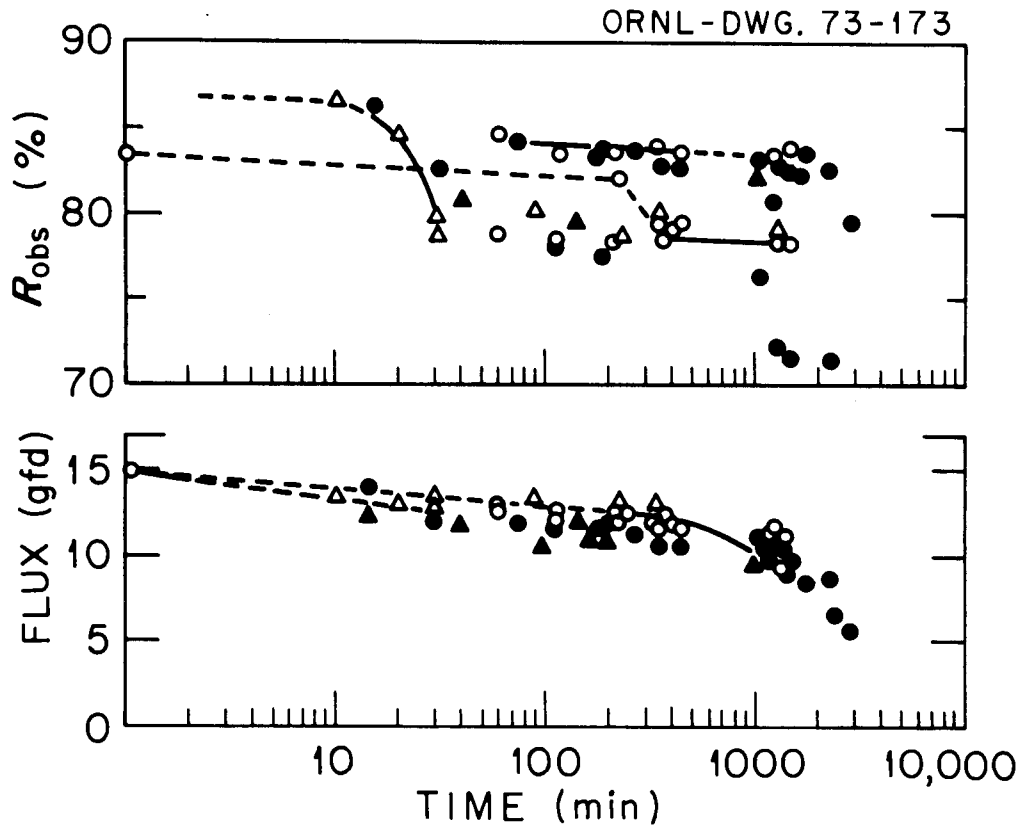
4. Possible degradation of polymetaphosphate: A word of caution about the interpretation of the results from the studies described above, and from any studies in which a feed solution is recirculated for extended periods of time, seems in order. Polyphosphates are usually highly rejected by cast film membranes, and, as a result of concentration polarization, their concentration in the boundary layer should be high. At

ORNL - DWG. 73-172



REJECTION AND FLUX OF 0.0176 M  $\text{CaSO}_4$  IN 0.05 M NaCl WITH CA MEMBRANES (Eastman KP 90) AS FUNCTION OF TIME AFTER VELOCITY DROPPED TO 0.5 fps. pH 5.5:  $\blacktriangle$ ; pH 8.5:  $\bullet$ . (500 psig, 25°C).

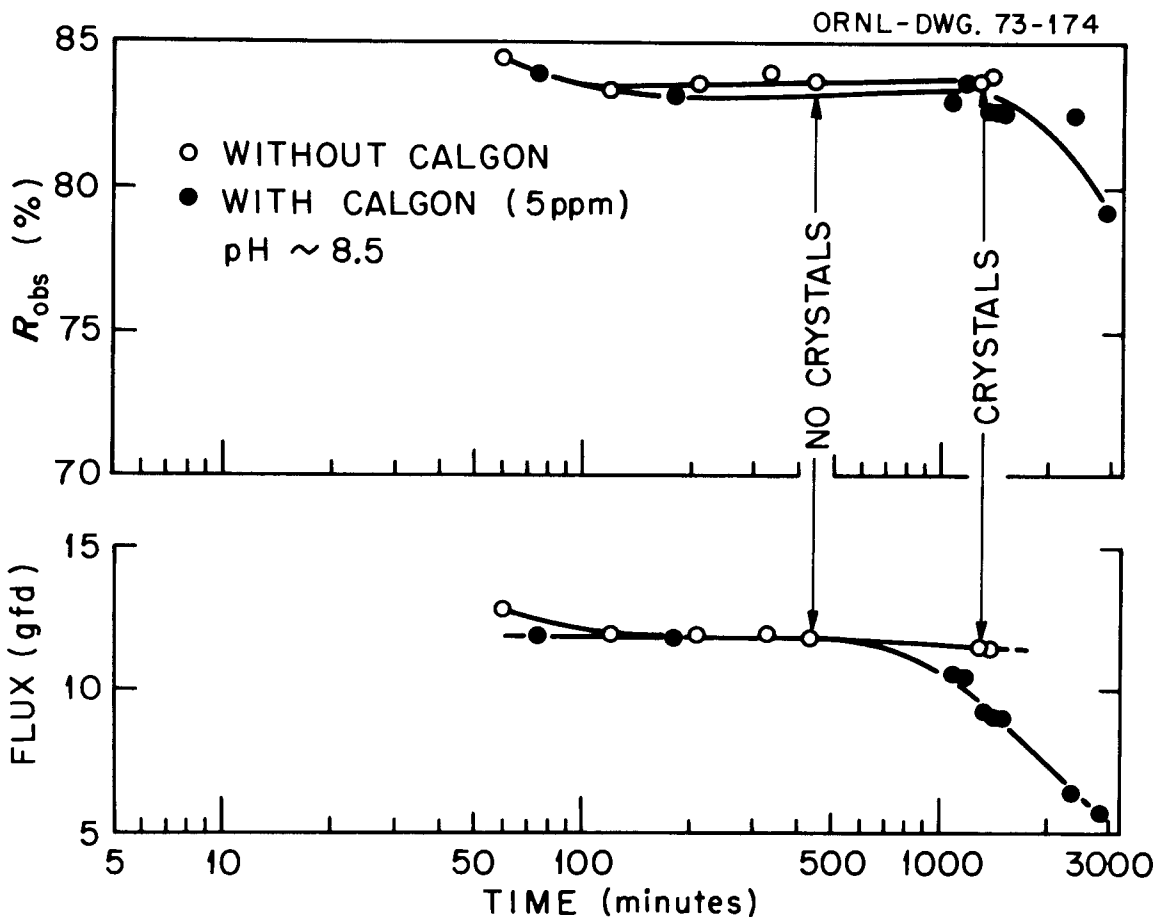
Fig. 4



REJECTION AND FLUX OF 0.0176 M  $\text{CaSO}_4$  IN 0.05 M NaCl WITH CA MEMBRANES (Eastman KP 90) AS FUNCTION OF TIME AFTER VELOCITY DROPPED TO 0.5 fps. (500 psig, 25°C).

pH	Calgon Concentration	
	0 ppm	5 ppm
5.5	△	▲
8.5	○	●

Fig. 5



REJECTION AND FLUX OF CA MEMBRANES (Eastman KP 90) AS FUNCTION OF TIME AFTER FLOW VELOCITY DROPPED TO 0.5 fps. ( $0.0176 M$   $CaSO_4$  in  $0.05 M$  NaCl,  $25^\circ C$ , 500 psig, pH 8.5).

Fig. 6

TABLE III

EFFECT OF pH AND CALGON (5 ppm) ON THE RATE OF APPEARANCE OF  $\text{CaSO}_4 \cdot 2\text{H}_2\text{O}$  CRYSTALLITES ON A CELLULOSE ACETATE MEMBRANE (EASTMAN KP 90) DURING SUPERSATURATION DUE TO CONCENTRATION POLARIZATION.

(0.0176  $\text{CaSO}_4$  in 0.05 NaCl, 500 psig, 25°C, 0.5 fps)

<u>Run No.</u>	<u>pH</u>	<u>Calgon</u>	<u>Crystals</u>	<u>Time (t) (min)</u>
1	8.5	No	Yes	~360
5	8.5	No	Yes	435 < t < 1290
7	8.5	No	No	>1330
2	5.5	No	Yes	~20
8	5.5	No	Yes	~90
4	8.5	Yes	No	>1695
6	8.5	Yes	No	>2820
9	8.5	Yes	No	>2355
3	5.5	Yes	Yes	190 < t < 1000
10	5.5	Yes	No	>260

least some of their beneficial effects in scale inhibition at very low bulk concentrations may arise from this fact. However, in experiments such as these, in which brine was recirculated, the polymetaphosphate may have been degraded over a period of time, either by hydrolysis or by action of the pump, or by both.

We attempted to determine additive degradation by following changes in the viscosities of the feed, but were surprised to find very little difference in the viscosities of saline solutions containing 0, 5, 10, and 15 ppm Calgon. An inquiry to Dr. T. W. Brooks of Calgon Corporation revealed that the molecular weight of the polyphosphate in commercially available Calgon is low, about 1200 to 1400. Through the courtesy of Dr. Brooks and of Mr. P. H. Ralston, also of Calgon Corporation, we obtained two samples of polyphosphates of somewhat higher molecular weights, namely about 2700 and 5600. Solutions of these at 5, 10, and 15 ppm also failed to show differences in viscosities larger than the experimental errors in our measurements. It became apparent that we were not able to follow polyphosphate degradation by this method.

C. Tests with commercial modules:

After the modules had been installed, they were tested briefly with 0.05 M NaCl solution. At 400 psig and 70°F, the DuPont flux was about 1.5 gfd at 46.5% single-pass water recovery. The GESCO module flux was about 13.3 gfd at 34% recovery. Average rejection, as determined by the difference in conductivity between product and feed, was about 90% for the DuPont module and 93% for the GESCO. Following these tests, we began a long series of experiments with simulated brackish waters. A chronological listing of these tests with operating conditions and flux and rejection data is given in Appendix A to this report. It must be emphasized at the outset that, while we were aware of limitations regarding salt concentrations and water recovery rates imposed by the manufacturers, we often violated these limitations in order to bring about measurable effects caused by exceeding solubility limits in the brine at the membrane-brine interface. This kind of treatment, of course, caused irreversible changes in the modules that would not have occurred had they been operated according to specifications.

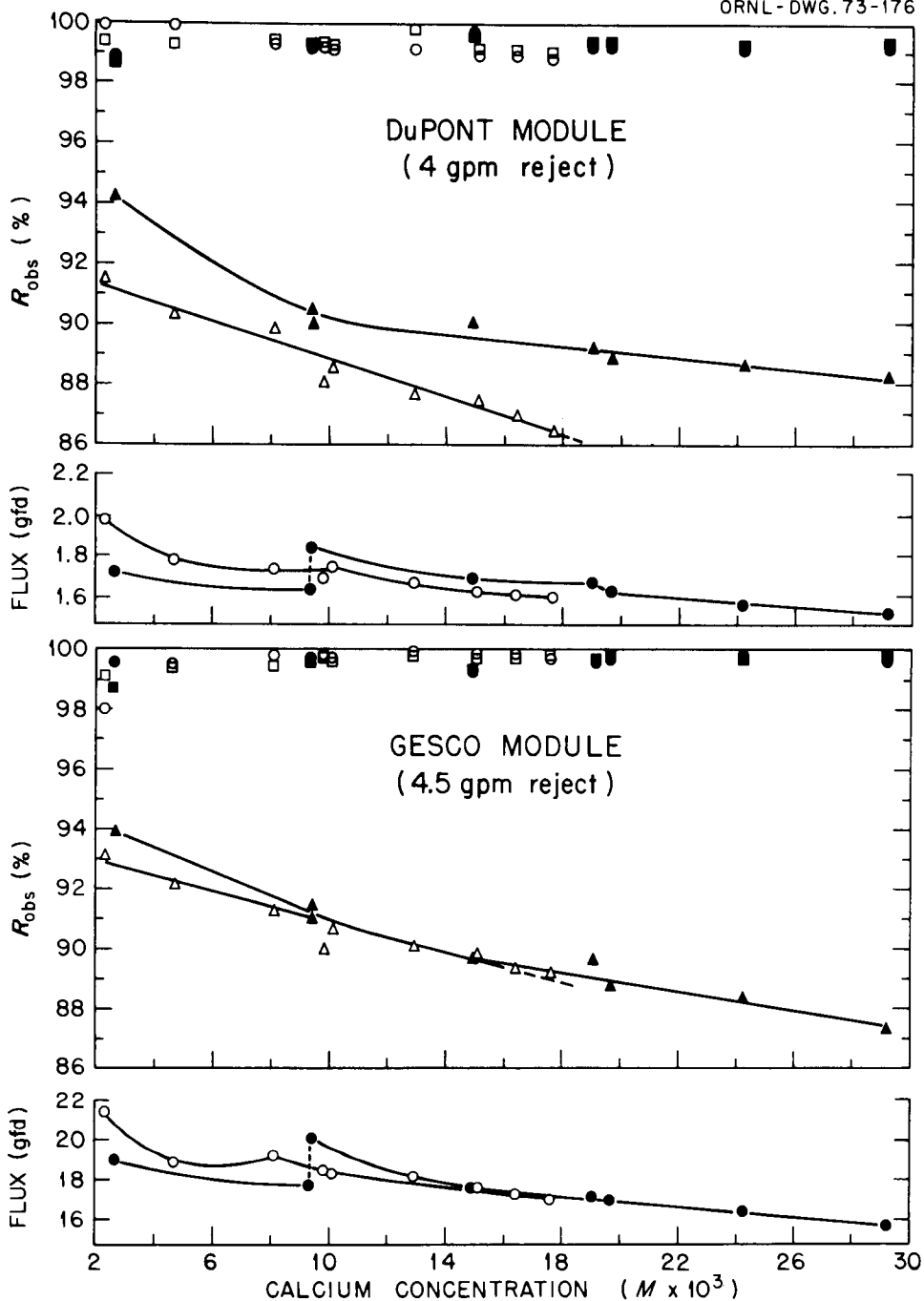
1. Tests with simulated Webster Water:

a. Incremental increases in salt concentration: We began the series of tests by circulating about 25 gallons of simulated Webster Water, with and without polymetaphosphate (Calgon), through the two modules operating in parallel (Runs 8a-2 and 3). Inlet pressure was maintained at about 400 psig, temperatures about 70°F, and the single pass recovery rates were adjusted to about 40% for the DuPont module and 25% for the GESCO. Product and reject were returned to the feed tank, except when product water was discarded incrementally to increase the concentration of the feed, thereby simulating conditions the modules might face in later sections of an in-field plant.

We had anticipated, based on our experience with  $\text{CaSO}_4$  crystal formation on CA membranes under fouling conditions (see Section II B), that, as we slowly increased the calcium concentration in the feed brine by discarding product, we would reach a point at which  $\text{CaSO}_4 \cdot 2\text{H}_2\text{O}$  would begin to plate out on the membrane surfaces. Because of concentration polarization at the membrane-feed interface, this point should occur before

the bulk solution reached saturation, and it should be indicated by an abrupt change in the slope of the flux vs. calcium concentration curve. However, no such change in slope was observed (see Fig. 7), even though we carried the water effective recovery to 80% without Calgon present, and to 93% in the presence of 20 ppm Calgon. Based on the solubility of  $\text{CaSO}_4 \cdot 2\text{H}_2\text{O}$  in Webster Water concentrates<sup>1</sup>, we had expected saturation to occur in the module at about 64% water recovery, assuming a 1.2 wall-to-bulk concentration factor. This expectation was derived from Fig. 8, which shows a plot of the calculated solubility product ( $Q_{\text{fsp}}$ ) of  $\text{CaSO}_4$  in Webster Water as a function of the percent of the water removed by RO, assuming complete rejection of all components of the solution. Also indicated in Fig. 8 are two curves showing the product of the concentrations of the Ca(II) ion and the sulfate ion in solutions corresponding to a given water recovery level. The lower of the two curves is drawn for bulk feed concentrations, while the upper curve would indicate the product of the concentrations at the feed-membrane interface if there were a 1.2 wall-to-bulk concentration factor due to polarization. Thus, saturation should occur in the bulk feed at about 74% water recovery and at the membrane at 64% water recovery. The situation in practice is considerably more complicated, of course, since there is a concentration gradient through the module. Membrane surfaces near the inlet see a relatively dilute brine, while those near the reject manifold see a brine concentrated by a factor  $100/(100 - \% \text{ recovery})$ , assuming 100% rejection. In addition, the leading membranes not only encounter a weaker brine, but also encounter a higher flow rate which tends to reduce concentration polarization. This is especially true of the DuPont module, where both the configuration and the product removal decrease flow rate along those membrane surfaces that see brines at the higher concentrations.

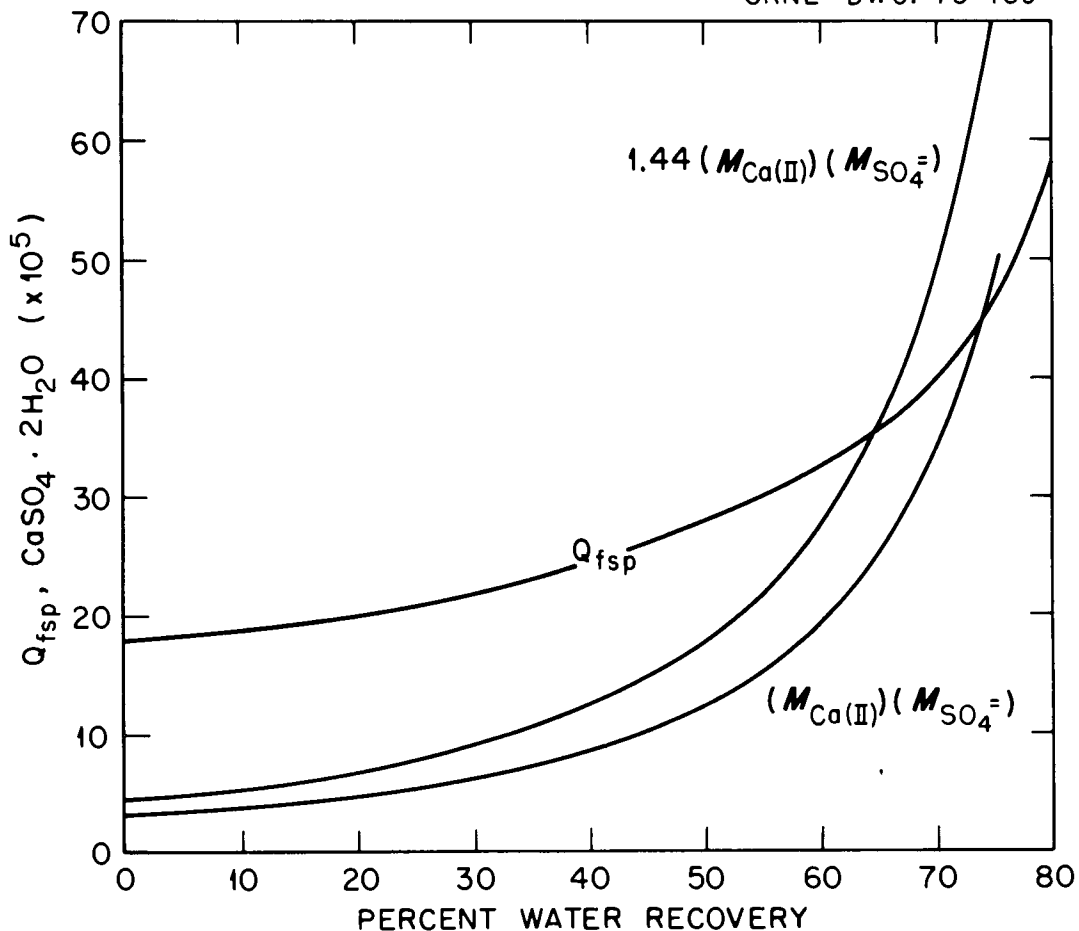
During the initial tests, we found that the rejection of Ca(II) and Mg(II) appeared to be independent of Ca(II) concentration over the range studied, but the rejection of  $\text{Cl}^-$  decreased monotonically as the feed solution became more concentrated in salt. The presence of poly-metaphosphate appeared not to affect rejections, except for that of  $\text{Cl}^-$  by the DuPont module, where chloride rejections were appreciably higher when Calgon was present at 20 ppm.



RUNS 8A-2 AND 3. FLUX AND REJECTION AS FUNCTION OF CALCIUM CONCENTRATION. (~400 psig, ~70°F).  
○ Ca plus Mg, □ Ca, △ Cl. Open Symbols, No Calgon; Closed Symbols, 20 ppm Calgon.

Fig. 7

ORNL - DWG. 73-169



$Q_{fsp}$  VERSUS PERCENT WATER RECOVERY FOR WEBSTER WATER, ASSUMING COMPLETE REJECTION FOR ALL COMPONENTS, AND USING THE DATA OF MARSHALL, YEATTS, AND LANTZ FOR THE SOLUBILITY OF  $\text{CaSO}_4 \cdot 2\text{H}_2\text{O}$  IN WEBSTER WATER (Ref. 1 in Text).

Fig. 8

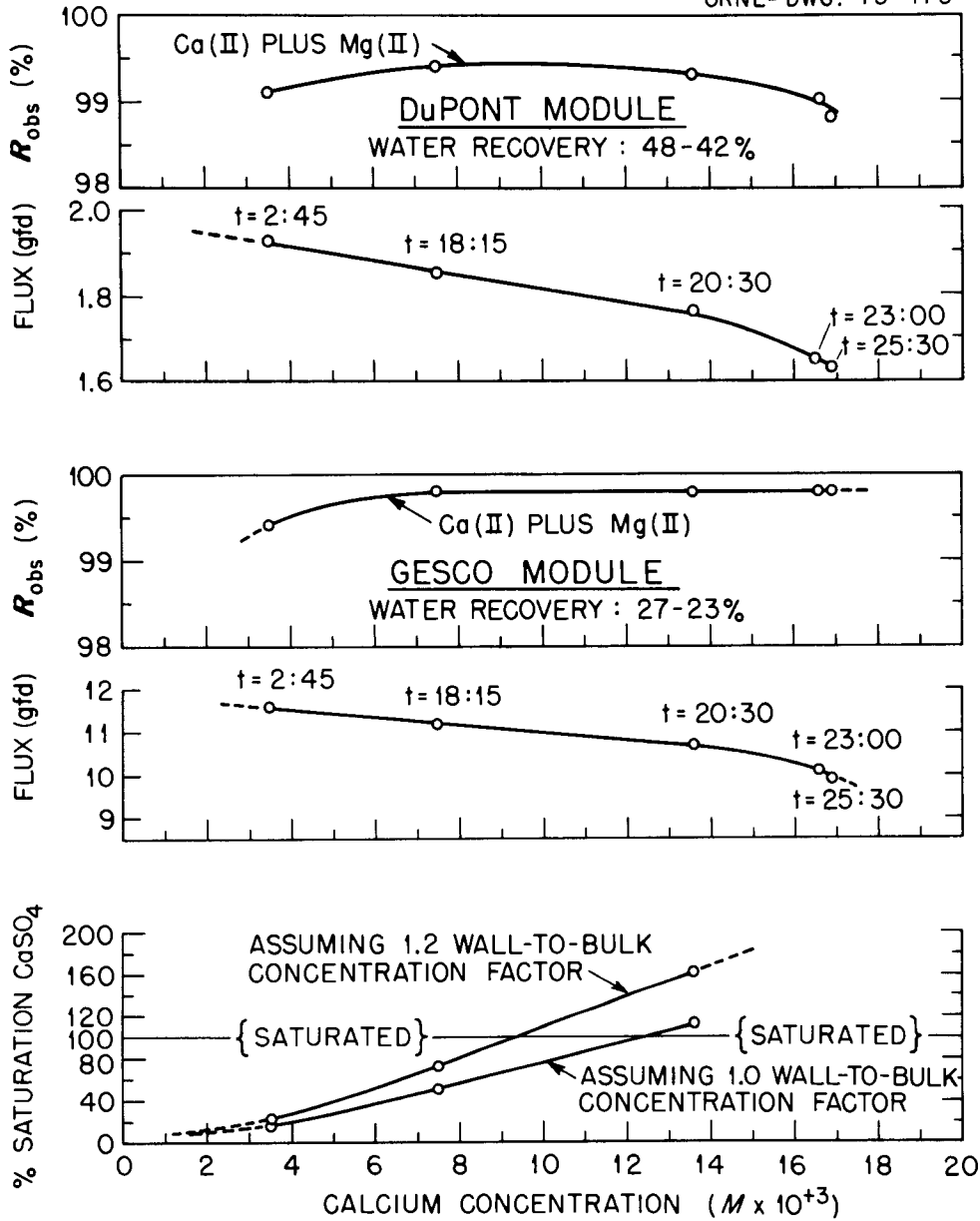
The run without Calgon was repeated (Run 8A-4) after first rinsing the modules with distilled water until fluxes were steady with time under normal operating conditions of pressure, flow, and temperature. As before, see Fig. 9, the rejection of divalent cations was relatively independent of concentration, while the flux decrease monotonically as the Ca(II) concentration increased.

We checked these results for Webster water at this point by repeating the experiments with a solution containing only an equivalent amount of NaCl. Although the decrease in flux at high water recovery levels was even more pronounced with the NaCl than with the Webster water, corrections made to account for increases in osmotic pressure and for concentration gradients through the modules indicated that while the permeabilities for NaCl increased slightly at high water recovery levels, those for Webster water showed about a 5% decrease. This decrease was so small, however, we were not convinced that it resulted from fouling in the module.

b. Attempts to achieve steady state: In the next run with Webster water, (8A-6), we modified our test procedure somewhat in that, after each incremental increase in brine concentration, the product rates were monitored until they reached some constant value for a period of at least one or two hours. Although slow rates of flux decline would not be detected in this manner, rapid rates might become apparent. The results of this test were similar to previous ones up to a water recovery level of about 70%, at which point the calcium depletion rate became appreciably larger. This was reflected by a break in the flux vs. log time plot (Fig. 10) at about 25 hours, by which time enough product had been discarded to bring the effective water recovery rate to about 70%.

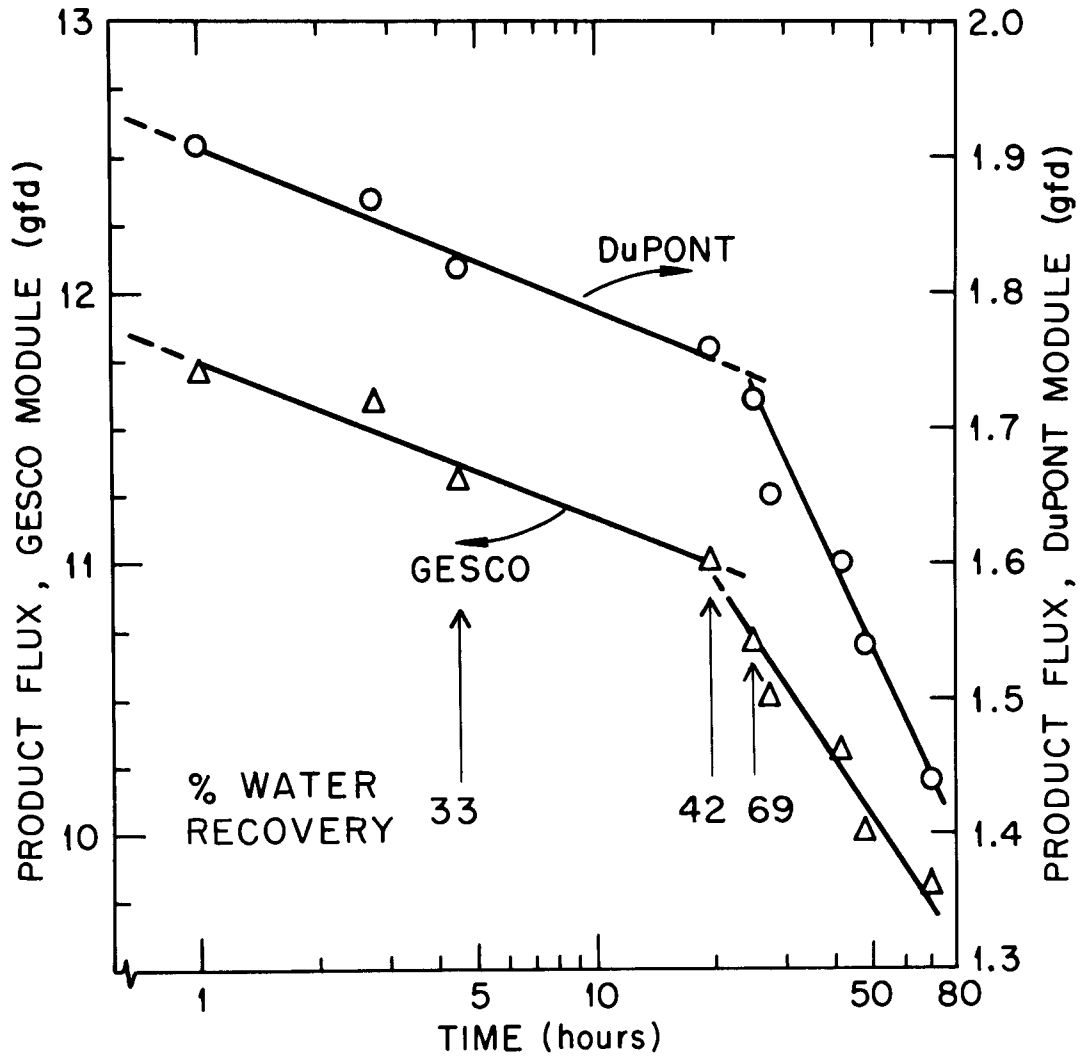
c. Long-term run at high, single-pass recovery rates: It is difficult, if not impossible, to infer fouling rates from the experiments described above, since the concentrations of fouling agents in the feed were being changed at arbitrary times. Our next experiment, 8A-7, attempted to correct this by operating both modules at higher single-pass recovery rates for an extended period of time while returning both product and reject to the feed tank in an attempt to maintain constant input brine composition. The DuPont was operated at about 68% recovery while the GESCO module was

ORNL- DWG. 73-175



FLUX AND REJECTION AS FUNCTION OF CALCIUM CONCENTRATION IN SIMULATED WEBSTER WATER. TIME POINT TAKEN INDICATED ON FLUX PLOT. (~ 400 psig; ~75° F; pH: 5.9-6.1).

Fig. 9



FLUX VERSUS LOG TIME FOR RO TREATMENT OF SIMULATED WEBSTER WATER WITH CONCURRENT INCREMENTAL INCREASES IN BRINE CONCENTRATION. Single-pass Recovery: 46-40% for DuPont Module, 30-26% for GGA. (~400 psig, 75°F, pH 6-6.1).

Fig. 10

operated at about 64% for the first 316 hours and at about 69% for the remainder of the run, to 500 hours. This technique, too, proved unsatisfactory, for the calcium in the feed was rapidly depleted to low levels, presumably by precipitation on membrane surfaces. These results indicated that, with limited feed volumes, the  $\text{CaSO}_4$  was rapidly depleted to levels at which supersaturation in the modules could not occur. It became evident that, to simulate field conditions, it was necessary to have an inexhaustible source of brine or to replace continuously those components in the brine that were removed by the modules.

We were able to garner some information about concentration polarization from these longer term tests. If, with limited feed volume, the composition of the feed and of the reject stream reaches a composition that remains unchanged with time, it might be assumed that a steady state equilibrium exists between the brine passing through the modules and any  $\text{CaSO}_4$  deposits that may have formed on the membrane surfaces. If so, the square root of the ratio of the formal solubility product for  $\text{CaSO}_4$  in a brine of the ionic strength characteristic of the reject stream to the actual concentration product found in the reject stream will be an estimate of the wall-to-bulk concentration factor holding under the conditions existing in the module. In six different cases during run 8A-7, we analyzed feed and reject concentrations; the results indicated a wall-to-bulk concentration factor that averaged about 1.24, with most values falling within 0.05 of this.

d. Periodic replacement of depleted salts: At this stage in the project, we added a 200-gallon stainless steel feed tank. We reasoned that the larger feed volume would decrease the rate at which the calcium and the sulfate were depleted, thereby making it easier to monitor fouling rates. We then decided to try to monitor feed composition and to replace periodically those components removed by the modules. In run 8A-9, reject flow rates were adjusted to give initial recovery rates between 65 and 70%; after about 180 hours, these rates were adjusted upward to about 72%. The pressure drop across the DuPont module was monitored as a possible indicator of fouling, and sufficient  $\text{Ca(II)}$  and  $\text{SO}_4^{=}$  were added about once a day to bring the concentration in the feed tank back to a composition

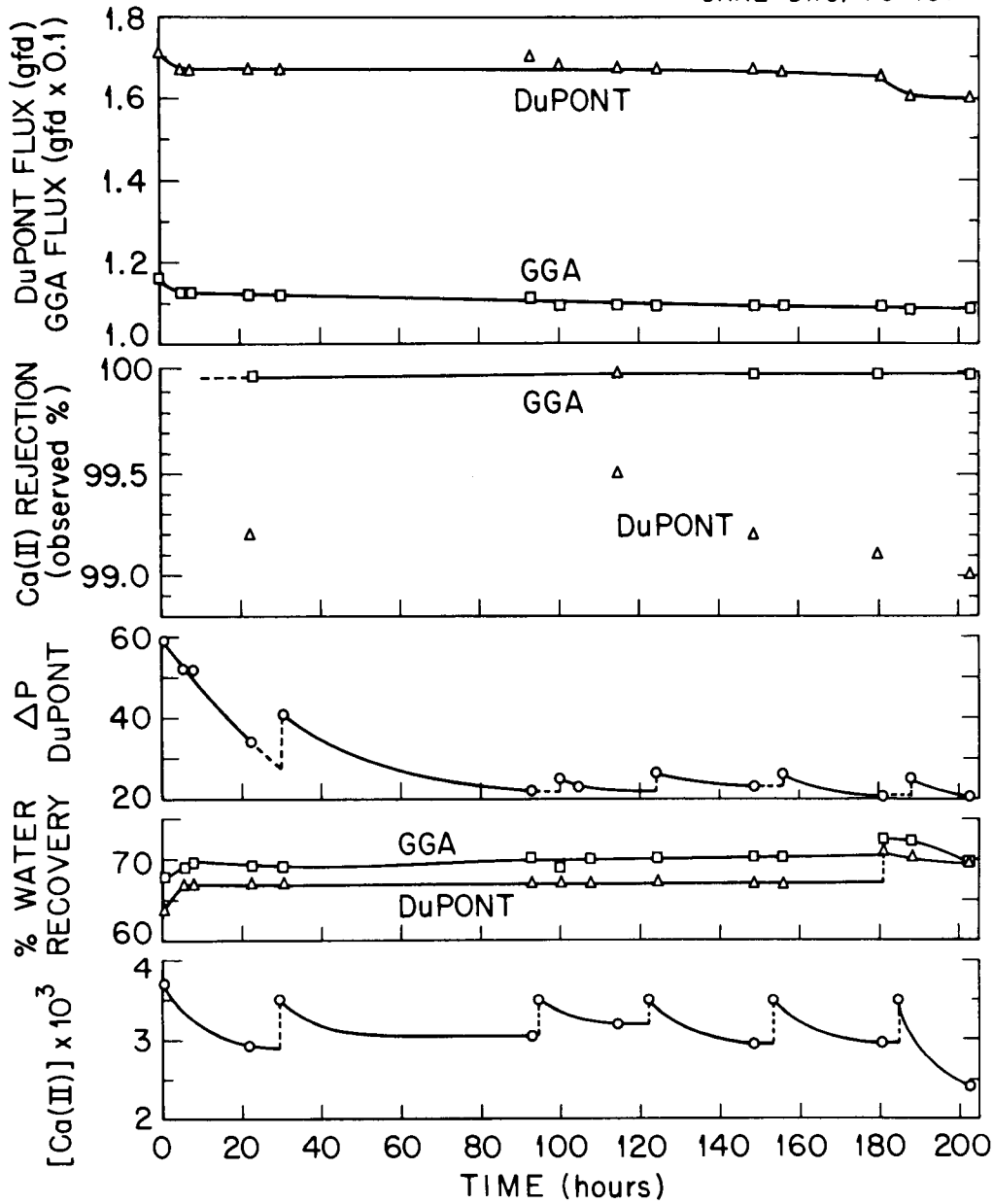
typical of Webster water. The results of the run are shown graphically in Fig. 11, and may be summarized as follows.

Each time calcium and sulfate were added to the feed solution to bring their concentration back to nominal, the rate at which they were removed appeared to increase. Within several hours, the depletion rates once again assumed low values, as evidenced by the results of a material balance between input, reject, and product concentrations. Each time  $\text{CaSO}_4$  was added to the feed tank, the pressure drop across the DuPont module first increased and subsequently decreased with time as the calcium and sulfate were depleted. This is contrary to our a priori assumption that the pressure would increase, because of increased fouling, as the foulants were removed from the brine. This contrary behavior may have resulted, however, from a temporary partial plugging of the module by the suspended  $\text{CaSO}_4$  newly added to the brine.  $\text{CaSO}_4$  dissolves slowly in cold water, and slow dissolution of particles trapped in the modules under flow conditions not conducive to supersaturation may then have led to the slow decrease in pressure drop observed.

When the single-pass recovery rates were increased slightly after about 180 hours, we found a significant increase in the  $\text{Ca(II)}$  depletion rate, and this indicated to us that the  $\text{Ca(II)}$  depletion rate may well be the most sensitive indicator of fouling. Prior to beginning a series of experiments designed to test this premise, we tried to remove as much of the precipitated  $\text{CaSO}_4$  from the modules as possible, using a series of washes with distilled water as well as with solutions containing several different sequestering agents.

We washed the modules first by operating with three separate 100 liter batches of distilled water for one hour each. At the end of the second wash, the  $\text{Ca(II)}$  concentration in the wash water was 0.0031 M; at the end of the third, it had fallen to 0.00062 M. We added 20 ppm Calgon to the third wash and ran for another hour;  $\text{Ca(II)}$  concentration in the wash water more than doubled. We rinsed the system with distilled water and operated the system over the weekend with 100 liters of distilled water with 20 ppm Calgon added; the  $\text{Ca(II)}$  concentration following this extended wash was 0.0092 M. We followed this with two three-hour washes, two overnight washes, and one 6-hour wash with Calgon-spiked distilled water, and then changed to distilled water containing 0.01 M EDTA for four hours.

ORNL-DWG. 73-181



CHRONOLOGICAL RECORD OF RUN 8A-9.  
DESALINATION OF SIMULATED WEBSTER WATER  
BY DuPONT AND GGA MODULES. (400 psig,  
75-76°F, pH 5.9-7.4).

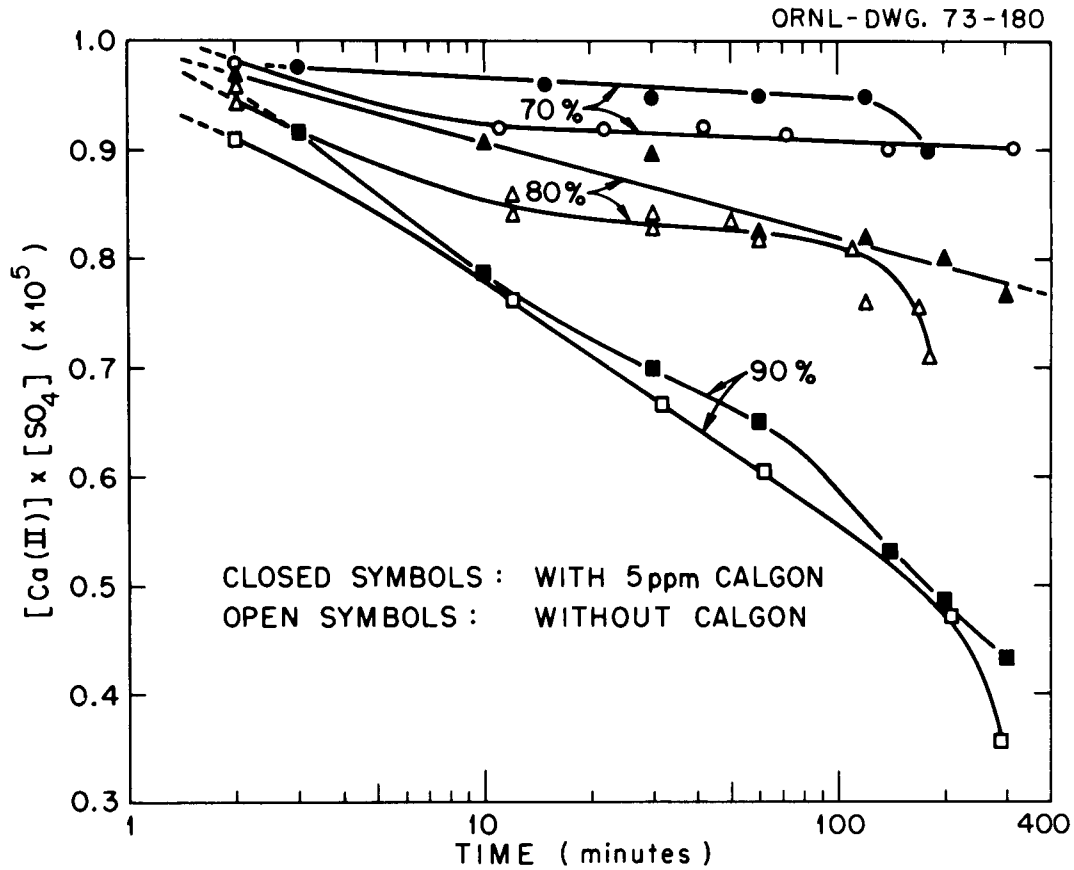
Fig. 11

The EDTA was rinsed out, and following another two-hour wash using Calgon, the Ca(II) concentration was still  $0.0004 \text{ M}$ ,

Following the advice of Mr. V. J. Tomsic, Supervisor of Technical Services, DuPont Corporation, we next resorted to a 2 wt% citric acid solution, buffered to pH 8 with  $\text{NH}_4\text{OH}$ . This wash solution was run overnight, then rinsed out, and replaced with 20 ppm Calgon solution. At the end of two more similar Calgon washes, the wash solution at the end of a four-hour wash was still  $0.0004 \text{ M}$  Ca(II), about 10% of the nominal concentration in Webster water. We rinsed overnight with distilled water, and began the experiments described below.

e. Depletion as a function of recovery rate: In the next experiment with Webster water (8A-10A), we chose a single-pass recovery rate, 45%, which should not have led to saturation in the modules and which, consequently, should not have led to a depletion in the concentration of calcium in the feed. However, there was still an 11% decrease in Ca(II) concentration with time during the initial fifty minutes of the run. After this time, the rate of decrease became much smaller. We then made three runs (8A-10B, C, and D) at about 70% single-pass recovery, and the results were similar to those at 45%. Between each run, we returned to 45% water recovery, and usually ran for at least fourteen hours under these conditions. When we went to 90% recovery (8A-10E), however, we noted a drastic change in the nature of the curve, with calcium depletion continuing at much lower feed concentrations.

We repeated the experiments with runs at 80 and 90% recovery levels, with and without 5 ppm Calgon added, and at 70% recovery with Calgon (Runs 8A-10F, G, I, J, and K). These results, shown in Fig. 12, with those of 8A-10C, indicate that  $\text{CaSO}_4$  is removed much more rapidly from the feed stream at the higher recovery rates, and somewhat more rapidly if Calgon is absent than if it is present. The data also indicated that we were approaching steady state conditions in these eight-hour tests only in those cases where the recovery rates were about 70%. At the higher rates, the reject streams were supersaturated in  $\text{CaSO}_4$ , see Table IV, and samples taken of the reject streams under these conditions soon showed precipitates unless they were diluted promptly. The effect of Calgon at 5 ppm was not great in these tests, and seemed to become less important the higher the recovery rate.



CHANGE IN PRODUCT OF CALCIUM CONCENTRATION AND SULFATE CONCENTRATION AS FUNCTION OF TIME AND WATER RECOVERY RATE FOR SIMULATED WEBSTER WATER, WITH AND WITHOUT 5ppm CALGON ADDED. DuPONT AND GGA MODULES USED IN PARALLEL. (400 psig, 75°F).

Fig. 12

TABLE IV

PROPERTIES OF THE REJECT STREAM AT THE  
FINAL POINTS OF EACH RUN SHOWN IN FIG. 12.

Webster water feed, 400 psig.

Run	Module	% Water Recovery	Calgon (ppm)	[Ca] x [SO <sub>4</sub> ] (x 10 <sup>5</sup> )	Q <sub>fsp</sub> *	$\frac{Q_{fsp}}{[Ca] \times [SO_4]}$ <sup>1/2</sup>
8A-10C	DuPont	69.5	0	33.8	39.3	1.08
	GESCO	67.8	0	21.1	36.7	1.32
8A-10K	DuPont	69.6	5	31.5	38.6	1.11
	GESCO	68.2	5	30.6	38.5	1.12
8A-10G	DuPont	79.3	0	36.7 <sup>†</sup>	43.0	1.08
	GESCO	80.7	0	48.4 <sup>†</sup>	48.0	0.996
8A-10J	DuPont	78.8	5	48.0	46.2	0.981
	GESCO	80.2	5	60.0	51.0	0.922
8A-10F	DuPont	89.5	0	73.3	58.0	0.890
	GESCO	90.4	0	92.2	65.2	0.841
8A-10I	DuPont	89.9	5	86.3	89.9	0.842
	GESCO	89.9	5	113.1	68.5	0.778

\*Based on the solubility data from reference 1 in text.

†Probably low values since samples contained precipitate.

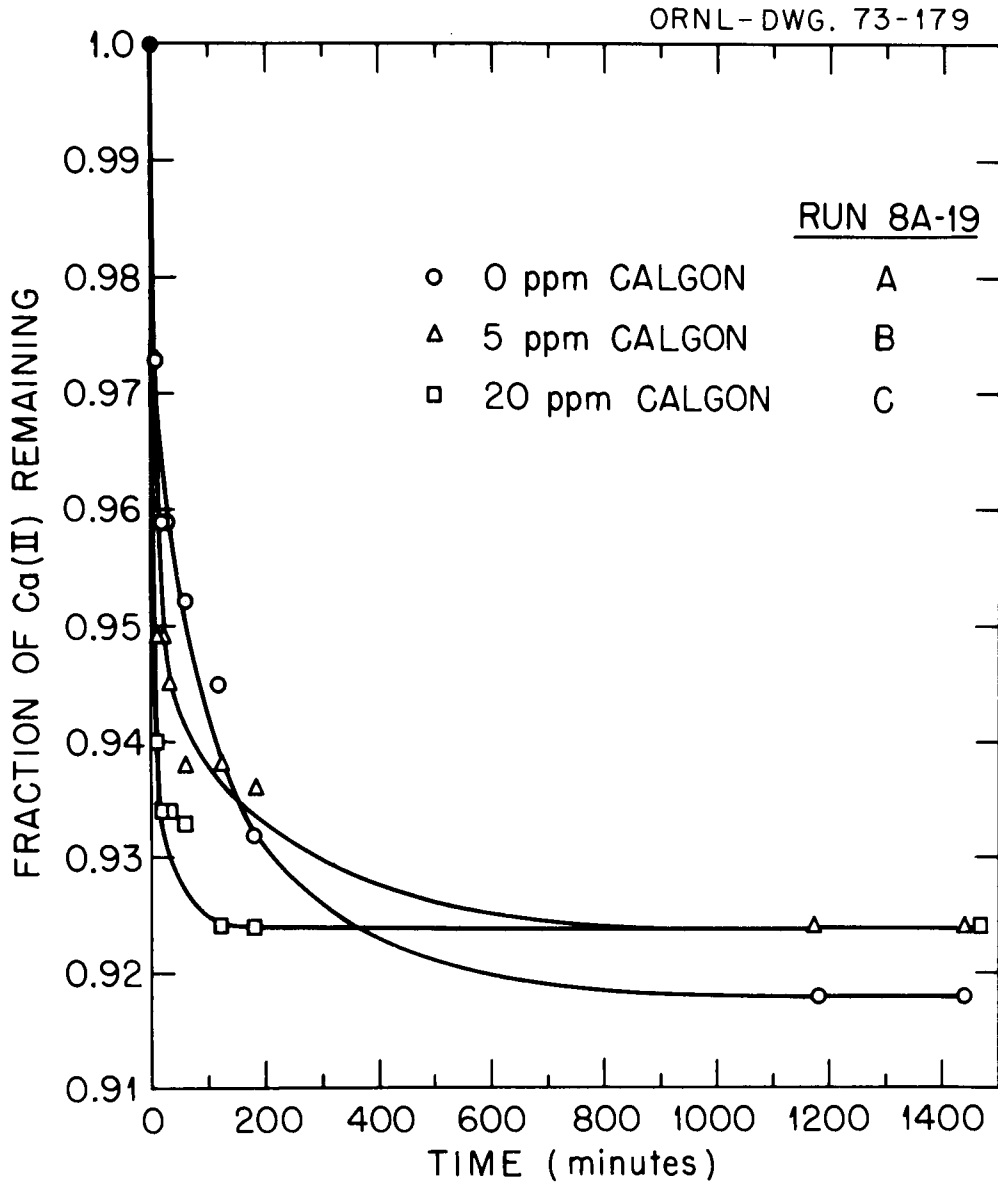
f. Simulated second-section feed concentrates: Following the tests on Webster water indicated above, we turned our attention to other waters for a time, as indicated in Appendix A. In runs 8A-11A and B, we worked with Webster water that had been pretreated by cross-flow filtration to remove substantial amounts of Ca(II) and Mg(II). In the runs of 8A-12 and 13, we worked with Wellton-Mohawk drainage canal water, and in those of 8A-15 with simulated Foss Reservoir water. After these runs, we returned to Webster water, in runs in which we attempted to operate the RO units under conditions in which the number of stagnant areas in the modules were minimized.

We doubled the concentration of each constituent in the simulated Webster water to make up a feed approximating a second or third stage section stream and operated the two units in parallel at single-pass recovery levels less than 30%. The net result was equivalent to operating

at about 65% water recovery, which should lead to incipient precipitation only near the reject end of the modules. Pressures were again maintained at 400 psig, and the temperatures about 75°F.

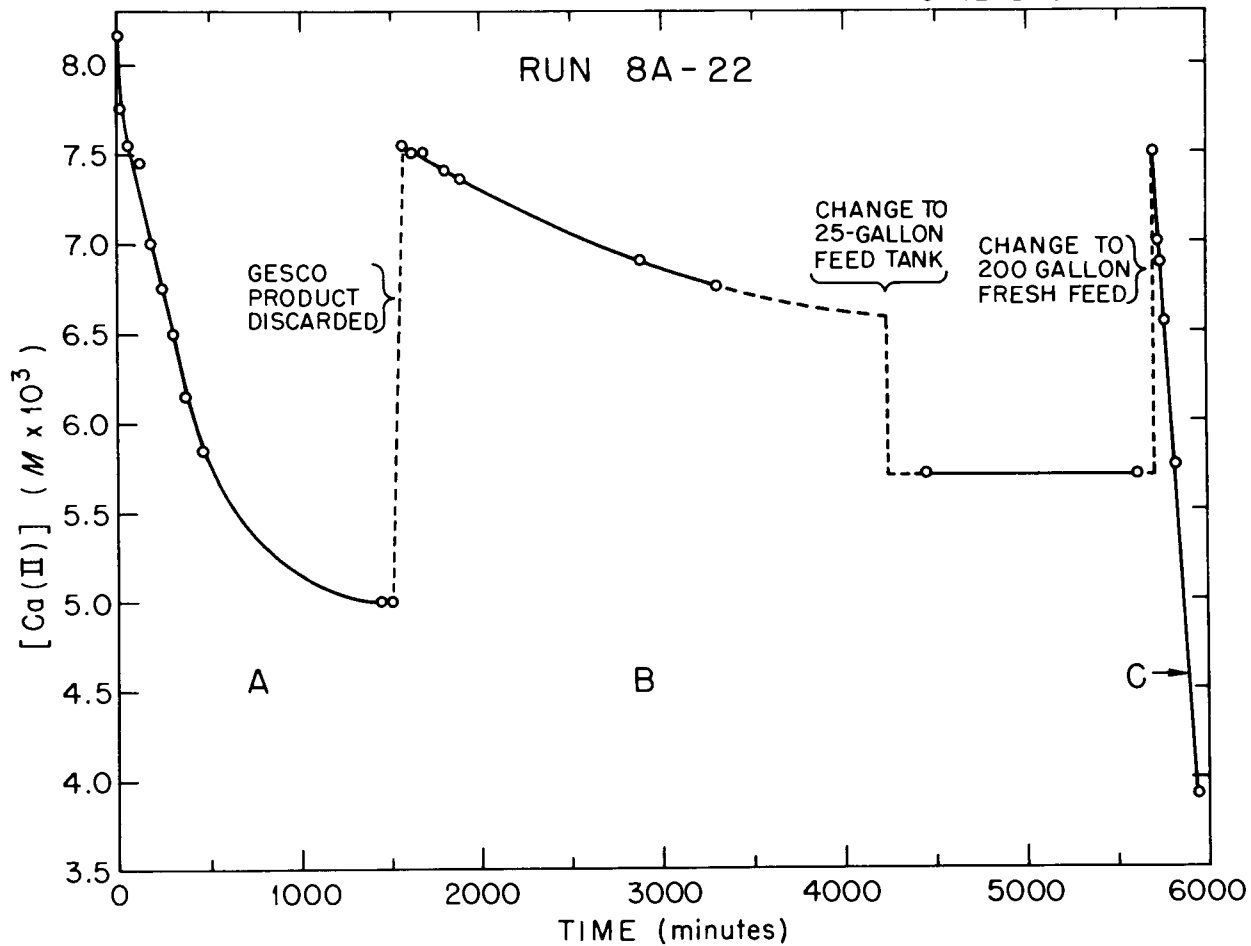
The rates at which Ca(II) was depleted for the first three runs (8A-19A through C), with 0, 5, and 20 ppm Calgon, are shown in Fig. 13, where the data have been normalized to compensate for small differences in concentrations. There is not much difference in the three curves. Without Calgon, the Ca(II) is apparently depleted more slowly in the early stages, but it falls to a slightly lower steady-state concentration over longer times. Even though we had lost Ca(II) in the modules, the reject streams at the end of these runs were not saturated in calcium sulfate. The differences between the product of the calcium and the sulfate concentrations and the formal solubility product indicated a wall-to-bulk concentration factor of 1.06 to 1.19 for the DuPont module and 1.04 to 1.21 for the GESCO module, somewhat lower than the values obtained in 8A-7.

Figure 14 shows the results of the next series of runs, 8A-22A, B, and C. We made up a fresh supply of 2X Webster water and operated the modules in parallel under the same conditions as in the test just described, except for some variations in the pH. During the first 1500 minutes of the run (A), the calcium concentration in the feed decreased rather rapidly. It did, however, appear to be approaching a steady state value around  $5 \times 10^{-3}$  M. We next increased the concentration of calcium back to near the starting level by discarding product from the GESCO module. This should have increased all constituents proportionately since the rejection by the GESCO module was well over 90% for everything that we have measured. As we continued the run (B), the rate of decrease of calcium was much lower, even though the initial concentration was almost as high as it was in A. At about 4200 minutes, we set aside a small tank of the feed being used and continued to operate the modules from that tank while we prepared a new batch of 2X feed in the 200 gallon main feed tank. When we switched to the new feed at about 5700 minutes, we again got a precipitous fall in calcium concentration (C). This decrease continued until we terminated the run at about 6000 minutes at which point the concentration of calcium



Ca(II) CONCENTRATION IN FEED VERSUS TIME FOR SIMULATED WEBSTER WATER. DuPONT AND GESCO MODULES IN PARALLEL OPERATION. (2X, 30% Single-Pass Recovery)

Fig. 13

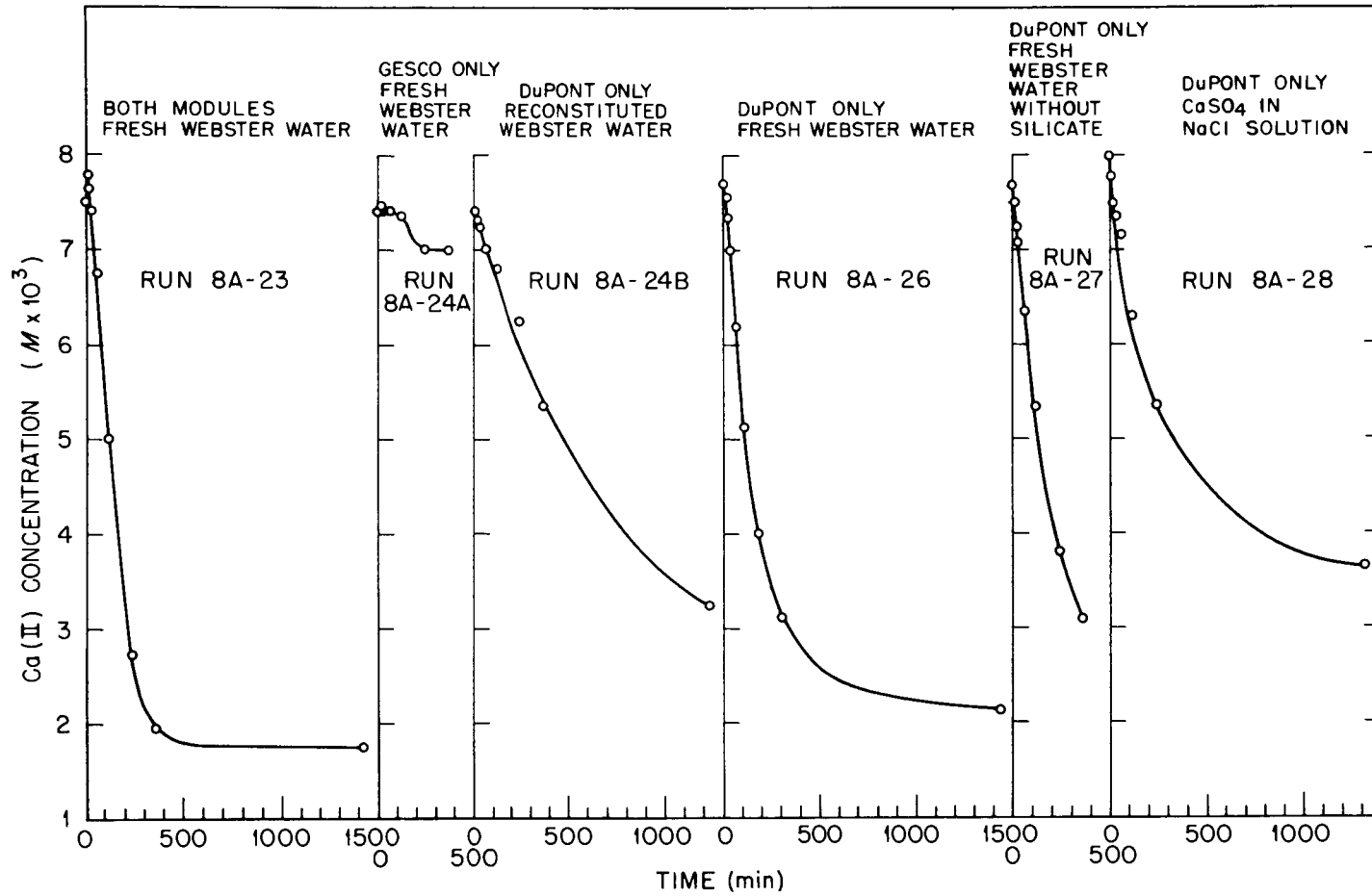


Ca(II) CONCENTRATION IN FEED VERSUS TIME FOR SIMULATED WEBSTER WATER. DuPONT AND GESCO MODULES IN PARALLEL OPERATION. (2X, 30% Single-Pass, 400 psig, 73-75 °F)

Fig. 14

was below  $4 \times 10^{-3}$  M. These results seemed to indicate that there was something in a freshly made up batch of Webster water feed, other than calcium and sulfate, that affected the rate at which calcium was removed.

The next series of tests with Webster water were designed to try to discover which components of the feed might be responsible for the loss of calcium and to determine if this loss is common to both modules. The results of these tests are shown in Fig. 15. All of the tests were run at 400 psig, 73 to 75°F, and at pH values between 5.1 and 6.1. Feed concentrations and single-pass recovery levels are indicated in Appendix A. In run 8A-23, a fresh 2X Webster water feed was directed through both modules operating in parallel. The decrease in calcium was very rapid and was very similar to the last part of run 8A-22. The calcium concentration appeared to be reaching an equilibrium value in the feed at about  $2 \times 10^{-3}$  M. At this point, we rinsed the modules with distilled water, prepared a new batch of 2X Webster water, and directed it to the GESCO module only (run 8A-24A). In this case, the decrease in calcium was quite low, appearing to reach steady state at about  $7 \times 10^{-3}$  M. We added a slight amount of calcium and sulfate to the feed in order to bring these constituents up to the nominal value in 2X Webster water, i.e., "reconstituted" the feed, and began run 8A-24B. During this run, the GESCO module was removed from the stream, and only the DuPont module was used. Although the rate of decrease in calcium was greater than it had been with the GESCO module, it was less than had been shown by both modules together with a fresh feed in 8A-23. Run 8A-26 is a repeat of 8A-24B with a fresh 2X Webster water feed. The results here look very similar to those of the earlier run, 8A-23, in which a fresh feed had also been used, i.e., the rate of decrease in calcium is again very rapid and again approaches  $2 \times 10^{-3}$  M near the end of the run. We examined samples of feed taken at the beginning of runs 8A-24A, 8A-24B, and 8A-26 and noticed a small amount of floc in the samples for 8A-24A and 8A-26 but none in 8A-24B. We analyzed the initial feed samples for silicate and for inorganic carbon, using the inorganic carbon analysis as an approximation for carbonate and bicarbonate. Silicate was near nominal levels in each of the samples, but the inorganic carbon was low in the feed for run 8A-24B while near nominal in the other two runs (see Table V). However, a decrease in calcium by precipitation



Ca(II) CONCENTRATION IN FEED vs TIME .  
 (2X Feed, 20-30% Single-Pass Recovery)

Fig. 15

TABLE V

SILICA AND BICARBONATE CONCENTRATIONS IN NOMINAL WEBSTER WATER AND IN INITIAL FEEDS FOR THREE RUNS WITH SIMULATED WEBSTER WATER

Run	Feed	Silica (M)	HCO <sub>3</sub> <sup>-</sup> (M)
	Nominal	0.0005	0.0049
8A-24A	Fresh	0.0012	0.0047
8A-24B	Recon.	0.0010	0.0002
8A-26	Fresh	0.0007	0.0050

of calcium carbonate at these acidic pH values seems unlikely. We postulated that some kind of precipitate with silicate might possibly increase the rate at which calcium is removed. We tested this premise in run 8A-27, where we made up a batch of 2X Webster water feed without any silicate in it. As can be seen from Fig. 15, the rate of decrease of calcium was as rapid as it had been when the silicate was present.

The final run with the DuPont module, 8A-28, was made with only calcium and sulfate present in a NaCl solution with an ionic strength equivalent to that of 2X Webster water. From Fig. 15, it is apparent that the results of this run are much more similar to those of run 8A-24B, with the reconstituted feed, than to any of those in which the DuPont module was used with a fresh feed of simulated Webster Water. It is further interesting to note that we continue to lose Ca(II) in these later runs even though the rejection by the DuPont module decreased drastically. We also found, see Table VI, that the reject stream became more and more unsaturated with respect to CaSO<sub>4</sub>, i.e., the wall-to-bulk concentration factor, F, became increasingly greater than 1, over the course of these experiments. When we dismantled the DuPont module, see next section, we found that a pin-hole leak had developed in the product end of the fiber bundle, and feed was evidently contaminating the product directly. The loss of Ca(II) was evidently associated with the formation of an unidentified (not CaSO<sub>4</sub>) precipitate found permeating the module on the brine side of the fibers. Attempts to identify this precipitate are described in the next section.

g. Analyses of solid deposits:\* During the final tests with the DuPont module, we had been bothered by reoccurring blockages and malfunctions

\*The semi-quantative spectrographic analyses were done by S. A. McIntyre, the X-ray analyses by R. L. Sherman, both of the ORNL Analytical Chemistry Division.

TABLE VI

RATIO OF SOLUBILITY PRODUCT QUOTIENTS IN REJECT STREAMS TO  
 $[Ca(II)][SO_4^{=}]$  CONCENTRATION PRODUCT.

(Data from final point in run.)

Run No.	Module	$[Ca(II)] \times [SO_4^{=}]$	$Q_{fsp}^a$	$F^b$
8A-19A	DuPont	$31.4 \times 10^{-5}$	$35 \times 10^{-5}$	1.06
	GESCO	27.6	34	1.11
8A-19B	DuPont	24.6	35	1.19
	GESCO	22.7	33	1.21
8A-19C	DuPont	25.0	31	1.11
	GESCO	31.1	33.5	1.04
8A-22A	DuPont	20.0	32	1.26
	GESCO	19.5	32	1.28
8A-22B <sup>c</sup>	DuPont	41.3	46	1.06
	GESCO	38.2	44	1.07
8A-22C	DuPont	13.2	32	1.56
	GESCO	15.5	35	1.50
8A-23	DuPont	3.8	25	2.60
	GESCO	7.9	34	2.07
8A-24A	GESCO	24.6	32	1.30
8A-24B	DuPont	15.7	35	1.49
8A-26	DuPont	3.2	21.5	2.61
8A-27	DuPont	5.2	24	2.15
8A-28	DuPont	1.2	15.7	3.57

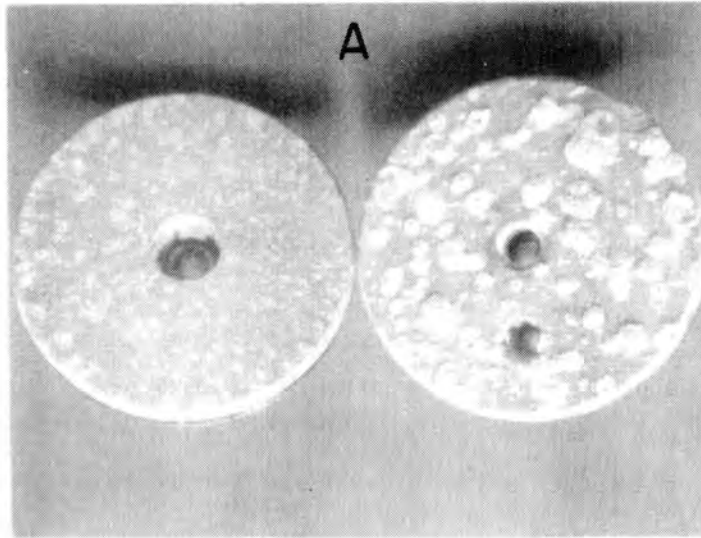
- 
- a.  $Q_{fsp}$  is the formal solubility product for  $CaSO_4 \cdot 2H_2O$  in Webster water, as determined from the data of Yeatts and Lantz (see Ref. 1 in text).
- b. The factor  $F = \{Q_{fsp}/[Ca(II)][SO_4^{=}]^{1/2}\}$  for the reject stream is a measure of concentration polarization near the exit, if  $CaSO_4$  has precipitated at the membrane-feed interface and if the  $Ca(II)$  concentration in the feed, under recycle operation, has become invariant with time.
- c. Data taken at 3300 minutes, Fig. 14.
-

in a control valve in the piping for the reject stream from the DuPont module. Upon close examination of the interior of the valve, we found that some small, hard deposits had formed, which were yellow-grey in color and which were probably responsible for the troubles in the valve. The deposits were found to contain an appreciable amount (>10% by weight) of aluminum, which must have come from the end plates of the DuPont modules, since there was no other aluminum in the system. Other major constituents in the deposits were silicon, (>5%); calcium, (~0.7%); magnesium, (~0.5%); and iron, (~0.2%). The solid may have been a complex silicate. The material of the deposits was only sparingly soluble, and we found less than  $10^{-5}$  M aluminum in the feed samples for runs 8A-24A and B and 8A-26 (Fig. 15). Aluminum concentrations in a fresh feed did not increase appreciably over the course of a run.

While we continued fouling experiments with the GESCO module, we dismantled the DuPont module, and found the end plates badly pitted and corroded (Fig. 16A), especially the end which came in direct contact with the reject stream. We also found a pin-hole leak in the product end of the fiber bundle, which allowed the feed to directly contaminate the product, and which was probably responsible for the very low rejections we found with the DuPont in the late runs. The deposits on the reject end plate proved to be very similar to those we had found on the reject-stream valve. They apparently contained slightly less Ca(II) and Mg(II), but the major constituents remained Al (>10%) and Si (~2%). These deposits were difficult to get into solution, and we resorted to aqua regia - that part of the sample that did go into solution (~98%) was apparently about 12% aluminum. We got no good X-ray powder pattern of the end-plate deposits; they were apparently amorphous.

We opened the fiber bundle of the DuPont module, and found the fibers permeated with a solid material which we have not been able to identify. As the module dried, the solid material became powdery; it was yellow-brown in the outer layers of the fiber bundle (nearly the color of the fibers themselves), but nearly white several layers into the module. Beginning from the outside of the fiber bundle, the amount of solid increased layer by layer, until, by the fourth layer, adjacent fibers were cemented together by the white precipitate (see Fig. 16B). We had at first assumed the

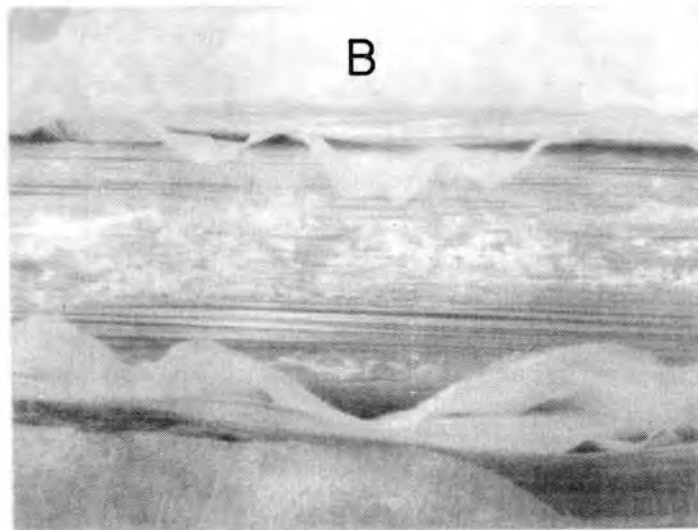
ORNL PHOTO 0289-73



Reject End

Product End

END PLATES OF DuPONT HOLLOW  
FIBER MODULE AT CONCLUSION  
OF TESTS.



SALT DEPOSITS ON HOLLOW FIBER  
IN INTERIOR OF DuPONT MODULE.

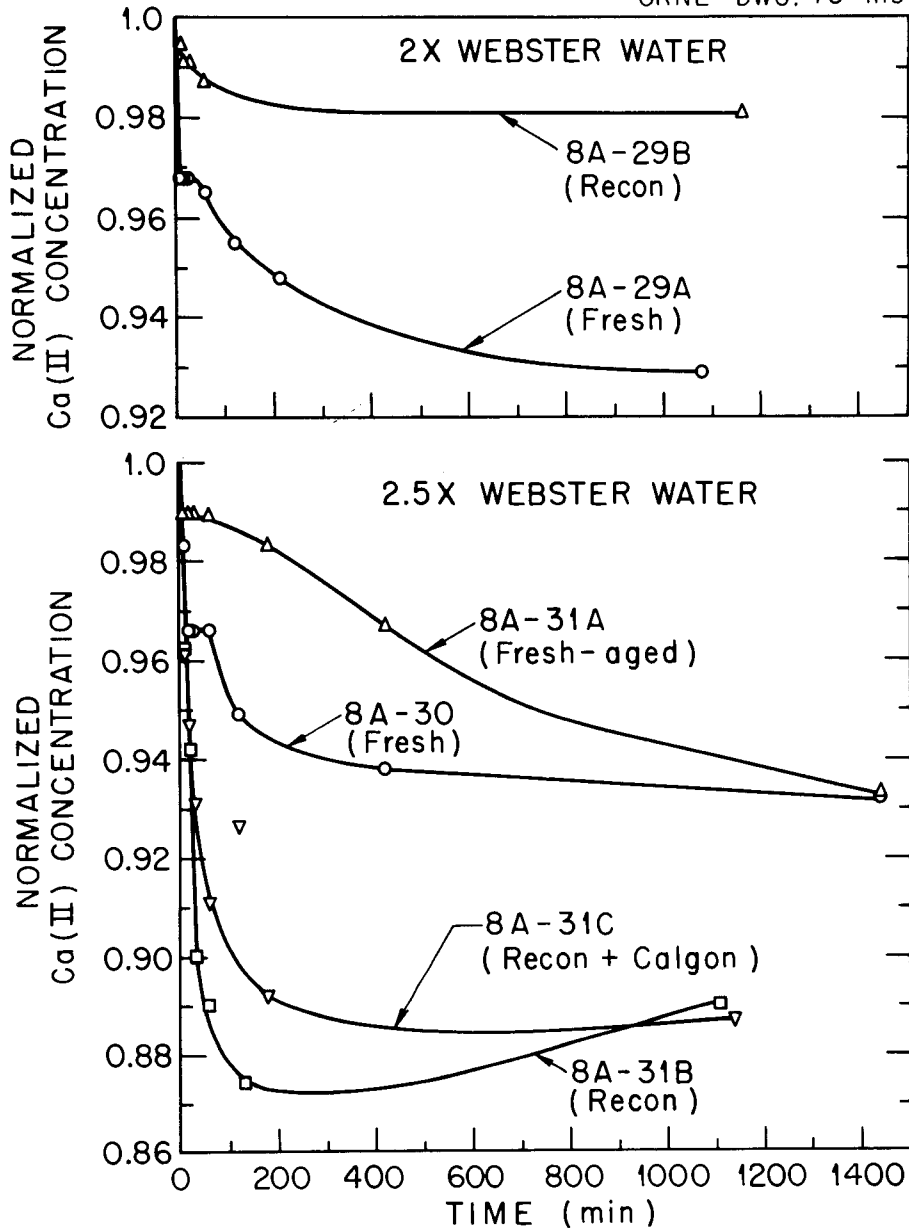
Fig. 16

powder was  $\text{CaSO}_4$ , and chemical analysis showed  $\text{Ca(II)}$  to be present to about 22 weight percent, but an X-ray powder pattern indicated that the  $\text{CaSO}_4$  was, at best, a minor constituent.  $\text{Mg(II)}$  was present to a smaller extent, perhaps as much as 3%, but no other cations constituted as much as 1% of the sample. Organic carbon, however, was present as a major constituent, amounting to about 22% of the sample. When the powder was slowly heated in air, it charred with some smoke, and lost about 67% by weight. The residue after firing was a white powder consisting of about 55%  $\text{Ca(II)}$  and about 12%  $\text{SO}_4^{=}$ . The powder, as deposited in the module, contained about 0.5% inorganic carbon, perhaps as the carbonate. The X-ray powder pattern suggests that the sample consists of a mixture of compounds, including some primarily organic in nature, but not easily identified as citrates or complexes with EDTA, which could conceivably have resulted from our wash procedures. The fibers themselves did not appear to have been dissolved or otherwise affected to any appreciable extent.

h. Tests with GESCO module only: The final series of tests in this project were carried out using the GESCO module only, with the single-pass recovery rate set at about 27%. This results in a reject flow rate of about 4 gpm, which is within the range specified by the manufacturer. Run 8A-29A, Fig. 17, was made with a fresh 2X Webster water feed, and once again there was a fairly rapid depletion of  $\text{Ca(II)}$  in the early (<200 minutes) part of the run. The results were very similar to those attained earlier under similar conditions, but with both modules in the system (see Fig. 13). At 27% and 2X concentration, which is equivalent to about 64% water recovery, incipient precipitation should take place only near the reject end of the module, again assuming a wall-to-bulk concentration factor of 1.2. We repeated the run, using reconstituted 2X water (8A-29B, Fig. 17), and got less than 2% depletion of the  $\text{Ca(II)}$  in a 20 hour period.

The lower portion of Fig. 17 shows the results of four runs with 2.5X Webster water, using the GESCO module set at about 27% single-pass recovery (effective recovery about 71%). In run 8A-30, a feed was made up and the run began immediately after the silicate and the bicarbonate

ORNL - DWG. 73-1119



NORMALIZED Ca(II) CONCENTRATION VERSUS TIME. GESCO MODULE WITH WEBSTER WATER CONCENTRATES. (400 psig, 73-75°F, pH 5.2-6.4, Single-pass Recovery ~ 27%).

Fig. 17

were added. In 8A-31A, a similar feed was stirred for 2 1/2 days before it was introduced into the module. There is appreciable difference in early depletion, but negligible difference at the end of 24 hours. In 8A-31B and C, we compared runs with reconstituted feeds, to one of which had been added 20 ppm Calgon. There is apparently little difference between the two cases, Fig. 17. The somewhat greater depletion of Ca(II) observed in these cases with the reconstituted feeds may have been caused by the somewhat higher initial concentrations of CaSO<sub>4</sub> in the last two runs. For example, the effective recovery rates at the beginning of the last two runs were about 73%, as compared to about 71.5% in the first two.

i. Comparison of runs with fresh and with reconstituted feeds:

Table VII lists all of the runs we made with 2X Webster water at effective recovery levels between 65 and 70%. The first six runs listed were carried out with freshly prepared solutions, the last six with reconstituted water. The fifth column in the table indicates the fraction of Ca(II) remaining in the feed solution after 180 minutes of operation. Except for the cases involving only the GESCO module, the rate of depletion of Ca(II) is much more rapid with the fresh solutions than with the reconstituted. With reconstituted solutions, there was appreciable depletion in the first three hours with the DuPont module only, some depletion when both modules were used, and very little with the GESCO only. These results might be explained if some of the Ca(II) is incorporated with undissolved materials in the fresh solutions, and if these materials are mechanically filtered from the solution during passage through the fibrous bundle in the DuPont module. The fact that in Run 8A-22B, where all components still remaining in solution after 8A-22A were concentrated back to the nominal 2X concentration at the beginning of the run, the loss of Ca(II) was minimal indicates that, indeed, something in the starting solution besides CaSO<sub>4</sub> has been removed.

j. Pretreatment to increase recovery: Because brine disposal is costly at inland locations, it is desirable to carry reverse osmosis treatment of brackish waters to high recovery levels. A recent study<sup>5</sup> has indicated that the lowest overall product costs are to be found at very high recovery rates. The most economical operating points were found

TABLE VII

Ca(II) DEPLETION, NORMALIZED, AT 180 MINUTES INTO A  
NUMBER OF RUNS FOR FRESH AND RECONSTITUTED 2X WEBSTER WATER.

(400 psig, pH 5.4-7.9)

<u>Run No.</u>	<u>Feed</u>	<u>Modules</u>	<u>Effective Recovery Level (%)</u>	<u>Normalized Ca(II) concentration at 180 minutes</u>
8A-22A	Fresh	Both	69	0.86
8A-22C	Fresh	Both	65	0.65
8A-23	Fresh	Both	67	0.50
8A-24A	Fresh	GESCO	65	0.96
8A-26	Fresh	DuPont	68	0.52
8A-29A	Fresh	GESCO	68	0.95
8A-19A	Recon	Both	66	0.93
8A-19B	Recon <sup>a</sup>	Both	65	0.94
8A-19C	Recon <sup>b</sup>	Both	68	0.92
8A-22B	Recon <sup>c</sup>	Both	66	0.98
8A-24B	Recon	DuPont	67	0.88
8A-29B	Recon	GESCO	68	0.99

a. Plus 5 ppm Calgon.

b. Plus 20 ppm Calgon.

c. Reconstituted by discarding GESCO product at end of 8A-22A.

to occur at recovery factors between 0.9 and 0.98. Because of this, we thought it would be informative to test pretreated Webster water with the DuPont and GESCO modules.

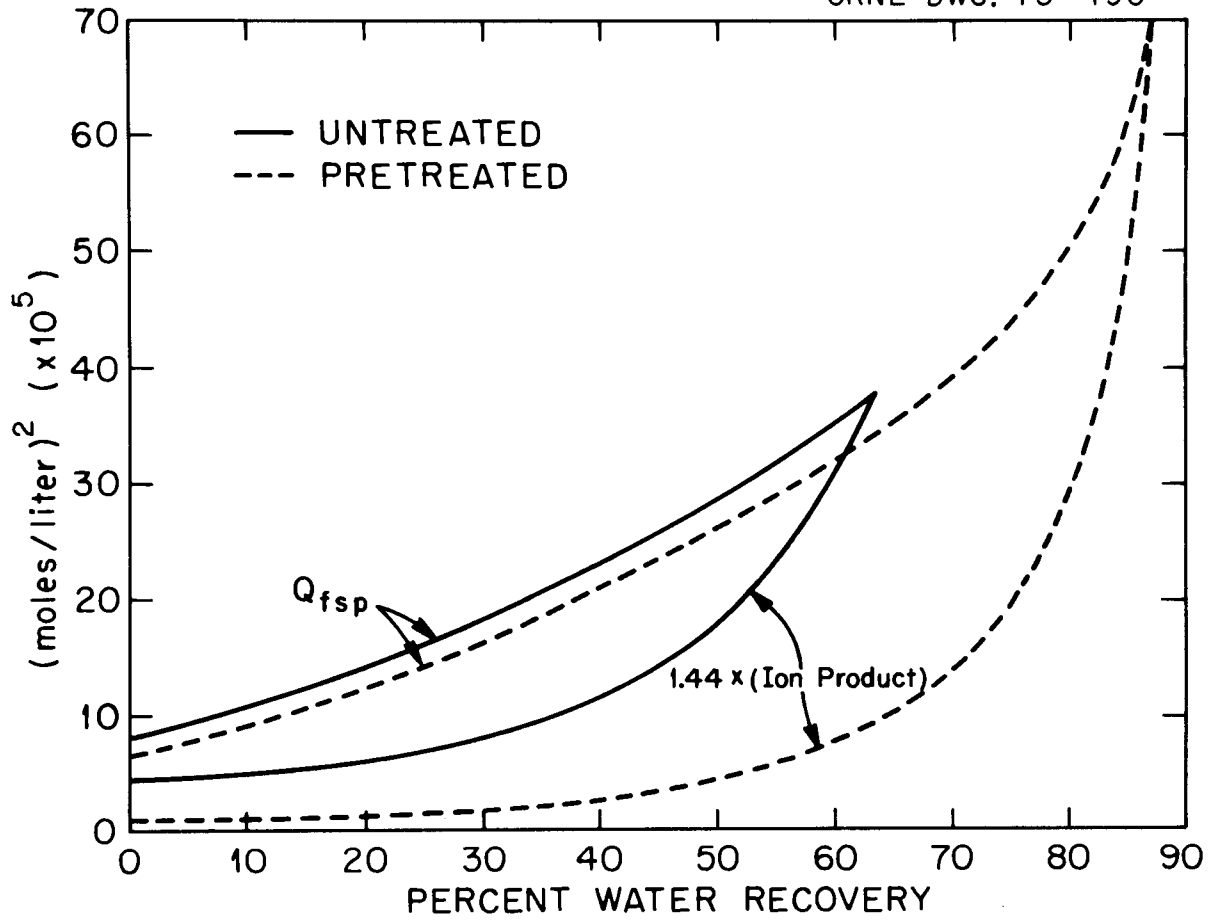
(1). Cross-flow pretreatments: We made up a quantity of simulated Webster water and pretreated it by cross-flow filtration after adding chemicals to precipitate most of the calcium as CaCO<sub>3</sub>. To do this, we added 0.135 g/l of CaO and 0.117 g/l of Na<sub>2</sub>CO<sub>3</sub>. We cross-flow filtered the resulting slurry, which was at pH 8.7, on a fire hose jacket with inside pressurization at 72°F and 20 pounds per square inch. The circulation velocity was below 10 ft/sec. Under these conditions, the flux fell from an initial value of 935 gfd to 618 gfd over ~7 hours. Since filters can be cleaned by a water wash, flux decline is not a serious problem. The original Webster water contained 0.0035 M Ca(II); the final cross-flow product contained 0.00084 M Ca(II), a removal of 76%. The cross-flow product was acidified with H<sub>2</sub>SO<sub>4</sub> to bring it to pH 6, which is

in the range suitable for operation with the commercial modules. This resulted in an increase in  $\text{SO}_4^{=}$  concentration from 0.00882  $\underline{\text{M}}$  in the original feed to 0.00978 in the cross-flow product. The  $\text{Ca(II)} \times (\text{SO}_4^{=})$  concentration product was reduced from an original value of  $3.09 \times 10^{-5}$  to  $0.82 \times 10^{-5}$ . As can be seen from Fig. 18, the reduction in calcium concentration resulted in a change in the percent water recovery possible before saturation from about 64% to about 87%, assuming a 1.2 wall-to-bulk concentration factor. The chemical costs of removal of calcium to this level would be about 6¢/kgal, including the cost of the  $\text{H}_2\text{SO}_4$  needed. If HCl had been used instead of  $\text{H}_2\text{SO}_4$ , the saturation limit would have been raised to about 88%.

In previous tests with cross-flow softening of brackish waters where both calcium and magnesium were removed, we have been able to achieve 97% removal of the calcium, much higher than that achieved in the present case. Perhaps it is necessary to precipitate some  $\text{Mg(OH)}_2$  in order to form a more effective filter cake on the filter surface. The chemical costs, however, for the removal of calcium and all magnesium are much higher. It might be possible to remove both during an initial part of a pretreatment run, and, once the filter cake is formed, to revert to the removal of calcium only. Alternatively, enough base could be added continuously to remove a small fraction of  $\text{Mg(II)}$ .

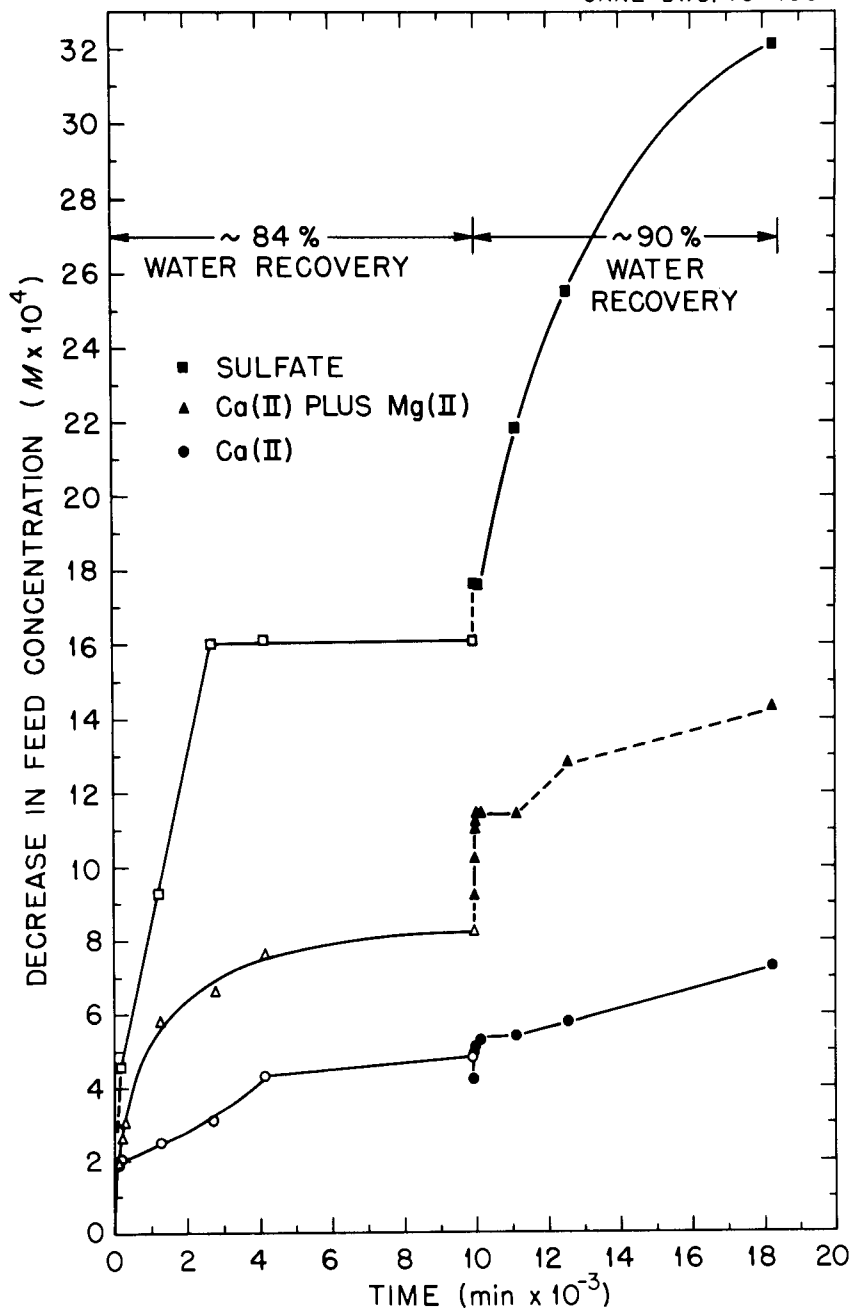
(2). Reverse osmosis of pretreated feed: We took 200 gallons of product from the pretreatment run and treated it with the DuPont and GESCO modules running in parallel. During the first part of the run (8A-11A), which lasted about 166 hours, we ran at an 84% recovery level. During the remainder of the run (8A-11B), lasting about 140 hours, we set the recovery level to the maximum possible with the apparatus, 89 to 92%. The change in concentration of the sulfate, of the  $\text{Ca(II)} + \text{Mg(II)}$ ; and of the  $\text{Ca(II)}$  alone are shown in Fig. 19 as a function of time. During both sections of the run, it is apparent that the decrease in sulfate concentration was much greater than that of calcium. This is hard to explain if one assumes that the fouling was due to  $\text{CaSO}_4$  precipitation, nor have we established a sink for  $\text{SO}_4^{=}$ . The loss of  $\text{Mg(II)}$  may be associated with the formation of the silicate crystals on the down-stream end plate of the DuPont module.

ORNL-DWG. 73-490



EFFECT OF PRETREATMENT ON MAXIMUM WATER RECOVERY WITH WEBSTER WATER

Fig. 18



DECREASE IN ION CONCENTRATIONS IN FEED (Pretreated Webster Water) WITH TIME AT TWO WATER RECOVERY LEVELS. (400 psig, 74-76°F).

Fig. 19

Under normal flow conditions, there should have been no loss in Ca(II) and  $\text{SO}_4^{=}$ , since the brine should not have been saturated in  $\text{CaSO}_4 \cdot 2\text{H}_2\text{O}$  anywhere in the modules. For example, at the beginning of the run, where the ion concentrations were highest, the Ca(II) and  $\text{SO}_4^{=}$  concentrations in the reject streams would have been 0.0056 M and 0.0652 M, respectively, assuming 100% rejection, the worst possible case for fouling, at 85% water recovery. This gives an ion concentration product of about  $36 \times 10^{-5}$ , compared to a  $Q_{\text{fsp}}$  of about  $62 \times 10^{-5}$ . Thus, to get saturation in the module, the wall-to-bulk concentration factor would have to exceed 1.3. The losses which did occur, however, may have resulted from very high concentration polarization arising from the low flow rates in the modules at the high recovery values used in this run.

At the time the recovery rate was changed to 90% in the middle of the run, before any change in feed concentration could occur, the ion concentration product in the reject stream should have been about  $45 \times 10^{-5}$ , again assuming 100% rejection of all components. Under these conditions,  $Q_{\text{fsp}}$  would be about  $90 \times 10^{-5}$ , and supersaturation could occur only if the wall-to-bulk concentration factor exceeded 1.4. Yet, from Fig. 19, there was an obvious and rapid decrease in the concentration of Ca(II), Mg(II), and  $\text{SO}_4^{=}$  when the recovery rates were changed.

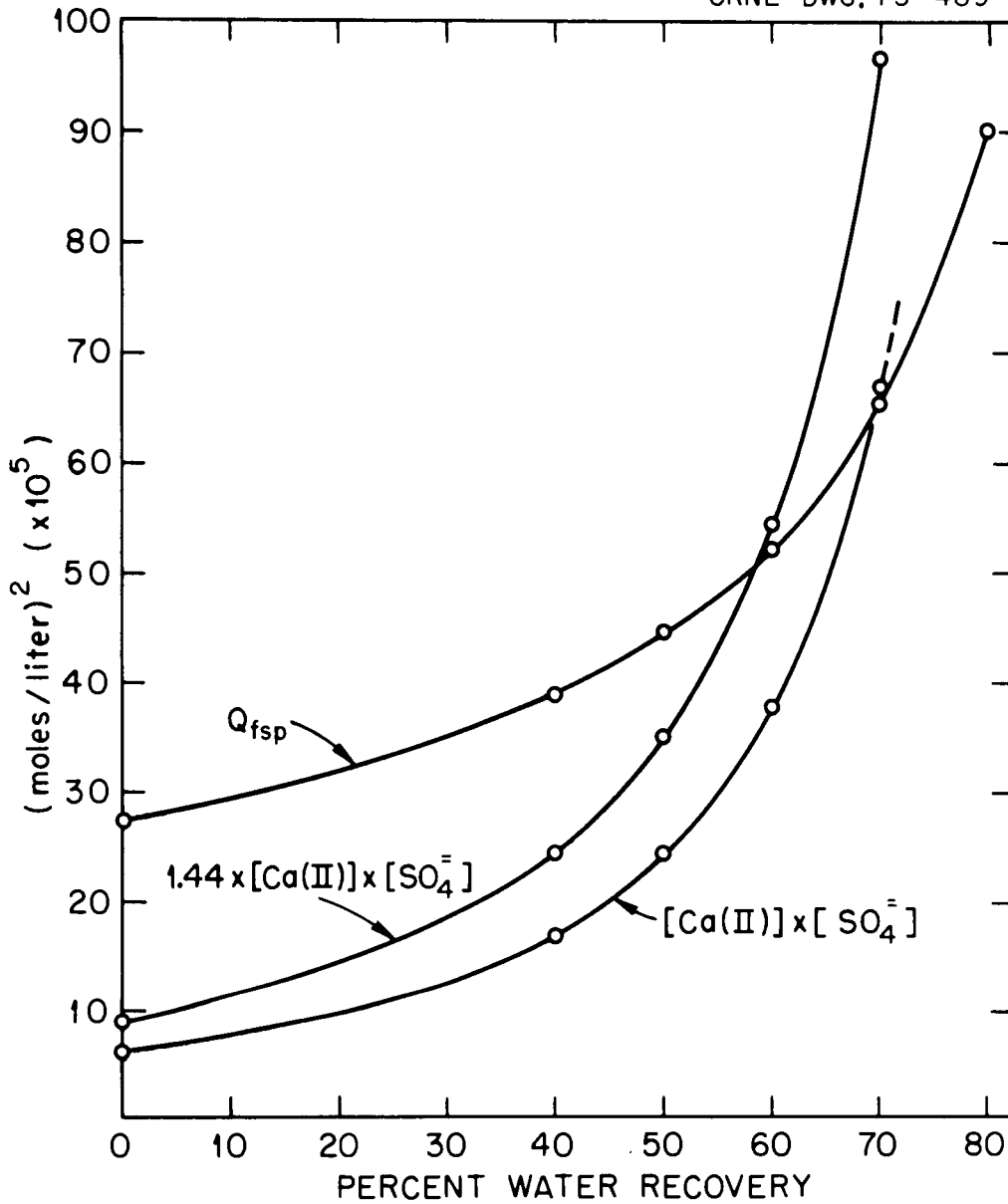
Toward the end of the run, there appeared to be a decrease in the rate at which the ions were being depleted from the feed. We had thought that concentrations at this point might give an indication of the level to which pretreatment must be carried to minimize fouling at high recovery rates. Since we know so little about the hydrodynamics, however, we cannot come to any firm conclusions. For the record, the Ca(II) concentration in the feed at the end of the run was 0.00032 M, a reduction of about 91% from the nominal concentration in Webster water. The final sulfate concentration was about 0.00322 M, down from 0.0083 in the original water. The product  $[\text{Ca(II)}] \times [\text{SO}_4^{=}]$  decreased from about  $1.0 \times 10^{-5}$  at the beginning of the RO run to about  $0.202 \times 10^{-5}$  at the end.

In retrospect, these runs should have been made at much lower single-pass recovery rates, with the feed brine concentrated, by discarding product, to give high effective recovery levels under operation more in accord with manufacturer's specifications.

2. Tests with simulated Wellton-Mohawk canal water: We also investigated the possibility of the fouling of commercial modules by the  $\text{CaSO}_4$  in a brackish water simulating that of the Wellton-Mohawk main conveyance channel. This water should be saturated in  $\text{CaSO}_4$  at about 70% water recovery if no concentration polarization occurred in the modules (Fig. 20). If a wall-to-bulk concentration factor of 1.2 prevailed, saturation should occur at the membrane-feed interface at a water recovery rate of about 58%. The curves of Fig. 20 were calculated assuming a 98% rejection of divalent ions and a 94% rejection of monovalent ions. The  $Q_{\text{fsp}}$  curve was calculated from the data of Yeatts et. al., reference 1.

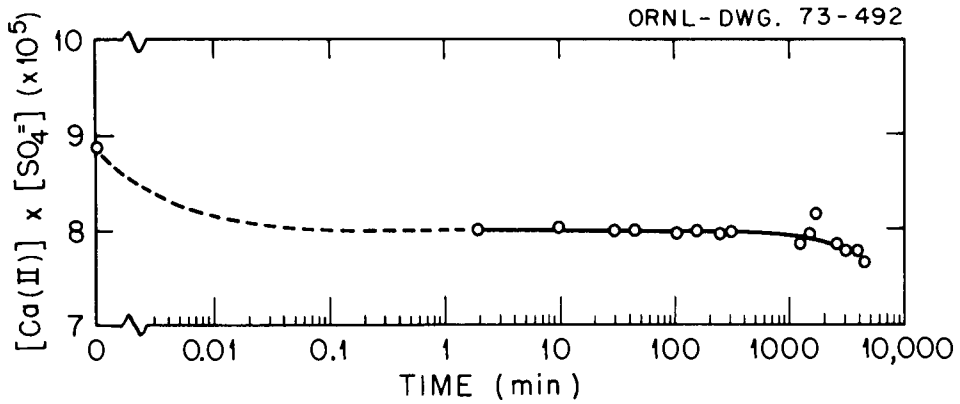
a. First section simulation: We first tested the brine at the nominal concentration provided by Dr. Fred Witmer of OSW setting the modules to 50% water recovery (Run 8A-12). Under these conditions, no saturation should have occurred in the modules, and no depletion of  $\text{Ca(II)}$  or  $\text{SO}_4^{=}$  should have been detected. Figure 21 is a plot of the product of the calcium and sulfate concentrations in the feed as a function of time for a run lasting about three days. Both product and reject were returned to the feed tank, which contained about 200 gallons of brine. There was a drop of about 10% in the product value in the first few minutes, similar to what we had seen with Webster water. The depletion rate slowed, however, over the remainder of the test. Figure 22 shows the changes in concentration of the individual components for the same run. For some unknown reason, the concentration of  $\text{Ca(II)}$  began to decrease at about 1500 minutes, accompanied by a concurrent increase in the sulfate concentration. The reject stream was unsaturated with respect to  $\text{CaSO}_4$ . At the end of the run,  $Q_{\text{fsp}}$  was  $44.5 \times 10^{-5}$  while the product of the concentration of the ions was about  $31.5 \times 10^{-5}$ . If the system was at steady state, this indicates a wall-to-bulk concentration factor of  $\sim 1.19$ .

b. Second section simulation: We next simulated a second section module by doubling the concentration of the feed, again operating the modules at about 50% recovery. This is equivalent to an overall recovery level of about 75%. We made three runs under these conditions, 8A-13A through 13C, the first with zero concentration of polymetaphosphate (Calgon), the second with 5 ppm, and the third with 20 ppm. The changes with time in the feed calcium and sulfate concentration for the three runs are shown in



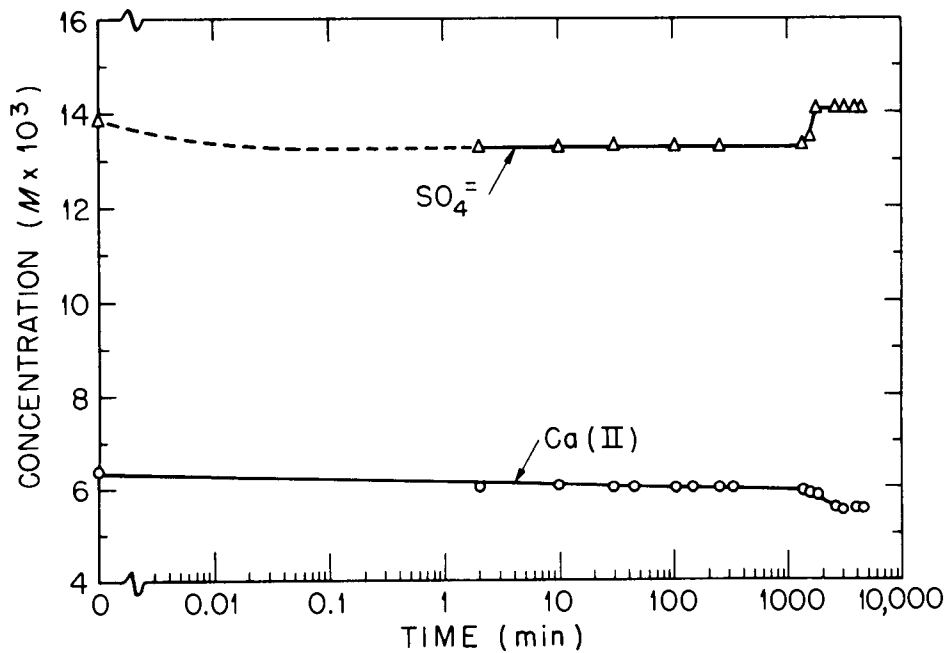
$\text{CaSO}_4$  SOLUBILITY PRODUCT CURVES FOR WELLTON-MOHAWK WATER, ASSUMING 98% REJECTION OF DIVALENT IONS AND 94% REJECTION OF MONOVALENT IONS.  $Q_{fsp}$  FROM REF. 1.

Fig. 20



[Ca(II)] x [SO<sub>4</sub><sup>2-</sup>] VERSUS TIME. WELLTON-MOHAWK FEED TREATED BY DuPONT AND GESCO MODULES IN PARALLEL. (400 psig, 76°F, 50% Recovery).

Fig. 21



CALCIUM AND SULFATE CONCENTRATION IN FEED VERSUS TIME. WELLTON-MOHAWK FEED TREATED BY DuPONT AND GESCO MODULES IN PARALLEL. (400 psig, 76°F, 50% Recovery).

Fig. 22

Fig. 23. With 5 ppm Calgon present, the rates of decrease in concentration were apparently less than when no phosphate was present. At 20 ppm Calgon, the calcium concentration decreased very slowly, but the concentration of sulfate behaved erratically. The products  $[Ca] \times [SO_4]$  vs. time are given in Fig. 24.

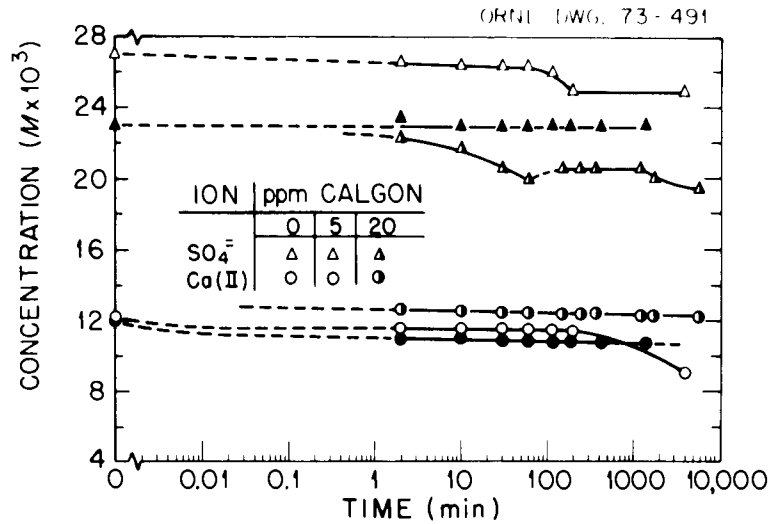
At the end of the three runs, analyses of the feed, product, and reject streams indicated that there was very little, if any, single-pass depletion in the calcium and sulfate; i.e., little precipitation was taking place in the module. However, the analyses showed that the reject stream was supersaturated with respect to  $CaSO_4$  in each case (Table VIII). Evidently the reject brine is not in steady-state equilibrium with crystals on the membrane surfaces. This behavior is very similar to that reported earlier for Webster water at higher recovery levels (see Table IV).

Rejections were quite constant throughout a run, but there was a slight decrease in flux during each run. The fluxes were lower than fluxes obtained with typical brackish waters when we first started using the modules, see Run 8A-2, Appendix A.

### 3. Tests with simulated Foss Reservoir water:

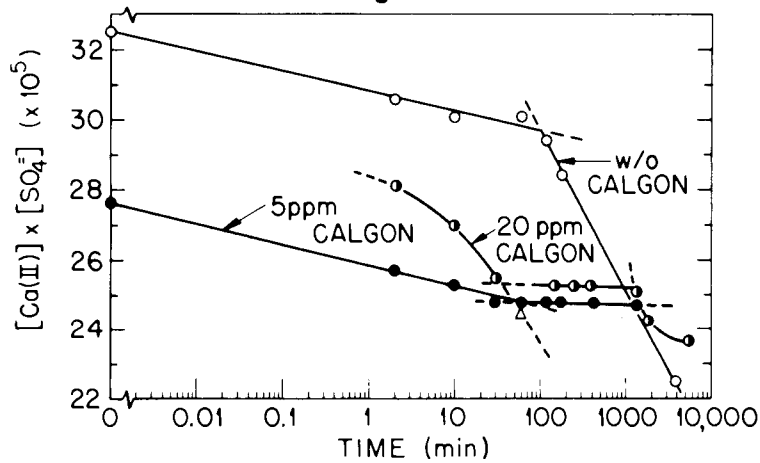
The third water we tested was one with a composition typical of the Foss Reservoir in Oklahoma.

This is a high-sulfate water (see Table I) that would come very close to  $CaSO_4 \cdot 2H_2O$  saturation in the modules at 50% recovery if there were a 1.2 wall-to-bulk concentration factor and a 95% average rejection of ions. We made three runs (8A-15A through 15C) at 50% recovery, two without added polymetaphosphate (Calgon), and one with 5 ppm Calgon added. For the first run, the top graph of Fig. 25 shows the decrease with time of the  $Ca(II)$  and  $SO_4^{=}$  concentrations in the feed, and of their product. There appears to be a slight decrease in the concentrations of the ions in the feed solution, and an analysis of the reject streams shows that the brine could be saturated at the membrane surface if a 1.2 wall-to-bulk concentration prevails. For example, with the GESCO module, the product of the calcium and sulfate ion concentrations in the reject was  $20.8 \times 10^{-5}$  at the time of the final point of the run.  $Q_{fsp}$  at the same point was  $27.5 \times 10^{-5}$ , assuming that the solubility of  $CaSO_4 \cdot 2H_2O$  in Foss Reservoir water is the



CALCIUM AND SULFATE CONCENTRATION IN FEED AS A FUNCTION OF TIME AND CALGON CONCENTRATION IN RO TREATMENT OF WELLTON-MOHAWK WATER (2X Concentration) BY DuPONT AND GESCO MODULES OPERATING IN PARALLEL AT 50% WATER RECOVERY LEVEL. (400 psig, 76°F).

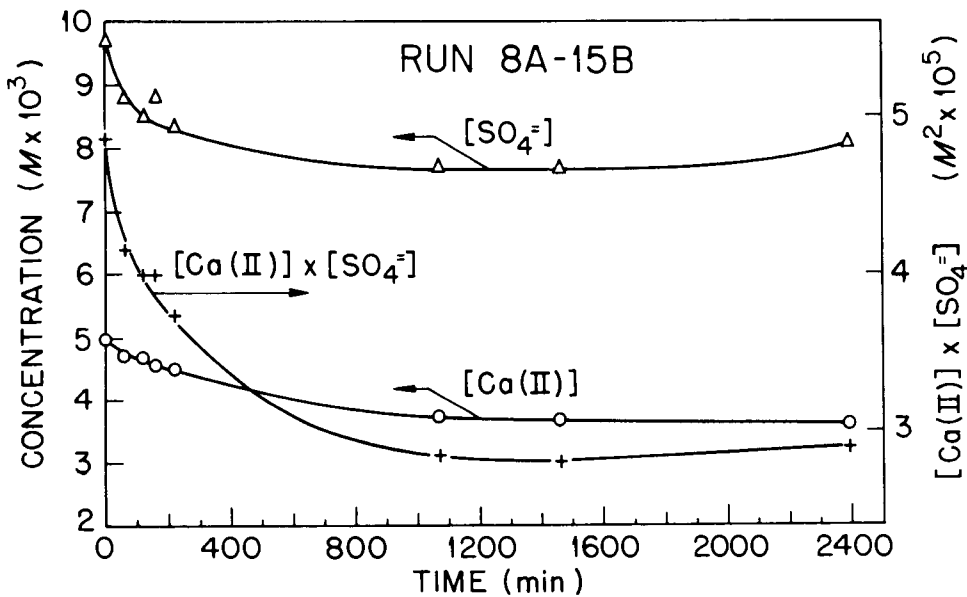
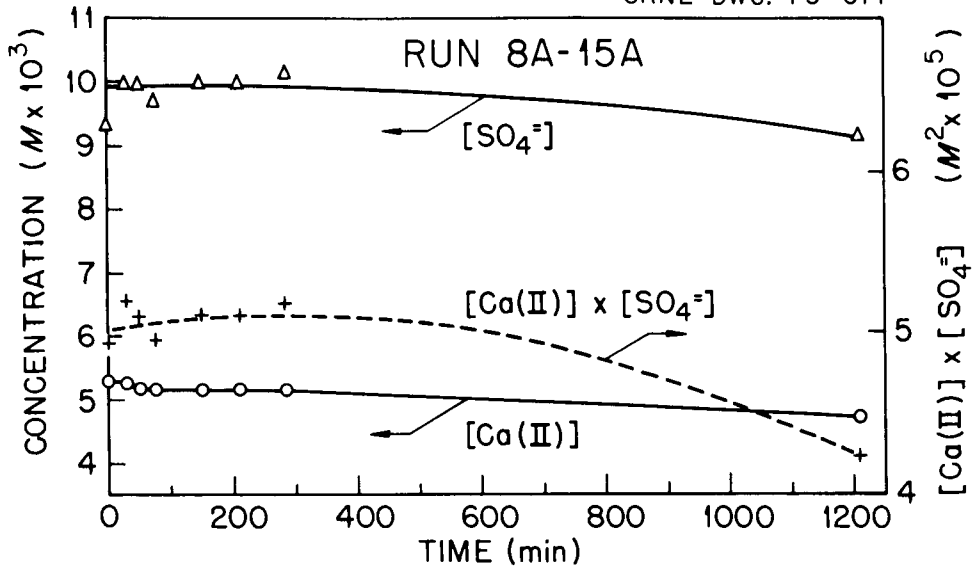
Fig. 23



$[Ca(II)] \times [SO_4^{2-}]$  IN FEED VERSUS TIME AND CALGON CONCENTRATION FOR WELLTON-MOHAWK WATER AT 2X CONCENTRATION. DuPONT AND GESCO MODULES OPERATED IN PARALLEL AT 50% WATER RECOVERY LEVEL. (400 psig, 76°F).

Fig. 24

ORNL-DWG. 73-671



TIME DEPENDENCE OF ION CONCENTRATIONS AND ION CONCENTRATION PRODUCT FOR A SIMULATED FOSS RESERVOIR WATER TREATED BY DUPONT AND GESCO MODULES OPERATED IN PARALLEL AT 50% WATER RECOVERY. (400 psig, 73-76°F).

Fig. 25

TABLE VIII  
 COMPARISON OF  $\text{CaSO}_4$  ION PRODUCTS WITH  $Q_{\text{fsp}}$  FOR THE  
 FINAL POINTS OF EACH OF THE THREE RUNS OF FIGS. 23 AND 24.  
 (400 psig; 70°C)

Time <sup>a</sup> (min)	Calgon (ppm)	Module	[Ca] x [SO <sub>4</sub> ] (x 10 <sup>5</sup> )	$Q_{\text{fsp}}$ <sup>b</sup> (x 10 <sup>5</sup> )	$\left(\frac{Q_{\text{fsp}}}{[\text{Ca}] \times [\text{SO}_4]}\right)^{1/2}$
3937	0	DuPont	112	90	0.896
		GESCO	103	76	0.859
1380	5	DuPont	94	70	0.863
		GESCO	109	73	0.818
1680	20	DuPont	95	68	0.846
		GESCO	96	68	0.842

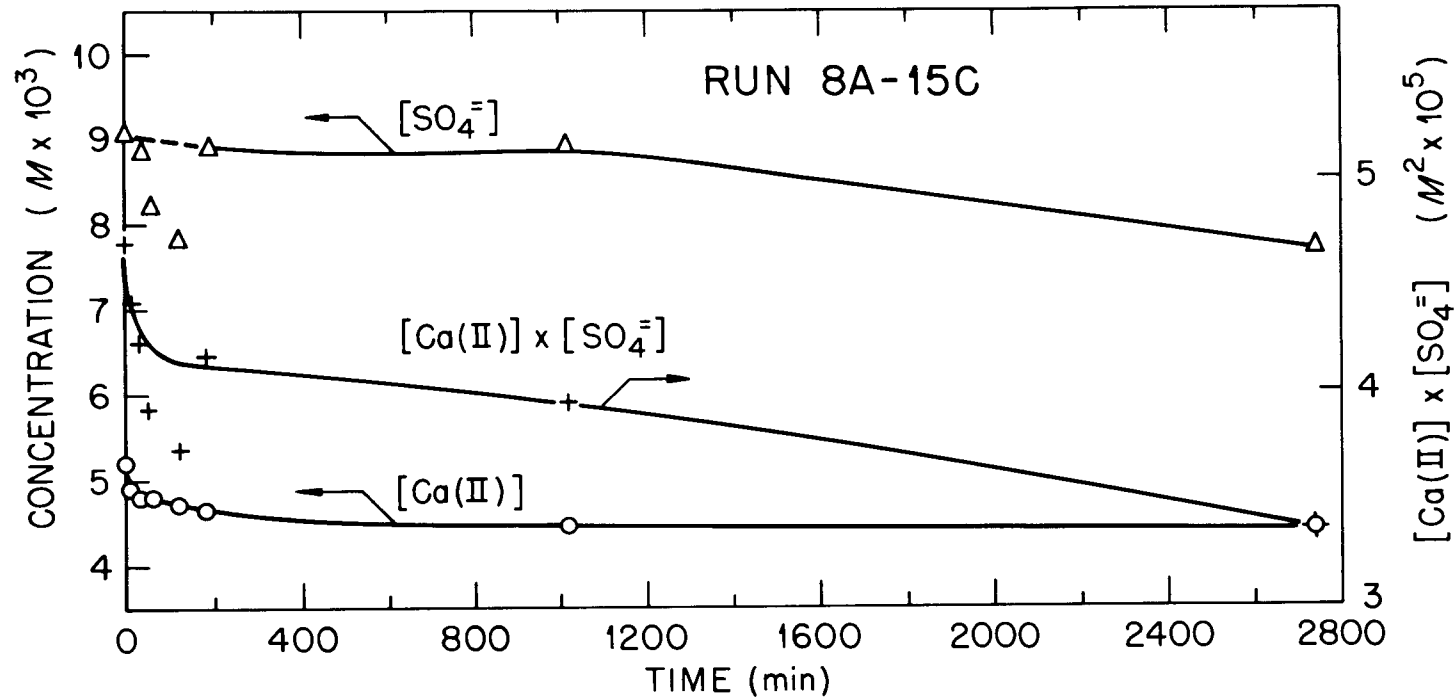
a. Time from beginning of each run.

b. Based on solubility data of reference 1, this report.

same as it would be in a NaCl solution of the same ionic strength. If both Ca(II) and  $\text{SO}_4^{=}$  were concentrated by 1.2, the ion product at the membrane surface would be about  $30 \times 10^{-5}$ , which exceeds  $Q_{\text{fsp}}$  by about 9%. Results for the DuPont module were similar.

The bottom part of Fig. 25 shows the results for the next run, again without added Calgon. Enough  $\text{CaSO}_4$  was added to the feed to bring it back to the nominal concentration before the run was started. In run 8A-15A, the modules had been rinsed for more than a week with distilled water; in run B they had been rinsed for about two days. However, the decrease in calcium and sulfate concentrations is much more pronounced in the second run than in the first, even though the starting concentrations and the recovery levels were almost the same. Concentrations after 1200 minutes of operation were appreciably lower in the second run. We did a complete chemical analysis of the reject, product, and feed taken at about 1460 minutes. Here, the ion concentration product appeared to be more than 30% below the solubility product limit. The reason for the differences in the two runs is not clear to us.

Results for the third run with Foss Reservoir water, to which 5 ppm Calgon had been added, are shown in Fig. 26 (run 8A-15C). The erratic results with the  $\text{SO}_4^{=}$  values prompted us to check on the reproducibility of



ION CONCENTRATIONS AND ION CONCENTRATION PRODUCT VERSUS TIME. SIMULATED FOSS RESERVOIR WATER WITH 5ppm CALGON ADDED. (400 psig, 73-75°F, 50% Water Recovery).

Fig. 26

TABLE IX  
REPRODUCIBILITY OF SULFATE ANALYSES IN SAMPLES OF  
FOSS RESERVOIR WATER CONTAINING 5 ppm CALGON.  
ANALYSES BY THE HACH TURBIDIMETRIC METHOD

<u>Sample No.</u>	<u>Analysis 1</u>	<u>Analysis 2</u>	<u>Analysis 3</u>	<u>Average</u>
F-0	0.00905	0.00905	0.00937	0.00916
F-1	0.00905	0.0090	0.00937	0.00914
F-2	0.00905	0.00889	0.00877	0.00890
F-3	0.00884	0.00898	0.00877	0.00886
F-4	0.00819	0.00791	0.00905	0.00838
F-5	0.00780	0.00791	0.00921	0.00831
F-6	0.00889	0.00819	0.00861	0.00856
F-7	0.00889	0.00819	0.00861	0.00856

our sulfate analyses, which were done by a turbidimetric method using a Hach\* Kit. The results of three sets of analyses done on the same samples are listed in Table IX. In some samples there is as much as a 6% deviation from the average value, and the difference between analyses of the same sample may run as high as 25%. Obviously, too much faith should not be placed in the values given for the sulfate concentrations. It might be that the Calgon added to the feed solution interferes with the analyses for sulfate.

In Fig. 26, the curve which represents the product of the ion concentrations reflects the erratic results for the sulfate ion. The curves for the decrease in concentration of the Ca(II) with time are quite similar for all three curves, and may be a more accurate guide to performance than those curves involving the sulfate. If so, there appears to be little effect from the addition of 5 ppm Calgon to the feed solution.

#### 4. Discussion and recommendations:

It became apparent very early in this program that some of the stated objectives were going to be very difficult to attain. A single commercial

---

\*Hach Chemical Company, Ames, Iowa.

module of a given type does not lend itself readily to repeated experiments under closely controlled conditions. This is true mainly because, to study fouling, one must cause it to happen, and consequently each experiment, especially those that lead to measurable changes in the properties of the modules, effected changes which proved to be, to some extent, irreversible in the modules. Thus, each subsequent experiment had different starting conditions, and inter-comparisons became unreliable.

We found the DuPont hollow-fiber module to be much more susceptible to irreversible change than was the GESCO spiral wound module. This in no way casts reflections on the relative merits of the modules in the field, where they would presumably be operated under vendor-specified conditions. Our chief deviations from specifications, in pursuit of our objectives, were that we sometimes operated at single-pass recovery levels much above those recommended. This, in turn, meant that flow rates in the modules were often below the minimums specified, and concentration polarization was probably excessive.

A second major source of difficulty lay in the need to recycle feed. Even under the lowest flow conditions we used (~90% single-pass recovery), about 2.4 gpm were required by each module, or about 280 gallons each hour when the modules were being operated in parallel. This was far above our capacity to replenish the synthesized water, and recycle was the only recourse. Under conditions in which no fouling occurred, i.e., in which no salt was retained in the modules, recycle would be feasible if both the product and the reject streams were returned to the feed tank. But then, of course, no changes would occur in the modules, and no information on fouling would result.

In the field, polymetaphosphate is continuously added to the feed brine as part of the pretreatment. In our experiments, it was added to the feed at the beginning of the run. Since the runs covered several hours, and sometimes days, we have no assurance that the polyphosphates were not degraded by hydrolysis or by mechanical abrasion in the pumping system.

In the experiments with modules, we began with a rather small (~50 gallon) feed tank, but soon changed to a 200 gallon tank. Even with

the larger volume, salts were often depleted so rapidly we could not complete analyses and replenish the feed water in any smooth or continuous way. We consequently resorted to monitoring the rate of depletion under given initial conditions as a possible indicator of relative fouling potential.

In practice, the attainment of "given initial conditions" was somewhat elusive. Not only did the modules change, as indicated above and as documented by the accumulative changes apparent from Appendix A, but the compositions of starting feeds may not have been always duplicated. For example, in our experiments with Webster water, we began many of the runs by adding all ingredients except the bicarbonate and the silicate to 200 gallons of distilled water, and stirring the mixture overnight, in order to get the  $\text{CaSO}_4$  completely into solution. In these runs, we did not add the bicarbonate until shortly before the run was to begin so that it would not be lost to the air as  $\text{CO}_2$ , and we withheld the silicate until last because it appeared that the solution was more stable toward precipitation without the silicate. After a sample of the feed was taken for analysis, the run was started. Sometimes, in a following run, we did not begin with a fresh solution, but simply added enough  $\text{CaSO}_4$  to replace that lost in the preceding run. This type of run is characterized as "reconstituted" in Appendix A. However, the rate of depletion of  $\text{Ca(II)}$  and of  $\text{SO}_4^{=}$  in "reconstituted" runs was invariably lower, especially in the early parts of the runs, than in runs with fresh solutions (see Table VII, for example). We had justified reconstitution, which saved considerable time over making up fresh solutions each experiment, by assuming that, under the conditions of operation, only the  $\text{CaSO}_4$  was being depleted. Our analysis of the crystallites found in a valve in the reject line from the DuPont module, which showed both  $\text{Mg(II)}$  and silicate, and our subsequent analyses of deposits in the DuPont module, all of which have been mentioned earlier, demonstrated that this assumption was wrong.

At the beginning of a run with fresh feed, there was always a slight turbidity present; at the beginning of a run with reconstituted feed, this turbidity was absent. It may be that much of the early losses in the measured constituents in the fresh-feed runs resulted from the removal of this turbidity by a mechanical filtering action in the modules. In

general, depletion of silicates and bicarbonates was not determined, but run 8A-27, Fig. 15, demonstrated that the silica was not primarily responsible for the Ca(II) depletion, i.e., the depletion was rapid in the absence of silicate.

We analysed the initial feed solutions for runs 8A-24A and B and 8A-26 for silicate and bicarbonate. The silicate concentration was nominal or greater in all three runs, but the bicarbonate was appreciably lower in the starting feed of the reconstituted run, 8A-24B (see Fig. 15 and Table V). It thus might be possible that the difference in the early depletion rates between fresh and reconstituted feeds result from the removal of crystallites of  $\text{CaCO}_3$ , formed in the fresh feeds under locally supersaturated conditions when the bicarbonate is added to the feed tank. These crystallites, if trapped in the modules, must subsequently dissolve, perhaps during the periodic water rinses we carried out between runs, since the solid deposits found in the fibers of the DuPont module appeared to contain very little inorganic carbon.

The work performed under this contract provides considerable information about the reverse osmosis treatment of brackish waters, even though the conclusions must be tempered by the uncertainties generated by the shortcomings noted above. In the early experiments with cast films in transparent test sections, we demonstrated that visible crystals can form at the feed-membrane interface at bulk concentrations below saturation, under conditions of high concentration polarization. Such crystal formation resulted in lower fluxes and lower rejections. We demonstrated that the average time to crystal formation increased as the concentration of polymetaphosphate increased in the feed brine, but that, once formed, the crystals were not readily removed by the addition of polymetaphosphate to the feed.

It appeared that, for reasons not clear, pH was at least as important as the presence of polyphosphate in preventing crystal growth, that crystal formation was much more rapid at pH 5.5 than at 8.5, and that if precipitation of  $\text{CaSO}_4 \cdot 2\text{H}_2\text{O}$  scaling were the only consideration, the best conditions for film membranes were the higher pH with polymetaphosphate present. The importance of adequate flow velocity to minimize precipitation caused by excessive concentration polarization was, of course, amply demonstrated.

In our work with brackish waters using commercial modules, we investigated changes in several parameters as possible indicators of incipient fouling. Almost all of them proved to be insensitive as short term indicators. Although we experienced abrupt changes in fluxes when crystals formed on the cast films in our transparent jacket experiments, we found none in our tests with modules. As feed concentration increased, fluxes did decrease, but these decreases could usually be explained as resulting from the increased osmotic pressure of the feeds at the high concentrations. Incipient precipitation should occur first on membrane surfaces near the reject ends of the modules. This results from two effects: 1) a concentration gradient through the modules caused by the loss of product water from the brine, and 2) increased concentration polarization resulting from decreased flow velocities. This increased concentration polarization would be most pronounced in the DuPont module, for the flow there is radial and the flow rate decreases as the square of the distance from the axis of the module. In each module, precipitation would occur initially on only a small fraction of the total membrane area, and the effect on total flux would be gradual and thus perceptible only over an appreciable period of time.

We attempted to measure the pressure drop across the module as an indicator of fouling, but this, too, proved to be unfruitful. Short-term fluctuations in the pressure drop were generally an appreciable fraction of the total, and were generally at least as large as any trends we were able to find. Rejections of the various components of the feed, although decreasing somewhat over the entire period of this study, were quite constant, for a given concentration, over the term of a single experiment.

During an early experiment, we monitored the Ca(II) concentration in the recirculating feed and found that, although Ca(II) was continuously depleted from the feed during most experiments, the rate at which it was depleted increased appreciably when conditions were such that  $\text{CaSO}_4 \cdot 2\text{H}_2\text{O}$  precipitation should have occurred. We suggest that the most sensitive and reliable method to determine fouling in commercial modules is to determine the material balance between feed on the one hand and reject and product streams on the other, for all components in the feed. For

limited feed volumes under recirculating conditions, this procedure also enables one to get a rough idea of the effective wall-to-bulk concentration factor under different operating conditions. If the feed concentration and the single-pass water recovery rates are such that precipitation occurs in the module; steady state conditions should prevail when the precipitating species has been depleted to the point that concentration polarization no longer leads to supersaturation. At this point, the reject stream should be unsaturated, and the ratio of the formal solubility product,  $Q_{fsp}$ , to the ion concentration product of the precipitating species should be the square of the wall-to-bulk concentration factor. If the reject stream is supersaturated, as sometimes happened (see Table IV), the factor computed in this way will be less than one, and steady state conditions will not exist. Supersaturation occurred most often at very high single-pass recovery levels. Conversely, if precipitation has occurred in the module and the reject stream at steady state conditions is not saturated, then the wall-to-bulk concentration factor will indicate the extent of the concentration polarization. Of course, if formation of precipitates other than  $\text{CaSO}_4$  is depleting these ions, the factor is not related in any simple way to concentration polarization. This apparently happened with the DuPont module in the later stages of the program (see Table VI).

When we resorted to multiple concentrates (2X, 2.5X, etc.) as initial feeds, the problems of arriving at a stable synthetic water increased, and the initial effects, such as increased turbidity, were exaggerated. However, the results of such experiments were much more pertinent to field problems, since the modules, in these cases, were operated as they would have been in the field.

The work of Yeatts, Lantz, and Marshall<sup>1</sup>, concurrent with that being reported here, has demonstrated that the presence of small amounts of poly-metaphosphate (PMP) leads to a small but measurable increase in the equilibrium solubility of  $\text{CaSO}_4 \cdot 2\text{H}_2\text{O}$  in simulated brackish waters and their concentrates. Equilibrium values may or may not be pertinent, however, to the study of the effect of PMP in the dynamic systems used in the field. The effect of PMP on the rate of precipitation from a given feed volume under operational conditions may be the controlling factor in the amelioration of fouling. This is suggested by our studies of crystal

formation on membranes in transparent test sections, see Table II, but it is not consistently apparent from our work on the modules.

PMP did not appear to have appreciable effect on the rejection of various components by the membranes in the modules, except, perhaps, for  $\text{Cl}^-$ , where rejections appeared to be somewhat better in its presence.

Both Wellton-Mohawk canal water and Foss Reservoir water are more difficult to treat to high recovery levels than is Webster water, because of the higher concentrations of  $\text{CaSO}_4$ . Since both are inland waters, it seems imperative that they be pretreated to remove a major part of the  $\text{Ca(II)}$ . The results of our experiments with pretreated Webster water (see Section II.C.10) were not compelling evidence for the truth of this statement, but they were run with a badly-fouled module under unreasonably high single-pass recovery rates. Further experiments here seem desirable: a properly designed pretreatment plant would not only remove  $\text{Ca(II)}$  to negligible levels, but might also remove  $\text{Fe(III)}$  and organic particulates, both fouling constituents of natural waters. The removal of  $\text{Fe(III)}$  would obviate the necessity for acidification, and the advantages we noted for higher pH values (Section II.B.3) could be realized. Cross-flow filtration has been demonstrated to be an effective pretreatment for Roswell water<sup>6</sup> prior to its hyperfiltration by dynamic membranes, and investigation of its applicability to pretreatment prior to RO desalination by commercial plants seems warranted.

### III. OSMOTIC PRESSURES OF SALINE WATERS

The second law of thermodynamics specifies that the pressure effective in causing water to flow through a solute-filtering membrane cannot be greater than the difference in hydrostatic pressure on the two sides of the membrane less the difference in osmotic pressure,  $\Pi$ , of the solutions at the membrane-solution interfaces. Knowledge of osmotic pressures are thus requisite for evaluation of membrane performance.

Although the magnitude of the osmotic pressure for solutions is primarily determined by the concentration of particles, reasonably accurate estimates at concentrations typical of most desalination feeds requires also that non-ideality of the solutions be taken into account. The most convenient representation of non-ideality for present purposes is the osmotic coefficient,  $\phi$ , defined by the equation

$$\phi = - \frac{N \ln a_I}{\sum_I v_{I-I} m_I} \quad (1)$$

where  $N$  is the number of moles of solvent in a kilogram of solvent (55.51 for water);  $v_{I-I}$  is the number of moles of ions per mole of component I (e.g. 2 for NaCl or MgSO<sub>4</sub>, or 3 for MgCl<sub>2</sub> or Na<sub>2</sub>SO<sub>4</sub>);  $m_I$  is the concentration of solute component I in moles per kilogram of solvent; and  $a_I$  is the activity of the solvent, the standard state being defined so that the activity of the pure solvent is one. The osmotic pressure,  $\Pi$ , of aqueous solutions may be obtained from the equation

$$\Pi = \left( \frac{RT}{\bar{V}_I} \right) \ln a_I = \left( \frac{RT}{\bar{V}_I} \right) \frac{\sum_I v_{I-I} m_I}{55.51} \phi \quad (2)$$

where  $R$  is the gas constant;  $T$  is the absolute temperature; and  $\bar{V}_I$ , the partial molal volume of water. Values of  $\left( \frac{RT}{55.51 \bar{V}_I} \right)$  in units selected to give  $\Pi$  in atmospheres and in psi when inserted in Equation 2 are listed in Table X. In these tables, the partial molal volume of water used is its one-atmosphere value in pure water, but, since variation with pressure and solute concentration is small, the approximation should not be of any moment for present purposes. For aqueous solutes at 25°C, osmotic pressures

TABLE X

$\frac{RT}{(55.51 \bar{V}_I)}$  FOR A NUMBER OF TEMPERATURES

Temperature			$\frac{RT}{55.51 \bar{V}_I}$	
(°C)	(°F)	T(°K)	Atmospheres	psi
0	32	273	22.4	329.3
10	50	283	23.2	341.2
20	68	293	24.0	352.9
25	77	298	24.4	358.5
30	86	303	24.8	364.0
50	122	323	26.2	384.9
75	167	348	27.9	409.3
100	212	373	29.3	431.3
125	257	398	30.7	450.9
150	302	423	31.9	468.1
175	347	448	32.8	482.1
200	392	473	33.5	492.2

(atmospheres) are to a good approximation

$$\Pi \approx 24.4 \phi \sum_I v_{I-I} m_I \quad (3)$$

The estimation of osmotic pressures of a water containing solutes thus involves knowledge of  $\phi$ . At first glance, with the infinity of compositions possible, this appears difficult. However, the ions present in major amounts in most natural waters of interest in desalination are sodium, chloride, magnesium, sulfate, and calcium. For practical purposes, it will usually be sufficient to represent the solute in terms of the first four of these, and to add the molalities of other ions to those of the four having the same valence--Ca(II) to Mg(II), potassium to sodium, bromide to chloride, silicate to sulfate, etc.

There are empirical equations in the literature fitting experimental measurements of osmotic coefficients of solutions containing these four ions.<sup>7</sup> The equations are not convenient for computation, and we have computed tables of osmotic coefficients for the range of compositions of primary interest here (Table XI). These tables could as easily have presented osmotic pressures. The reason for not doing so are twofold. Osmotic coefficients vary much less rapidly with composition than osmotic pressure, and interpolation is therefore much easier for  $\phi$ . Probably for most purposes, it will be sufficient to use the concentration close to that of the water in question, without interpolation. Second, the values in the table are for 25°C. However,  $\phi$  varies much less with temperature than  $\Pi$ , and practically useful estimates can be made as high as the boiling point with ambient temperature values of  $\phi$ .

Since it is concentration in numbers of particles which counts in computation of  $\Pi$ , concentrations on the molality scale, moles/kilogram of solvent, are much more appropriate than in terms of weight of solute (mg/liter, ppm, for example). With brackish waters, at least, molarity, moles per liter, will ordinarily be an acceptable approximation to molality. In Fig. 27, computed from International Critical Tables data, it can be seen that even for solutions in the ppm level of seawater the difference between molarity and molality is less than 2%.

ORNL-DWG. 73-4261

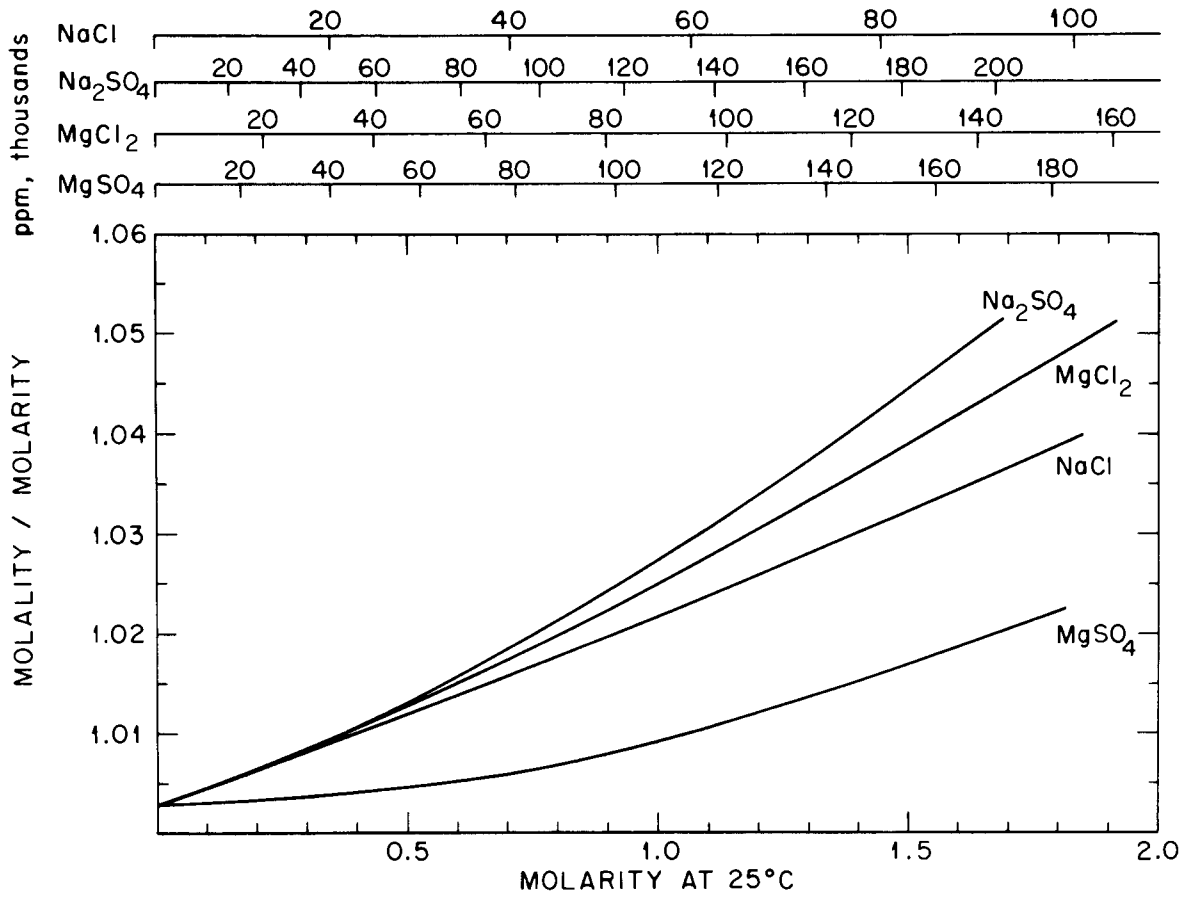


Fig. 27. RELATIONSHIP BETWEEN MOLARITY (moles/liter) AND MOLALITY (moles/kg water) FOR SINGLE-SALT SOLUTIONS, COMPOSED OF IONS TYPICALLY FOUND IN NATURAL WATERS

The values for  $\phi$  in Table XI were evaluated in terms of equivalent concentrations,  $\underline{m}'_i$ , of the four ions:  $\underline{m}'_{Na} = \underline{m}_{Na}$ ;  $\underline{m}'_{Cl} = \underline{m}_{Cl}$ ;  $\underline{m}'_{Mg} = 2\underline{m}_{Mg}$ ;  $\underline{m}'_{SO_4} = 2\underline{m}_{SO_4}$ . The total equivalent molality, or, as it is called in Table XI, the total equivalent concentration, of salt components is half the sum of the equivalent concentrations of ions present. Table XI provides  $\phi$  at intervals of total equivalent molality ranging from 0.0025 to 2.0. Each table, for a given total equivalent concentration, is entered with the equivalent fractions of cations and of anions.

The procedure for calculating osmotic pressures, given feed concentrations, is as follows:

I. If the concentrations are in parts per million (ppm) or milligrams per liter (mg/l), for each ionic species,  $i$ , convert the measured concentration to the equivalent concentration,  $\underline{m}'_i$ . For concentrations in ppm, use:

$$\underline{m}'_i = \frac{(\text{ppm})_i Z_i}{(\text{IW}) \left(1000 - \frac{\text{TDS}}{1000}\right)}, \quad (4a)$$

$$\approx \frac{(\text{ppm})_i Z_i}{1000 (\text{IW})}; \quad (4b)$$

and for concentrations in mg/l, use:

$$\underline{m}'_i = \frac{(\text{mg/l})_i Z_i}{(\text{IW}) \left(1000\rho - \frac{\text{TDS}}{1000}\right)}, \quad (5a)$$

$$\approx \frac{(\text{mg/l})_i Z_i}{1000 (\text{IW})}; \quad (5b)$$

where  $Z_i$  is 1 for monovalent ions, 2 for divalent ions, etc.; IW is the ionic weight in grams; TDS is the concentration of total dissolved solids, in ppm for Eq. (4) and mg/l in Eq. (5); and  $\rho$  is the solution density.

Equations (4a) and (5a) are exact, and should be used for concentrated feeds such as seawater. Equations (4b) and (5b) are approximate, but should be accurate enough for use with most dilute brines or brackish waters. For brines of less than 10,000 ppm TDS, values of  $\underline{m}'_i$  sufficiently accurate for most field work may be obtained from Fig. 28, which is a plot of  $\underline{m}'_i$  vs. ppm, and hence very closely  $\underline{m}'_i$  vs. mg/l, for a number of ions

ORNL-DWG. 73-4262

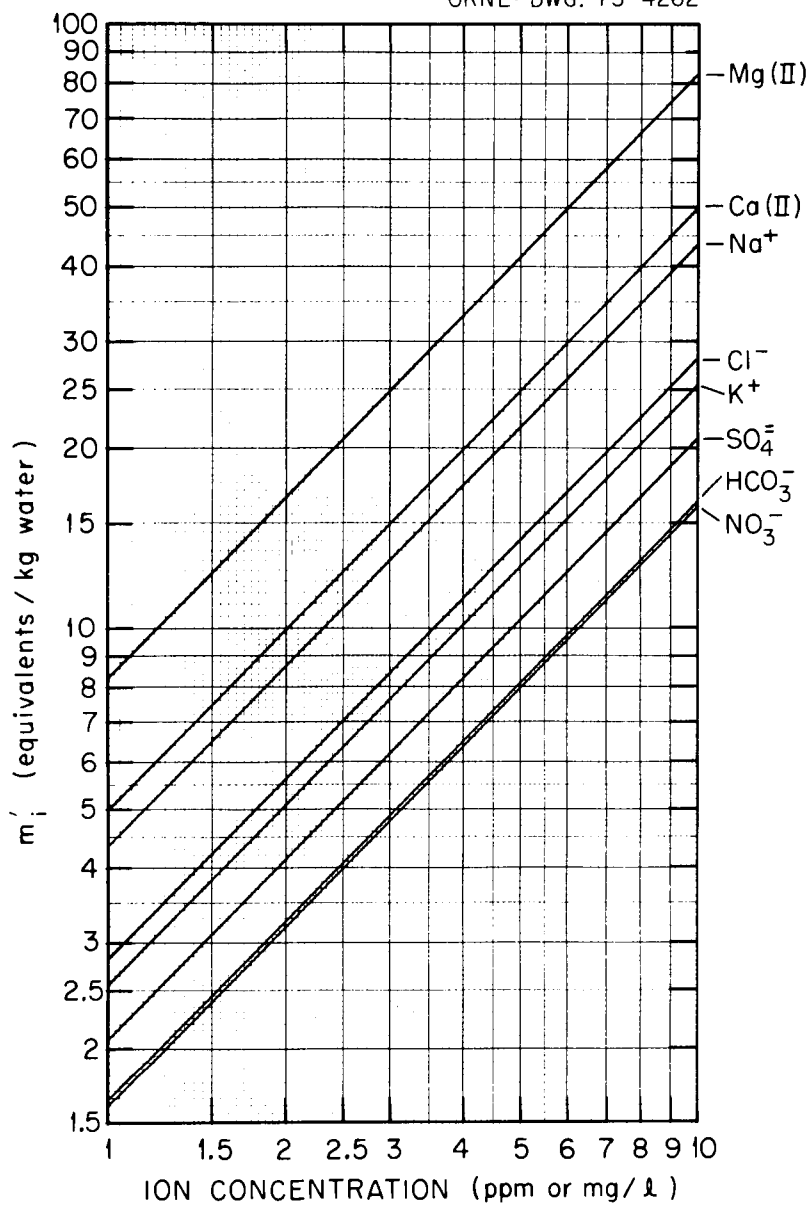


Fig. 28.  $m'_i$  vs ION CONCENTRATION.

(TDS = 3000 ppm,  $\rho = 1.0$ )

If Ion Concentration Is :	Multiply Ordinate By :
1 - 10	$10^{-5}$
10 - 100	$10^{-4}$
100 - 1000	$10^{-3}$
1000 - 10000	$10^{-2}$

commonly found in brackish waters. Values taken from the plot will be less accurate than those calculated from 4a or 5a, but should be more accurate than those calculated by 4b or 5b. The single plot may be used for several decades of ionic concentration. For example, if the ion concentration is between 1 and 10 ppm, multiply the ordinate by  $10^{-5}$ ; if it is between 10 and 100 ppm, multiply by  $10^{-4}$ ; if it is between 100 and 1000 ppm, multiply by  $10^{-3}$ ; and if between 1000 and 10,000, multiply by  $10^{-2}$ . The lines drawn in Fig. 28 were calculated assuming a TDS of 3000 and a solution density of 1.0 at 25°C (77°F).

II. Sum the equivalent concentrations of monovalent cations:

$$\underline{m}'_{(1+)} = \underline{m}'_{\text{Na}} + \underline{m}'_{\text{K}} + \text{etc.} ; \quad (6)$$

of divalent cations:

$$\underline{m}'_{(2+)} = \underline{m}'_{\text{Ca(II)}} + \underline{m}'_{\text{Mg(II)}} + \text{etc.} \quad (7)$$

of monovalent anions:

$$\underline{m}'_{(1-)} = \underline{m}'_{\text{Cl}^-} + \underline{m}'_{\text{HCO}_3^-} + \text{etc.}; \quad (8)$$

and of divalent anions:

$$\underline{m}'_{(2-)} = \underline{m}'_{\text{SO}_4^{2-}} + \text{etc.} \quad (9)$$

III. Calculate the equivalent fraction of (1+):

$$\text{EF}_{(1+)} = \frac{\underline{m}'_{(1+)}}{\underline{m}'_{(1+)} + \underline{m}'_{(2+)}} , \quad (10)$$

and the equivalent fraction of (1-):

$$\text{EF}_{(1-)} = \frac{\underline{m}'_{(1-)}}{\underline{m}'_{(1-)} + \underline{m}'_{(2-)}} . \quad (11)$$

IV. Calculate the total equivalent concentration,  $\underline{m}'$ :

$$\begin{aligned} \underline{m}' &= 1/2 \sum_i \underline{m}'_i , \\ &= 1/2(\underline{m}'_{(1+)} + \underline{m}'_{(2+)} + \\ &\quad \underline{m}'_{(1-)} + \underline{m}'_{(2-)}). \end{aligned} \quad (12)$$

V. Obtain the osmotic coefficient from the tables:

- A. Select table that corresponds most closely to total equivalent concentration calculated in step IV.
- B. Pick column that corresponds most closely to equivalent fraction of (1+), from III.
- C. Pick row that corresponds most closely to equivalent fraction of (1-), from III.
- D. The osmotic coefficient,  $\phi$ , lying at the intersection of the column and row chosen in B and C above will generally be sufficiently accurate to use directly in calculating osmotic pressures. Should a closer value be desired, it may be obtained by interpolating between adjacent tables and adjacent rows and columns.

VI. Calculate the osmotic pressure from:

$$\Pi = \left( \frac{RT}{55.51 \bar{V}_1} \right) \phi (m^1_{(1+)} + m^1_{(1-)} + m^1_{(2+)}/2 + m^1_{(2-)} / 2). \quad (13)$$

For computations of permeabilities of membranes, one needs the difference in osmotic pressures between the solution at the membrane-brine interface and the effluent. Precise values may therefore require an estimate of concentration polarization.

Sample Calculation

Consider a brackish well water from Webster, South Dakota, which may have the following ionic compositions:

<u>Ion</u>	<u>Ionic Weight</u>	<u>ppm</u>
Na <sup>+</sup>	23	200
K <sup>+</sup>	39.1	16
Ca(II)	40.08	140
Mg(II)	24.312	105
HCO <sub>3</sub> <sup>-</sup>	61	300
Cl <sup>-</sup>	35.453	10
SO <sub>4</sub> <sup>-</sup>	96.06	845
TDS	---	1616

What is the osmotic pressure at 25°C?

I. Calculate the equivalent concentrations:

Ion	ppm	$\underline{m}'_i$	
		Eq. (4)	Fig. 2
Na <sup>+</sup>	200	0.00871	0.00865
K <sup>+</sup>	16	0.00041	0.00041
Ca(II)	140	0.00700	0.00695
Mg(II)	105	0.00865	0.00868
HCO <sub>3</sub> <sup>-</sup>	300	0.00493	0.00488
Cl <sup>-</sup>	10	0.00028	0.00028
SO <sub>4</sub> <sup>=</sup>	845	0.01762	0.0176

II. Sum equivalent concentrations [Eqs. (6) through (9)]:

$$\underline{m}'_{(1+)} = 0.00871 + 0.00041 = 0.00912$$

$$\underline{m}'_{(2+)} = 0.01565$$

$$\underline{m}'_{(1-)} = 0.00521$$

$$\underline{m}'_{(2-)} = 0.01762$$

III. Calculate equivalent fractions [Eqs. (10) and (11)]:

$$\begin{aligned} EF_{(1+)} &= \frac{0.00912}{0.00912 + 0.01565} \\ &= 0.368 \end{aligned}$$

$$\begin{aligned} EF_{(1-)} &= \frac{0.00521}{0.00521 + 0.01762} \\ &= 0.228 \end{aligned}$$

IV. Calculate total equivalent concentration [Eq. (12)]:

$$\begin{aligned} \underline{m}' &= 1/2(0.00912 + 0.01565 + 0.00521 + 0.01762) \\ &= 0.0238 \end{aligned}$$

V. Obtain osmotic coefficient from table most closely corresponding to  $\underline{m}' = 0.0238$ , i.e., 0.025; from column most closely corresponding to  $EF_{(1+)} = 0.368$ , i.e., 0.4; and from row most closely corresponding to  $EF_{(1-)} = 0.228$ , i.e., 0.2. The value of  $\phi$  at the intersection of column

0.4 and row 0.2 is

$$\phi = 0.854$$

For a more accurate value we may interpolate between tables and rows and columns. In the present example, from the table for  $\underline{m}' = 0.020$ , we find

$$\phi_I = \frac{[0.854 + 0.68(0.011)] + [0.854 + 0.28(0.012)]}{2} = 0.859$$

From the table for  $\underline{m}' = 0.025$ , we find:

$$\phi_2 = 1/2[0.843 + 0.68(0.011)] + 1/2[0.843 + 0.28(0.013)] = 0.849$$

Interpolating between the two tables, we get:

$$\begin{aligned} \phi &= 0.859 - \left( \frac{0.0238 - 0.0200}{0.0250 - 0.0200} \right) (0.859 - 0.849) = 0.859 - \frac{38}{50} (0.859 - 0.849) \\ &= 0.851 \end{aligned}$$

VI. Calculate osmotic pressure,  $\Pi$ , from Eq. (13). From Table X at 25°,  $\frac{RT}{55.51 \bar{V}_I} = 24.4$  atm. Then

$$\begin{aligned} \Pi &= 24.4 \times 0.851 (0.00912 + 0.00521 + 0.01565/2 \\ &\quad + 0.01762/2) \\ &= 0.64 \text{ atm.} \end{aligned}$$

TABLE XI. OSMOTIC COEFFICIENTS,  $\phi$ , AS A FUNCTION OF TOTAL EQUIVALENT  
CONCENTRATIONS AND EQUIVALENT FRACTIONS OF SEVERAL COMMON IONS

(pages 73-94)

TABLE XI. OSMOTIC COEFFICIENTS,  $\phi$ , AS A FUNCTION OF TOTAL EQUIVALENT CONCENTRATIONS AND EQUIVALENT FRACTIONS OF SEVERAL COMMON IONS

OSMOTIC COEFFICIENT,  $\phi$

TOTAL EQ CONCENTRATION, m' = 0.002500 EQ PER KG-WATER

EQ FRACTION OF SODIUM

	0.0	0.1	0.2	0.3	0.4	0.5	0.6	0.7	0.8	0.9	1.0		
0.0	0.904	0.911	0.918	0.925	0.931	0.936	0.941	0.945	0.950	0.953	0.957	1.0	
0.1	0.912	0.919	0.925	0.931	0.936	0.941	0.946	0.950	0.954	0.957	0.960	0.9	
0.2	0.919	0.925	0.931	0.936	0.941	0.946	0.950	0.954	0.957	0.961	0.964	0.8	
0.3	0.926	0.931	0.937	0.941	0.946	0.950	0.954	0.957	0.961	0.964	0.967	0.7	
0.4	0.932	0.937	0.942	0.946	0.950	0.954	0.958	0.961	0.964	0.967	0.969	0.6	
EQ FRACTION OF CHLORIDE	0.5	0.937	0.942	0.946	0.950	0.954	0.958	0.961	0.964	0.967	0.969	0.972	0.5
	0.6	0.942	0.947	0.951	0.954	0.958	0.961	0.964	0.967	0.970	0.972	0.974	0.4
	0.7	0.947	0.951	0.955	0.958	0.961	0.964	0.967	0.970	0.972	0.974	0.977	0.3
	0.8	0.951	0.955	0.958	0.962	0.965	0.967	0.970	0.972	0.975	0.977	0.979	0.2
	0.9	0.955	0.958	0.962	0.965	0.967	0.970	0.972	0.975	0.977	0.979	0.981	0.1
	1.0	0.959	0.962	0.965	0.968	0.970	0.973	0.975	0.977	0.979	0.981	0.982	0.0
	1.0	0.9	0.8	0.7	0.6	0.5	0.4	0.3	0.2	0.1	0.0		

EQ FRACTION OF MAGNESIUM

EQ FRACTION OF SULFATE

TABLE XI (cont'd)

OSMOTIC COEFFICIENT,  $\phi$

TOTAL EQ CONCENTRATION,  $m'$  = 0.005000 EQ PER KG-WATER

EQ FRACTION OF SODIUM

	0.0	0.1	0.2	0.3	0.4	0.5	0.6	0.7	0.8	0.9	1.0	
	0.871	0.881	0.890	0.899	0.907	0.914	0.920	0.926	0.932	0.937	0.941	1.0
	0.882	0.891	0.899	0.907	0.914	0.921	0.927	0.932	0.937	0.942	0.946	0.9
	0.891	0.900	0.907	0.915	0.921	0.927	0.932	0.937	0.942	0.946	0.951	0.8
	0.900	0.908	0.915	0.921	0.927	0.933	0.938	0.942	0.947	0.951	0.955	0.7
	0.908	0.915	0.922	0.928	0.933	0.938	0.943	0.947	0.951	0.955	0.958	0.6
EQ FRACTION OF CHLORIDE	0.916	0.922	0.928	0.933	0.938	0.943	0.947	0.951	0.955	0.959	0.962	0.5
	0.923	0.928	0.934	0.939	0.943	0.948	0.952	0.955	0.959	0.962	0.965	0.4
	0.929	0.934	0.939	0.944	0.948	0.952	0.956	0.959	0.962	0.965	0.968	0.3
	0.935	0.940	0.944	0.948	0.952	0.956	0.959	0.963	0.966	0.968	0.971	0.2
	0.940	0.945	0.949	0.953	0.956	0.960	0.963	0.966	0.969	0.971	0.974	0.1
	0.945	0.949	0.953	0.957	0.960	0.963	0.966	0.969	0.972	0.974	0.976	0.0
	1.0	0.9	0.8	0.7	0.6	0.5	0.4	0.3	0.2	0.1	0.0	

EQ FRACTION OF MAGNESIUM

EQ FRACTION OF SULFATE

TABLE XI (cont'd)

OSMOTIC COEFFICIENT,  $\phi$

TOTAL EQ CONCENTRATION,  $m'$  = 0.010000 EQ PER KG-WATER

		EQ FRACTION OF SODIUM											
		0.0	0.1	0.2	0.3	0.4	0.5	0.6	0.7	0.8	0.9	1.0	
EQ FRACTION OF CHLORIDE	0.0	0.830	0.843	0.855	0.866	0.876	0.886	0.894	0.902	0.909	0.916	0.922	1.0
	0.1	0.844	0.856	0.867	0.877	0.886	0.895	0.902	0.910	0.916	0.922	0.928	0.9
	0.2	0.857	0.868	0.878	0.887	0.895	0.903	0.910	0.917	0.923	0.929	0.934	0.8
	0.3	0.869	0.879	0.888	0.896	0.904	0.911	0.917	0.924	0.929	0.934	0.939	0.7
	0.4	0.880	0.889	0.897	0.905	0.912	0.918	0.924	0.930	0.935	0.940	0.944	0.6
	0.5	0.890	0.898	0.905	0.912	0.919	0.925	0.930	0.935	0.940	0.945	0.949	0.5
	0.6	0.899	0.906	0.913	0.919	0.925	0.931	0.936	0.941	0.945	0.950	0.953	0.4
	0.7	0.907	0.914	0.920	0.926	0.932	0.937	0.941	0.946	0.950	0.954	0.958	0.3
	0.8	0.914	0.921	0.927	0.932	0.937	0.942	0.946	0.951	0.954	0.958	0.961	0.2
	0.9	0.921	0.927	0.933	0.938	0.943	0.947	0.951	0.955	0.958	0.962	0.965	0.1
	1.0	0.928	0.933	0.938	0.943	0.947	0.952	0.955	0.959	0.962	0.965	0.968	0.0
		1.0	0.9	0.8	0.7	0.6	0.5	0.4	0.3	0.2	0.1	0.0	

EQ FRACTION  
OF  
SULFATE

EQ FRACTION OF MAGNESIUM

TABLE XI (cont'd)

OSMOTIC COEFFICIENT,  $\phi$

TOTAL EQ CONCENTRATION,  $m'$  = 0.015000 EQ PER KG-WATER

		EQ FRACTION OF SODIUM												
		0.0	0.1	0.2	0.3	0.4	0.5	0.6	0.7	0.8	0.9	1.0		
EQ FRACTION OF CHLORIDE	0.0	0.803	0.818	0.832	0.844	0.856	0.866	0.876	0.885	0.893	0.901	0.908	1.0	EQ FRACTION OF SULFATE
	0.1	0.819	0.833	0.846	0.857	0.867	0.877	0.886	0.894	0.902	0.909	0.915	0.9	
	0.2	0.834	0.847	0.858	0.869	0.878	0.887	0.895	0.903	0.910	0.916	0.922	0.8	
	0.3	0.848	0.859	0.870	0.879	0.888	0.896	0.904	0.911	0.917	0.923	0.929	0.7	
	0.4	0.861	0.871	0.880	0.889	0.897	0.904	0.911	0.918	0.924	0.929	0.935	0.6	
	0.5	0.872	0.881	0.890	0.898	0.905	0.912	0.919	0.925	0.930	0.935	0.940	0.5	
	0.6	0.882	0.891	0.899	0.906	0.913	0.920	0.925	0.931	0.936	0.941	0.945	0.4	
	0.7	0.892	0.900	0.907	0.914	0.920	0.926	0.932	0.937	0.942	0.946	0.950	0.3	
	0.8	0.901	0.908	0.915	0.921	0.927	0.932	0.938	0.942	0.947	0.951	0.955	0.2	
	0.9	0.909	0.916	0.922	0.928	0.933	0.938	0.943	0.947	0.952	0.955	0.959	0.1	
	1.0	0.917	0.923	0.929	0.934	0.939	0.944	0.948	0.952	0.956	0.960	0.963	0.0	
		1.0	0.9	0.8	0.7	0.6	0.5	0.4	0.3	0.2	0.1	0.0		
EQ FRACTION OF MAGNESIUM														

TABLE XI (cont'd)

OSMOTIC COEFFICIENT,  $\phi$

TOTAL EQ CONCENTRATION,  $m' = 0.020000$  EQ PER KG-WATER

EQ FRACTION OF SODIUM

	0.0	0.1	0.2	0.3	0.4	0.5	0.6	0.7	0.8	0.9	1.0	
1.0	0.782	0.798	0.814	0.827	0.840	0.852	0.862	0.872	0.881	0.889	0.897	1.0
0.9	0.800	0.815	0.829	0.842	0.853	0.864	0.873	0.882	0.891	0.898	0.905	0.9
0.8	0.817	0.831	0.843	0.854	0.865	0.875	0.883	0.892	0.899	0.907	0.913	0.8
0.7	0.832	0.844	0.856	0.866	0.876	0.885	0.893	0.900	0.908	0.914	0.920	0.7
0.6	0.846	0.857	0.868	0.877	0.886	0.894	0.902	0.909	0.915	0.921	0.927	0.6
0.5	0.859	0.869	0.878	0.887	0.895	0.903	0.910	0.916	0.922	0.928	0.933	0.5
0.4	0.870	0.880	0.888	0.896	0.904	0.911	0.917	0.923	0.929	0.934	0.939	0.4
0.3	0.881	0.890	0.898	0.905	0.912	0.918	0.924	0.930	0.935	0.940	0.944	0.3
0.2	0.891	0.899	0.906	0.913	0.919	0.925	0.931	0.936	0.941	0.945	0.950	0.2
0.1	0.920	0.907	0.914	0.920	0.926	0.932	0.937	0.942	0.946	0.950	0.954	0.1
0.0	0.909	0.915	0.922	0.927	0.933	0.938	0.943	0.947	0.951	0.955	0.959	0.0
	1.0	0.9	0.8	0.7	0.6	0.5	0.4	0.3	0.2	0.1	0.0	

EQ FRACTION  
OF  
CHLORIDE

EQ FRACTION  
OF  
SULFATE

EQ FRACTION OF MAGNESIUM

TABLE XI (cont'd)

OSMOTIC COEFFICIENT,  $\phi$

TOTAL EQ CONCENTRATION,  $m'$  = 0.025000 EQ PER KG-WATER

		EQ FRACTION OF SODIUM											
		0.0	0.1	0.2	0.3	0.4	0.5	0.6	0.7	0.8	0.9	1.0	
EQ FRACTION OF CHLORIDE	0.0	0.765	0.783	0.799	0.814	0.827	0.840	0.851	0.861	0.871	0.880	0.888	1.0
	0.1	0.785	0.801	0.816	0.829	0.841	0.853	0.863	0.873	0.881	0.890	0.897	0.9
	0.2	0.823	0.817	0.831	0.843	0.854	0.864	0.874	0.883	0.891	0.899	0.906	0.8
	0.3	0.819	0.833	0.845	0.856	0.866	0.875	0.884	0.892	0.900	0.907	0.913	0.7
	0.4	0.834	0.846	0.857	0.867	0.877	0.886	0.894	0.901	0.908	0.915	0.921	0.6
	0.5	0.848	0.859	0.869	0.878	0.887	0.895	0.902	0.909	0.916	0.922	0.927	0.5
	0.6	0.861	0.871	0.880	0.888	0.896	0.904	0.911	0.917	0.923	0.929	0.934	0.4
	0.7	0.872	0.881	0.890	0.898	0.905	0.912	0.918	0.924	0.930	0.935	0.940	0.3
	0.8	0.883	0.891	0.899	0.906	0.913	0.919	0.925	0.931	0.936	0.941	0.945	0.2
	0.9	0.893	0.901	0.908	0.915	0.921	0.927	0.932	0.937	0.942	0.946	0.951	0.1
	1.0	0.902	0.909	0.916	0.922	0.928	0.933	0.938	0.943	0.947	0.952	0.955	0.0
		1.0	0.9	0.8	0.7	0.6	0.5	0.4	0.3	0.2	0.1	0.0	

EQ FRACTION OF SULFATE

EQ FRACTION OF MAGNESIUM

TABLE XI (cont'd)

OSMOTIC COEFFICIENT,  $\phi$

TOTAL EQ CONCENTRATION,  $m^1 = 0.030000$  EQ PER KG-WATER

EQ FRACTION OF SODIUM

	0.0	0.1	0.2	0.3	0.4	0.5	0.6	0.7	0.8	0.9	1.0	
0.0	0.751	0.770	0.787	0.802	0.816	0.829	0.841	0.852	0.863	0.872	0.881	1.0
0.1	0.772	0.789	0.804	0.818	0.831	0.843	0.854	0.864	0.874	0.882	0.890	0.9
0.2	0.791	0.806	0.820	0.833	0.845	0.856	0.866	0.875	0.884	0.892	0.899	0.8
0.3	0.809	0.822	0.835	0.847	0.858	0.868	0.877	0.885	0.893	0.901	0.908	0.7
0.4	0.825	0.837	0.849	0.859	0.869	0.878	0.887	0.895	0.902	0.909	0.915	0.6
EQ FRACTION OF CHLORIDE	0.839	0.851	0.861	0.871	0.880	0.888	0.896	0.904	0.910	0.917	0.923	0.5
0.6	0.853	0.863	0.873	0.882	0.890	0.898	0.905	0.912	0.918	0.924	0.929	0.4
0.7	0.865	0.875	0.883	0.892	0.899	0.907	0.913	0.919	0.925	0.931	0.936	0.3
0.8	0.876	0.885	0.893	0.901	0.908	0.915	0.921	0.927	0.932	0.937	0.942	0.2
0.9	0.887	0.895	0.903	0.910	0.916	0.922	0.928	0.933	0.938	0.943	0.947	0.1
1.0	0.897	0.904	0.911	0.918	0.924	0.929	0.935	0.939	0.944	0.948	0.953	0.0
	1.0	0.9	0.8	0.7	0.6	0.5	0.4	0.3	0.2	0.1	0.0	

EQ FRACTION  
OF  
SULFATE

EQ FRACTION OF MAGNESIUM

TABLE XI (cont'd)

OSMOTIC COEFFICIENT,  $\phi$

TOTAL EQ CONCENTRATION,  $m^{\pm}$  = 0.035000 EQ PER KG-WATER

EQ FRACTION OF SODIUM

	0.0	0.1	0.2	0.3	0.4	0.5	0.6	0.7	0.8	0.9	1.0	
0.0	0.739	0.758	0.776	0.792	0.807	0.821	0.833	0.845	0.855	0.865	0.874	1.0
0.1	0.761	0.778	0.795	0.809	0.823	0.835	0.846	0.857	0.867	0.876	0.884	0.9
0.2	0.781	0.797	0.812	0.825	0.837	0.848	0.859	0.869	0.878	0.886	0.894	0.8
0.3	0.799	0.814	0.827	0.839	0.850	0.861	0.870	0.879	0.888	0.895	0.902	0.7
0.4	0.816	0.829	0.841	0.852	0.863	0.872	0.881	0.889	0.897	0.904	0.911	0.6
0.5	0.832	0.844	0.855	0.865	0.874	0.883	0.891	0.899	0.906	0.912	0.918	0.5
0.6	0.846	0.857	0.867	0.876	0.885	0.893	0.900	0.907	0.914	0.920	0.926	0.4
0.7	0.859	0.869	0.878	0.887	0.894	0.902	0.909	0.915	0.921	0.927	0.932	0.3
0.8	0.871	0.880	0.888	0.896	0.904	0.910	0.917	0.923	0.928	0.934	0.939	0.2
0.9	0.882	0.890	0.898	0.905	0.912	0.918	0.924	0.930	0.935	0.940	0.944	0.1
1.0	0.892	0.900	0.907	0.914	0.920	0.926	0.931	0.937	0.941	0.946	0.950	0.0
	1.0	0.9	0.8	0.7	0.6	0.5	0.4	0.3	0.2	0.1	0.0	

EQ FRACTION OF CHLORIDE

EQ FRACTION OF SULFATE

EQ FRACTION OF MAGNESIUM

TABLE XI (cont'd)

OSMOTIC COEFFICIENT,  $\phi$

TOTAL EQ CONCENTRATION, m' = 0.040000 EQ PER KG-WATER

EQ FRACTION OF SODIUM

	0.0	0.1	0.2	0.3	0.4	0.5	0.6	0.7	0.8	0.9	1.0	
0.0	0.728	0.748	0.767	0.783	0.799	0.813	0.826	0.838	0.849	0.859	0.868	1.0
0.1	0.751	0.769	0.786	0.801	0.815	0.828	0.840	0.851	0.861	0.870	0.879	0.9
0.2	0.772	0.789	0.804	0.818	0.830	0.842	0.853	0.863	0.872	0.881	0.889	0.8
0.3	0.791	0.806	0.820	0.833	0.844	0.855	0.865	0.874	0.882	0.890	0.898	0.7
0.4	0.809	0.823	0.835	0.846	0.857	0.867	0.876	0.884	0.892	0.900	0.906	0.6
EQ FRACTION OF CHLORIDE	0.825	0.837	0.849	0.859	0.869	0.878	0.886	0.894	0.901	0.908	0.915	0.5
0.6	0.840	0.851	0.861	0.871	0.880	0.888	0.896	0.903	0.910	0.916	0.922	0.4
0.7	0.853	0.864	0.873	0.882	0.890	0.898	0.905	0.912	0.918	0.924	0.929	0.3
0.8	0.866	0.875	0.884	0.892	0.900	0.907	0.913	0.920	0.925	0.931	0.936	0.2
0.9	0.878	0.886	0.894	0.902	0.909	0.915	0.921	0.927	0.932	0.937	0.942	0.1
1.0	0.888	0.896	0.904	0.911	0.917	0.923	0.929	0.934	0.939	0.944	0.948	0.0
	1.0	0.9	0.8	0.7	0.6	0.5	0.4	0.3	0.2	0.1	0.0	

EQ FRACTION  
OF  
SULFATE

EQ FRACTION OF MAGNESIUM

TABLE XI (cont'd)

OSMOTIC COEFFICIENT,  $\phi$

TOTAL EQ CONCENTRATION,  $m' = 0.045000$  EQ PER KG-WATER

EQ FRACTION OF SODIUM

	0.0	0.1	0.2	0.3	0.4	0.5	0.6	0.7	0.8	0.9	1.0		
EQ FRACTION OF CHLORIDE	0.0	0.718	0.739	0.758	0.776	0.791	0.806	0.819	0.831	0.843	0.853	0.863	1.0
	0.1	0.743	0.761	0.778	0.794	0.808	0.822	0.834	0.845	0.855	0.865	0.874	0.9
	0.2	0.764	0.781	0.797	0.811	0.824	0.835	0.847	0.858	0.867	0.875	0.884	0.8
	0.3	0.784	0.800	0.814	0.827	0.839	0.850	0.860	0.869	0.878	0.886	0.894	0.7
	0.4	0.803	0.816	0.829	0.841	0.852	0.862	0.871	0.880	0.888	0.896	0.903	0.6
	0.5	0.819	0.832	0.844	0.854	0.864	0.874	0.882	0.890	0.898	0.905	0.911	0.5
	0.6	0.835	0.846	0.857	0.867	0.876	0.884	0.892	0.900	0.907	0.913	0.919	0.4
	0.7	0.849	0.859	0.869	0.878	0.886	0.894	0.902	0.908	0.915	0.921	0.926	0.3
	0.8	0.862	0.871	0.880	0.889	0.896	0.904	0.910	0.917	0.923	0.928	0.933	0.2
	0.9	0.874	0.883	0.891	0.899	0.906	0.912	0.919	0.924	0.930	0.935	0.940	0.1
	1.0	0.885	0.893	0.901	0.908	0.914	0.921	0.926	0.932	0.937	0.942	0.946	0.0
	1.0	0.9	0.8	0.7	0.6	0.5	0.4	0.3	0.2	0.1	0.0		EQ FRACTION OF SULFATE

EQ FRACTION OF MAGNESIUM

TABLE XI (cont'd)

OSMOTIC COEFFICIENT,  $\phi$

TOTAL EQ CONCENTRATION, m' = 0.050000 EQ PER KG-WATER

EQ FRACTION OF SODIUM

	0.0	0.1	0.2	0.3	0.4	0.5	0.6	0.7	0.8	0.9	1.0	
0.0	0.710	0.731	0.751	0.769	0.795	0.800	0.813	0.826	0.837	0.848	0.858	1.0
0.1	0.735	0.754	0.772	0.798	0.802	0.816	0.828	0.840	0.850	0.860	0.869	0.9
0.2	0.757	0.775	0.791	0.805	0.819	0.831	0.842	0.853	0.863	0.872	0.880	0.8
0.3	0.778	0.794	0.808	0.821	0.834	0.845	0.855	0.865	0.874	0.882	0.890	0.7
0.4	0.797	0.811	0.824	0.836	0.847	0.858	0.867	0.876	0.884	0.892	0.899	0.6
EQ FRACTION OF CHLORIDE	0.814	0.827	0.839	0.850	0.860	0.870	0.878	0.887	0.894	0.901	0.908	0.5
0.6	0.830	0.842	0.853	0.863	0.872	0.881	0.889	0.896	0.903	0.910	0.916	0.4
0.7	0.845	0.855	0.865	0.875	0.883	0.891	0.899	0.906	0.912	0.918	0.924	0.3
0.8	0.858	0.868	0.877	0.886	0.893	0.901	0.908	0.914	0.920	0.926	0.931	0.2
0.9	0.871	0.880	0.888	0.896	0.903	0.910	0.916	0.922	0.928	0.933	0.938	0.1
1.0	0.882	0.890	0.898	0.905	0.912	0.918	0.924	0.930	0.935	0.940	0.944	0.0
	1.0	0.9	0.8	0.7	0.6	0.5	0.4	0.3	0.2	0.1	0.0	

EQ FRACTION OF SULFATE

EQ FRACTION OF MAGNESIUM

TABLE XI (cont'd)

OSMOTIC COEFFICIENT,  $\phi$

---

TOTAL EQ CONCENTRATION, m' = 0.100000 EQ PER KG-WATER

---

EQ FRACTION OF SODIUM

	0.0	0.1	0.2	0.3	0.4	0.5	0.6	0.7	0.8	0.9	1.0		
0.0	0.655	0.679	0.702	0.722	0.741	0.758	0.773	0.787	0.801	0.813	0.824	1.0	
0.1	0.685	0.707	0.727	0.746	0.762	0.778	0.792	0.805	0.817	0.828	0.839	0.9	
0.2	0.713	0.733	0.751	0.767	0.782	0.796	0.809	0.821	0.832	0.842	0.852	0.8	
0.3	0.738	0.756	0.772	0.787	0.801	0.813	0.825	0.836	0.846	0.856	0.864	0.7	
0.4	0.761	0.777	0.792	0.805	0.818	0.829	0.840	0.850	0.859	0.868	0.876	0.6	
EQ FRACTION OF CHLORIDE	0.5	0.782	0.797	0.810	0.822	0.834	0.844	0.854	0.863	0.872	0.880	0.887	EQ FRACTION OF SULFATE
0.6	0.801	0.815	0.827	0.838	0.849	0.858	0.867	0.876	0.883	0.891	0.897	0.4	
0.7	0.819	0.831	0.843	0.853	0.862	0.871	0.879	0.887	0.894	0.901	0.907	0.3	
0.8	0.836	0.847	0.857	0.866	0.875	0.883	0.891	0.898	0.904	0.911	0.916	0.2	
0.9	0.852	0.861	0.871	0.879	0.887	0.895	0.901	0.908	0.914	0.920	0.925	0.1	
1.0	0.866	0.875	0.883	0.891	0.898	0.905	0.912	0.917	0.923	0.928	0.933	0.0	
	1.0	0.9	0.8	0.7	0.6	0.5	0.4	0.3	0.2	0.1	0.0		

EQ FRACTION OF MAGNESIUM

---

TABLE XI (cont'd)

OSMOTIC COEFFICIENT,  $\phi$

TOTAL EQ CONCENTRATION,  $m'$  = 0.200000 EQ PER KG-WATER

EQ FRACTION OF SODIUM

	0.0	0.1	0.2	0.3	0.4	0.5	0.6	0.7	0.8	0.9	1.0	
0.0	0.634	0.631	0.656	0.578	0.628	0.717	0.733	0.749	0.763	0.776	0.792	1.0
0.1	0.641	0.665	0.687	0.706	0.724	0.741	0.756	0.770	0.783	0.795	0.806	0.9
0.2	0.674	0.695	0.715	0.732	0.749	0.764	0.777	0.790	0.802	0.812	0.822	0.8
0.3	0.704	0.723	0.741	0.757	0.771	0.785	0.797	0.808	0.819	0.829	0.838	0.7
0.4	0.732	0.749	0.764	0.779	0.792	0.804	0.815	0.826	0.835	0.844	0.852	0.6
0.5	0.757	0.772	0.787	0.799	0.811	0.822	0.833	0.842	0.851	0.859	0.866	0.5
0.6	0.781	0.794	0.807	0.819	0.829	0.839	0.849	0.857	0.865	0.872	0.879	0.4
0.7	0.802	0.815	0.826	0.837	0.846	0.855	0.864	0.871	0.878	0.885	0.891	0.3
0.8	0.823	0.834	0.844	0.854	0.862	0.870	0.878	0.885	0.891	0.897	0.903	0.2
0.9	0.842	0.852	0.861	0.869	0.877	0.884	0.891	0.897	0.903	0.909	0.914	0.1
1.0	0.859	0.868	0.876	0.884	0.891	0.898	0.904	0.909	0.915	0.919	0.924	0.0
	1.0	0.9	0.8	0.7	0.6	0.5	0.4	0.3	0.2	0.1	0.0	

EQ FRACTION  
OF  
CHLORIDE

EQ FRACTION  
OF  
SULFATE

EQ FRACTION OF MAGNESIUM

TABLE XI (cont'd)

OSMOTIC COEFFICIENT,  $\phi$

TOTAL EQ CONCENTRATION,  $m'$  = 0.300000 EQ PER KG-WATER

EQ FRACTION OF SODIUM

	0.0	0.1	0.2	0.3	0.4	0.5	0.6	0.7	0.8	0.9	1.0	
EQ FRACTION OF CHLORIDE	0.578	0.606	0.632	0.655	0.675	0.694	0.711	0.727	0.741	0.754	0.766	1.0
	0.619	0.643	0.666	0.686	0.705	0.721	0.737	0.751	0.764	0.775	0.786	0.9
	0.655	0.677	0.697	0.715	0.732	0.747	0.760	0.773	0.785	0.795	0.805	0.8
	0.689	0.708	0.726	0.742	0.757	0.770	0.783	0.794	0.804	0.814	0.822	0.7
	0.720	0.737	0.753	0.767	0.780	0.792	0.803	0.813	0.823	0.831	0.839	0.6
	0.748	0.764	0.778	0.790	0.802	0.813	0.823	0.832	0.840	0.848	0.855	0.5
	0.775	0.788	0.801	0.812	0.822	0.832	0.841	0.849	0.856	0.863	0.869	0.4
	0.799	0.811	0.822	0.832	0.842	0.850	0.858	0.865	0.872	0.878	0.883	0.3
	0.822	0.833	0.842	0.851	0.860	0.867	0.874	0.880	0.886	0.892	0.896	0.2
	0.843	0.853	0.861	0.869	0.876	0.883	0.889	0.895	0.900	0.905	0.909	0.1
	0.863	0.871	0.879	0.886	0.892	0.898	0.904	0.908	0.913	0.917	0.921	0.0
	1.0	0.9	0.8	0.7	0.6	0.5	0.4	0.3	0.2	0.1	0.0	

EQ FRACTION OF MAGNESIUM

TABLE XI (cont'd)

OSMOTIC COEFFICIENT,  $\phi$

TOTAL EQ CONCENTRATION,  $m' = 0.400000$  EQ PER KG-WATER

EQ FRACTION OF SODIUM

	0.0	0.1	0.2	0.3	0.4	0.5	0.6	0.7	0.8	0.9	1.0		
0.0	0.562	0.590	0.616	0.639	0.660	0.679	0.696	0.711	0.725	0.738	0.750	1.0	
0.1	0.605	0.630	0.653	0.673	0.692	0.709	0.724	0.737	0.750	0.761	0.772	0.9	
0.2	0.645	0.667	0.697	0.705	0.721	0.735	0.750	0.762	0.773	0.783	0.792	0.8	
0.3	0.682	0.701	0.718	0.734	0.749	0.762	0.774	0.784	0.794	0.803	0.812	0.7	
0.4	0.715	0.732	0.747	0.761	0.774	0.786	0.796	0.806	0.815	0.823	0.830	0.6	
EQ FRACTION OF CHLORIDE	0.5	0.746	0.761	0.774	0.787	0.798	0.808	0.817	0.826	0.834	0.841	0.847	0.5
	0.6	0.775	0.788	0.800	0.810	0.820	0.829	0.837	0.845	0.851	0.858	0.863	0.4
	0.7	0.801	0.813	0.823	0.833	0.841	0.849	0.856	0.863	0.868	0.874	0.879	0.3
	0.8	0.826	0.836	0.845	0.853	0.861	0.868	0.874	0.879	0.884	0.889	0.893	0.2
	0.9	0.849	0.858	0.866	0.873	0.879	0.885	0.891	0.895	0.900	0.904	0.907	0.1
1.0	0.871	0.878	0.885	0.891	0.897	0.902	0.906	0.911	0.914	0.917	0.920	0.0	
	1.0	0.9	0.8	0.7	0.6	0.5	0.4	0.3	0.2	0.1	0.0		

EQ FRACTION OF MAGNESIUM

EQ FRACTION OF SULFATE

TABLE XI (cont'd)

OSMOTIC COEFFICIENT,  $\phi$

TOTAL EQ CONCENTRATION,  $m^{\pm}$  = 0.500000 EQ PER KG-WATER

EQ FRACTION OF SODIUM

	0.0	0.1	0.2	0.3	0.4	0.5	0.6	0.7	0.8	0.9	1.0	
0.0	0.550	0.579	0.605	0.628	0.649	0.667	0.684	0.699	0.713	0.726	0.737	1.0
0.1	0.597	0.622	0.644	0.665	0.683	0.699	0.714	0.727	0.740	0.751	0.760	0.9
0.2	0.639	0.661	0.681	0.698	0.714	0.729	0.742	0.754	0.764	0.774	0.783	0.8
0.3	0.678	0.697	0.714	0.730	0.744	0.756	0.768	0.778	0.787	0.796	0.803	0.7
0.4	0.714	0.730	0.745	0.759	0.771	0.782	0.792	0.801	0.809	0.816	0.823	0.6
EQ FRACTION OF CHLORIDE	0.747	0.761	0.774	0.786	0.797	0.806	0.815	0.823	0.830	0.836	0.842	0.5
	0.777	0.790	0.801	0.811	0.821	0.829	0.836	0.843	0.849	0.854	0.859	0.4
	0.806	0.817	0.827	0.835	0.843	0.850	0.856	0.862	0.867	0.872	0.876	0.3
	0.833	0.842	0.850	0.858	0.864	0.870	0.876	0.880	0.885	0.888	0.892	0.2
	0.858	0.866	0.872	0.879	0.884	0.889	0.894	0.898	0.901	0.904	0.907	0.1
1.0	0.881	0.888	0.893	0.899	0.903	0.907	0.911	0.914	0.917	0.919	0.921	0.0
	1.0	0.9	0.8	0.7	0.6	0.5	0.4	0.3	0.2	0.1	0.0	

EQ FRACTION  
OF  
SULFATE

EQ FRACTION OF MAGNESIUM

TABLE XI (cont'd)

OSMOTIC COEFFICIENT, $\phi$													
TOTAL EQ CONCENTRATION, m' = 0.750000 EQ PER KG-WATER													
EQ FRACTION OF SODIUM													
	0.0	0.1	0.2	0.3	0.4	0.5	0.6	0.7	0.8	0.9	1.0		
	0.0	0.532	0.561	0.587	0.609	0.630	0.648	0.664	0.678	0.691	0.702	0.712	1.0
	0.1	0.585	0.610	0.632	0.651	0.669	0.684	0.698	0.710	0.721	0.730	0.739	0.9
	0.2	0.633	0.654	0.673	0.690	0.705	0.718	0.730	0.740	0.749	0.757	0.765	0.8
	0.3	0.678	0.696	0.712	0.726	0.738	0.750	0.760	0.768	0.776	0.783	0.789	0.7
	0.4	0.719	0.734	0.747	0.759	0.770	0.779	0.788	0.795	0.801	0.807	0.812	0.6
EQ FRACTION OF CHLORIDE	0.5	0.756	0.769	0.781	0.791	0.799	0.807	0.814	0.820	0.825	0.830	0.833	0.5
	0.6	0.792	0.802	0.812	0.820	0.827	0.833	0.839	0.844	0.848	0.851	0.854	0.4
	0.7	0.825	0.833	0.841	0.847	0.853	0.858	0.862	0.866	0.869	0.871	0.873	0.3
	0.8	0.856	0.862	0.868	0.873	0.878	0.882	0.885	0.887	0.889	0.891	0.892	0.2
	0.9	0.884	0.890	0.894	0.898	0.901	0.904	0.906	0.908	0.909	0.909	0.910	0.1
	1.0	0.912	0.916	0.919	0.921	0.923	0.925	0.926	0.927	0.927	0.927	0.927	0.0
		1.0	0.9	0.8	0.7	0.6	0.5	0.4	0.3	0.2	0.1	0.0	
EQ FRACTION OF MAGNESIUM													

EQ FRACTION OF SULFATE

TABLE XI (cont'd)

OSMOTIC COEFFICIENT,  $\phi$

TOTAL EQ CONCENTRATION,  $m^1 = 1.000000$  EQ PER KG-WATER

EQ FRACTION OF SODIUM

	0.0	0.1	0.2	0.3	0.4	0.5	0.6	0.7	0.8	0.9	1.0	
0.0	0.522	0.551	0.576	0.598	0.618	0.635	0.649	0.663	0.674	0.684	0.692	1.0
0.1	0.581	0.605	0.626	0.645	0.661	0.675	0.688	0.699	0.708	0.716	0.723	0.9
0.2	0.635	0.655	0.673	0.688	0.701	0.713	0.723	0.732	0.740	0.746	0.752	0.8
0.3	0.684	0.701	0.715	0.728	0.739	0.749	0.757	0.764	0.770	0.775	0.779	0.7
0.4	0.730	0.743	0.755	0.765	0.774	0.782	0.788	0.794	0.798	0.802	0.805	0.6
EQ FRACTION OF CHLORIDE	0.772	0.783	0.792	0.800	0.807	0.813	0.818	0.822	0.825	0.828	0.829	0.5
0.6	0.812	0.820	0.827	0.833	0.838	0.842	0.846	0.848	0.850	0.852	0.853	0.4
0.7	0.849	0.855	0.860	0.864	0.868	0.870	0.872	0.874	0.875	0.875	0.875	0.3
0.8	0.883	0.887	0.891	0.893	0.895	0.897	0.897	0.898	0.898	0.897	0.896	0.2
0.9	0.916	0.918	0.920	0.921	0.922	0.922	0.921	0.921	0.919	0.918	0.916	0.1
1.0	0.947	0.947	0.948	0.948	0.947	0.946	0.944	0.942	0.940	0.938	0.935	0.0
	1.0	0.9	0.8	0.7	0.6	0.5	0.4	0.3	0.2	0.1	0.0	

EQ FRACTION  
OF  
SULFATE

EQ FRACTION OF MAGNESIUM

TABLE XI (cont'd)

OSMOTIC COEFFICIENT,  $\phi$

---

TOTAL EQ CONCENTRATION, m' = 1.250000 EQ PER KG-WATER

---

EQ FRACTION OF SODIUM

	0.0	0.1	0.2	0.3	0.4	0.5	0.6	0.7	0.8	0.9	1.0	
0.0	0.518	0.546	0.570	0.591	0.610	0.625	0.639	0.651	0.661	0.669	0.677	1.0
0.1	0.582	0.605	0.625	0.643	0.657	0.670	0.681	0.691	0.699	0.705	0.711	0.9
0.2	0.641	0.660	0.676	0.690	0.702	0.712	0.721	0.728	0.734	0.739	0.743	0.8
0.3	0.695	0.710	0.723	0.734	0.743	0.751	0.757	0.763	0.767	0.770	0.773	0.7
0.4	0.745	0.757	0.767	0.775	0.782	0.787	0.792	0.796	0.798	0.800	0.801	0.6
EQ FRACTION OF CHLORIDE	0.5	0.792	0.800	0.808	0.813	0.818	0.822	0.825	0.827	0.828	0.828	0.5
	0.6	0.835	0.841	0.846	0.850	0.852	0.854	0.855	0.856	0.856	0.855	0.4
	0.7	0.876	0.879	0.882	0.884	0.885	0.885	0.885	0.884	0.882	0.881	0.3
	0.8	0.914	0.915	0.916	0.916	0.915	0.914	0.912	0.910	0.908	0.905	0.2
	0.9	0.950	0.950	0.948	0.947	0.945	0.942	0.939	0.936	0.932	0.928	0.1
1.0	0.984	0.982	0.979	0.976	0.972	0.968	0.964	0.960	0.955	0.951	0.946	0.0
	1.0	0.9	0.8	0.7	0.6	0.5	0.4	0.3	0.2	0.1	0.0	

EQ FRACTION OF MAGNESIUM

EQ FRACTION  
OF  
SULFATE

TABLE XI (cont'd)

OSMOTIC COEFFICIENT, $\phi$												
TOTAL EQ CONCENTRATION, m' = 1.500000 EQ PER KG-WATER												
EQ FRACTION OF SODIUM												
	0.0	0.1	0.2	0.3	0.4	0.5	0.6	0.7	0.8	0.9	1.0	
0.0	0.518	0.545	0.568	0.588	0.605	0.619	0.632	0.642	0.651	0.658	0.663	1.0
0.1	0.587	0.609	0.627	0.643	0.657	0.668	0.678	0.685	0.692	0.697	0.701	0.9
0.2	0.651	0.668	0.682	0.695	0.705	0.713	0.720	0.726	0.730	0.733	0.736	0.8
0.3	0.710	0.723	0.733	0.742	0.750	0.756	0.760	0.764	0.766	0.768	0.769	0.7
0.4	0.764	0.773	0.781	0.787	0.792	0.795	0.798	0.800	0.800	0.800	0.800	0.6
0.5	0.815	0.821	0.825	0.829	0.831	0.833	0.833	0.833	0.833	0.831	0.829	0.5
0.6	0.862	0.865	0.867	0.868	0.869	0.868	0.867	0.865	0.863	0.860	0.857	0.4
0.7	0.906	0.907	0.906	0.905	0.904	0.902	0.899	0.896	0.892	0.888	0.884	0.3
0.8	0.948	0.946	0.944	0.941	0.937	0.933	0.929	0.925	0.920	0.915	0.909	0.2
0.9	0.987	0.983	0.979	0.974	0.969	0.964	0.958	0.952	0.946	0.940	0.934	0.1
1.0	1.025	1.019	1.013	1.006	0.999	0.993	0.986	0.979	0.972	0.964	0.957	0.0
	1.0	0.9	0.8	0.7	0.6	0.5	0.4	0.3	0.2	0.1	0.0	

EQ FRACTION OF MAGNESIUM

EQ FRACTION OF SULFATE

TABLE XI (cont'd)

OSMOTIC COEFFICIENT, $\phi$													
TOTAL EQ CONCENTRATION, m <sup>l</sup> = 1.750000 EQ PER KG-WATER													
EQ FRACTION OF SODIUM													
	0.0	0.1	0.2	0.3	0.4	0.5	0.6	0.7	0.8	0.9	1.0		
	0.0	0.521	0.546	0.568	0.587	0.602	0.615	0.626	0.635	0.642	0.648	0.652	1.0
	0.1	0.596	0.616	0.632	0.646	0.658	0.668	0.676	0.682	0.687	0.690	0.693	0.9
	0.2	0.664	0.679	0.692	0.702	0.710	0.717	0.722	0.726	0.729	0.730	0.731	0.8
	0.3	0.727	0.738	0.747	0.753	0.759	0.763	0.765	0.767	0.768	0.767	0.766	0.7
	0.4	0.786	0.792	0.798	0.801	0.804	0.805	0.806	0.805	0.804	0.802	0.800	0.6
EQ FRACTION OF CHLORIDE	0.5	0.840	0.843	0.845	0.846	0.846	0.846	0.844	0.842	0.839	0.836	0.832	0.5
	0.6	0.891	0.891	0.890	0.889	0.887	0.884	0.880	0.876	0.872	0.867	0.862	0.4
	0.7	0.938	0.936	0.933	0.929	0.925	0.920	0.915	0.909	0.903	0.897	0.891	0.3
	0.8	0.983	0.978	0.973	0.967	0.961	0.954	0.947	0.940	0.933	0.926	0.918	0.2
	0.9	1.026	1.019	1.011	1.003	0.995	0.987	0.978	0.970	0.962	0.953	0.944	0.1
	1.0	1.067	1.057	1.048	1.038	1.028	1.018	1.008	0.999	0.989	0.979	0.970	0.0
		1.0	0.9	0.8	0.7	0.6	0.5	0.4	0.3	0.2	0.1	0.0	
EQ FRACTION OF MAGNESIUM													

EQ FRACTION OF SULFATE

TABLE XI (cont'd)

OSMOTIC COEFFICIENT, $\phi$													
TOTAL EQ CONCENTRATION, m <sup>l</sup> = 2.000000 EQ PER KG-WATER													
EQ FRACTION OF SODIUM													
	0.0	0.1	0.2	0.3	0.4	0.5	0.6	0.7	0.8	0.9	1.0		
EQ FRACTION OF CHLORIDE	0.0	0.527	0.551	0.571	0.588	0.602	0.613	0.623	0.630	0.636	0.640	0.643	1.0
	0.1	0.607	0.625	0.640	0.652	0.662	0.670	0.676	0.681	0.684	0.686	0.687	0.9
	0.2	0.680	0.693	0.703	0.711	0.718	0.722	0.726	0.728	0.729	0.728	0.727	0.8
	0.3	0.747	0.756	0.762	0.766	0.769	0.771	0.772	0.772	0.770	0.769	0.766	0.7
	0.4	0.810	0.814	0.816	0.818	0.818	0.817	0.815	0.813	0.810	0.806	0.802	0.6
	0.5	0.868	0.868	0.867	0.866	0.863	0.860	0.856	0.852	0.847	0.841	0.836	0.5
	0.6	0.922	0.919	0.916	0.911	0.906	0.901	0.895	0.889	0.882	0.875	0.868	0.4
	0.7	0.973	0.967	0.961	0.954	0.947	0.939	0.932	0.924	0.915	0.907	0.899	0.3
	0.8	1.021	1.013	1.004	0.995	0.985	0.976	0.967	0.957	0.947	0.938	0.928	0.2
	0.9	1.067	1.056	1.045	1.034	1.022	1.011	1.000	0.989	0.978	0.967	0.956	0.1
1.0	1.111	1.097	1.084	1.071	1.058	1.045	1.032	1.020	1.007	0.995	0.983	0.0	
	1.0	0.9	0.8	0.7	0.6	0.5	0.4	0.3	0.2	0.1	0.0		
EQ FRACTION OF MAGNESIUM													

EQ FRACTION OF SULFATE

IV. CONCENTRATION POLARIZATION IN HYPERFILTRATION OF NaCl  
SOLUTIONS CONTAINING TRACE AMOUNTS OF Ca(II) and  $\text{SO}_4^{=*$

Lawrence Dresner

ABSTRACT

Wall concentrations of  $\text{Ca}^{++}$  and  $\text{SO}_4^{--}$  have been calculated for the hyperfiltration of NaCl solutions containing trace amounts of these ions. The common-ion effect (solute-solute friction) and the variation of activity coefficients with composition have been taken into account. Laminar and turbulent flow across the membrane are both considered. In laminar flow, both developing and fully developed concentration profiles are considered.

A. Introduction:

Concentration polarization in NaCl solutions containing  $\text{Ca}^{++}$  and  $\text{SO}_4^{--}$  is of interest because if the water in a hyperfiltration plant can be considered as such a solution and if it is close to saturation in  $\text{CaSO}_4$ , a small amount of concentration polarization may cause precipitation of  $\text{CaSO}_4$  at the membrane.

Concentration polarization in hyperfiltration has been studied exhaustively.<sup>8</sup> Solute concentration at the wall has been calculated for both perfect and imperfect membranes assuming either no flow, laminar flow, or turbulent flow across the face of the membrane. In the latter two cases, developing as well as fully developed concentration profiles have been studied. Unfortunately, for two reasons mentioned below, the results of these calculations cannot be used directly to estimate wall concentrations in solutions of  $\text{Na}^+$ ,  $\text{Cl}^-$ ,  $\text{Ca}^{++}$ , and  $\text{SO}_4^{--}$ .

In the first place, all the calculations of concentration polarization to date have dealt with two-component solutions (water plus one solute). When two or more solutes are present in the feed water, each may affect the diffusion of the other. In the parlance of Spiegler's frictional model of

---

\* Cosponsored by the Office of Saline Water, Membrane Division, and by the National Science Foundation/RANN.

irreversible thermodynamics<sup>9</sup> (which it should be noted is perfectly general) solute-solute friction may exist. Use of the "two-component" results is tantamount to neglecting solute-solute friction. When the solutes are electrolytes, it seems reasonable to ignore ion-ion friction, especially in dilute feed solutions. However, it can be shown<sup>10</sup> that when the equations of irreversible thermodynamics in the ionic form with ion-ion friction neglected are recast into the molecular form, solute-solute friction terms occur, coupling any pair of solutes having a common ion. This coupling arises because the chemical potentials of the two solutes both depend on the concentration of the common ion. There is no consistent physical approximation in which it can properly be ignored (which incidentally raises an objection to recent work of Srinivasan and Tien<sup>11</sup>).

Second, all the calculations to date have dealt with ideal solutions, i.e., have ignored the variation with concentration of the activity coefficient of the solute. In many cases this is a reasonable thing to do; for example, in the range of ionic strengths 0.1 - 1 M, the mean activity coefficient of NaCl is a weak function of concentration, varying at most by about 8% from its mean value. However, the mean activity coefficient of CaSO<sub>4</sub> in mixed CaSO<sub>4</sub>-NaCl solutions is a much stronger function of ionic strength in the same range of ionic strengths, and it is not right to treat such a solution as ideal.

The coupling between solutes with a common ion and the non-ideality of the solution greatly complicate the calculation of concentration polarization. A further complication is introduced by the possibility that the rejections of different solutes by the membrane may be different. This is certainly true with ion-exchange membranes, which reject salts with divalent cations far better than salts with univalent cations. Even neutral membranes like cellulose acetate reject CaSO<sub>4</sub> far more completely than they do NaCl. These complications make a general solution of the problem of concentration polarization in multicomponent solutions rather difficult. Much of the difficulty can be avoided, however, if Ca<sup>++</sup> and SO<sub>4</sub><sup>--</sup> are only present in trace quantities, i.e., if they make a negligible contribution to the ionic strength. Owing to the sparing solubility of CaSO<sub>4</sub> in NaCl solutions, the assumption that Ca<sup>++</sup> and SO<sub>4</sub><sup>--</sup> are present only in trace amounts in solutions of moderate ionic strength is not a bad one, and we make it throughout the rest of this discussion.

In the calculations performed below, both laminar and turbulent flow across the membrane are considered. The velocity profiles are taken to be fully developed. In turbulent flow, the concentration profile develops rapidly, and we consider it to be fully developed even at the inlet. In laminar flow, both developing and fully developed concentration profiles are considered. When the concentration profile is fully developed, it is necessary to assume that the membrane is completely rejecting and that the water flux through it is constant down the channel, but when the concentration profile is developing, both of these restrictions can be relaxed. In laminar flow with fully developed concentration profiles, the computations are restricted to slit geometry. In laminar flow with developing concentration profiles, when the concentration polarization is small, or in turbulent flow, there is no such restriction.

Numerical results for trace  $\text{CaSO}_4$  in NaCl solutions are to be presented in Fig. 30. Directions for the use of this figure are given in Section H, and the reader who does not wish to explore the details of the calculations may go directly to Section H from this point. Section I gives a short discussion of the magnitude of the correction introduced by the coupling between solutes with a common ion and the non-ideality of the solution.

B. Basic equations:

The motion of ions in a dilute solution in either laminar or turbulent flow is made up of the following parts: convection, molecular diffusion, eddy diffusion (absent in laminar flow), and migration caused by electric fields. Ionic flow can be described by the following equations:

$$\vec{j}_i = \vec{v}c_i - D_i \nabla c_i - D_i c_i \nabla \ln \gamma_i - \frac{\vec{\epsilon}}{z_i} \cdot \nabla c_i + z_i c_i D_i \frac{\vec{FE}}{RT} \quad (1)$$

where

- $\vec{j}_i$  is the current density of ions of type i (moles  $\text{m}^{-2} \text{sec}^{-1}$ ),
- $\vec{v}$  is the bulk flow velocity of the solution ( $\text{m sec}^{-1}$ ),
- $c_i$  is the concentration of ions of type i (moles  $\text{m}^{-3}$ ),
- $\gamma_i$  is the practical activity coefficient of ions of type i,
- $D_i$  is the diffusion coefficient of ions of type i ( $\text{m}^2 \text{sec}^{-1}$ ),

$\vec{\epsilon}$  is the eddy diffusivity\* (= 0 in laminar flow)  $\text{m}^2 \text{sec}^{-1}$ ),

$z_i$  is the charge of ions of type  $i$  in units of the proton charge (eq mole<sup>-1</sup>),

$F$  is the Faraday (96,500 coulombs mole<sup>-1</sup>),

$\vec{E}$  is the electric field vector (volt  $\text{m}^{-1}$ ),

$R$  is the universal gas constant (8.315 joule mole<sup>-1</sup>deg<sup>-1</sup>), and

$T$  is the absolute temperature (deg.).

In addition to (1), the ionic concentrations obey the equation of electro-neutrality:

$$\sum_i z_i c_i = 0 \quad (2a)$$

In steady-state hyperfiltration no electric current flows:

$$\sum_i z_i \vec{j}_i = 0 \quad (2b)$$

We introduce the following notation: subscripts 1, 2, 3, and 4 refer, respectively, to  $\text{Na}^+$ ,  $\text{Cl}^-$ ,  $\text{Ca}^{++}$ , and  $\text{SO}_4^{--}$ . Primed quantities refer to NaCl, doubly primed quantities refer to  $\text{CaSO}_4$ . Using this notation, for example, we can write Nernst's relation between the diffusion coefficient of NaCl and those of  $\text{Na}^+$  and  $\text{Cl}^-$  in pure NaCl solutions as

$$D' = 2(D_1^{-1} + D_2^{-1})^{-1} \quad (3)$$

We account for the non-ideality of NaCl solutions containing trace quantities of  $\text{Ca}^{++}$  and  $\text{SO}_4^{--}$  by approximating

$$\frac{d\ln\gamma_1}{d\ln c'} = \frac{d\ln\gamma_2}{d\ln c'} = \frac{d\ln\gamma_{\pm}'}{d\ln c'} = \text{constant} \equiv -k' \quad (4a)$$

$$\frac{d\ln\gamma_3}{d\ln c'} = \frac{d\ln\gamma_4}{d\ln c'} = \frac{d\ln\gamma_{\pm}''}{d\ln c'} = \text{constant} \equiv -k'' \quad (b)$$

over the range of concentration being considered. In the range 0.1 - 1 M in NaCl,  $k' = 0.070$  and  $k'' = 0.465$ .<sup>12</sup>

\*Most generally, the eddy diffusivity is a tensor of second rank; cf., e.g., Turbulence, An Introduction to Its Mechanism and Theory, J. O. Henze, McGraw-Hill, New York, 1959, p. 25; especially equations (1-29) and (1-30).

When  $\text{Ca}^{++}$  and  $\text{SO}_4^{--}$  are present in trace amounts, the electric field is simply related to the concentration gradient of NaCl. For if  $c_3, c_4 \ll c_1, c_2$ , then (2a) becomes simply  $c_1 = c_2 = c'$ . Similarly (2b) becomes  $\vec{j}_1 = \vec{j}_2 = \vec{j}'$ . Substituting these values into (1) for  $i = 1$  and 2, and subtracting gives

$$\frac{\vec{FE}}{RT} = (1 - k') \frac{D_1 - D_2}{D_1 + D_2} \nabla \ln c' \quad (5a)$$

Multiplying (1) by  $D_i^{-1}$ , adding the equations for  $i = 1$  and 2, and taking the divergence, gives, for steady-state laminar flow ( $\vec{\epsilon} = 0$ )

$$\vec{v} \cdot \nabla c' - (1 - k') D' \nabla^2 c' = 0 \quad (5b)$$

an equation we need later.

We introduce a variable  $\Gamma$  which we call the concentration polarization defined by

$$\Gamma = \frac{c}{\bar{c}} - 1 \quad (6)$$

where  $\bar{c}$  is the cup-mixing concentration at the position down the channel being considered. The cup-mixing concentration is the concentration of the fluid that would be collected if the channel were chopped off at the position being considered and the fluid issuing forth collected in a cup. When the concentration boundary layers are thin and little water has been withdrawn (entrance region), the cup-mixing concentration is nearly the same as the feed concentration.

C. Small concentration polarization--laminar flow.

When  $\Gamma \ll 1$ , (5a) becomes

$$\frac{\vec{FE}}{RT} = (1 - k') \frac{D_1 - D_2}{D_1 + D_2} \nabla \Gamma' \quad (7)$$

Substituting (7) into (1) [with  $\vec{\epsilon} = 0$ ], we find for  $i = 3, 4$

$$\vec{j}_i = \vec{v}c_i - D_i \nabla c_i + a_i D_i c_i \nabla \Gamma' \quad (8)$$

where

$$a_1 = k'' + z_1(1 - k') \frac{D_1 - D_2}{D_1 + D_2} \quad (9)$$

Here we have used (4b) and also set

$$\nabla \ln c' = \frac{\nabla \Gamma'}{1 + \Gamma'} + \nabla \ln \bar{c}' \approx \nabla \Gamma' \quad (10)$$

To justify (10) we note that  $\nabla \ln \bar{c}'$ , which only has a component in the axial direction, is of the order  $v_w/\bar{u}\ell$ , where  $v_w$  is the transpiration velocity of the water at the wall,  $\bar{u}$  is the mean stream velocity in the axial direction, and  $\ell$  is the transverse dimension of the channel (e.g., half-width for a slit).  $\nabla \Gamma'$ , on the other hand, is of the order of  $\Gamma'_w/\delta$ , where  $\delta$  is the thickness of the concentration boundary layer, and the subscript  $w$  refers to the wall. For (10) to be a good approximation,  $1 \gg \Gamma' \gg v_w \delta/\bar{u}\ell$ . If  $v_w = 30 \text{ gal ft}^{-2} \text{ day}^{-1}$  and  $\bar{u} = 1 \text{ cm sec}^{-1}$ ,  $v_w/\bar{u} = 1.4 \times 10^{-3}$ . In the entrance region where the concentration profile is developing,  $\delta \ll \ell$ ; when the concentration profile is fully developed,  $\delta \sim \ell$ . Hence for practical purposes (10) should be good down to values of  $\Gamma'$  so low we are no longer interested ( $\lesssim 0.1\%$ ). It should be good up to values of  $\Gamma' \sim 10\%$ .

If we note that  $\nabla \cdot \vec{j}_i = \nabla \cdot \vec{v} = 0$  and take the divergence of (8) we get

$$\vec{v} \cdot \nabla \Gamma_i - D_i \nabla^2 \Gamma_i + a_i D_i \nabla^2 \Gamma' = 0 \quad (11)$$

to terms of lowest order in the  $\Gamma$ 's. The transition from  $c_i$  to  $\Gamma_i$  involves an argument similar to that given immediately above.

As a solution to (11) we try

$$\Gamma_i = \frac{a_i D_i}{D_i - (1 - k') D'} \Gamma' + \left( \frac{R_i}{R'} - \frac{a_i D_i}{D_i - (1 - k') D'} \right) \Lambda_i \quad (12)$$

where  $\Lambda_i$  is a function yet to be determined,  $R_i$  is the rejection of ion  $i$ , and  $R'$  is the rejection of NaCl. When we substitute (12) into (11), we find

$$\vec{v} \cdot \nabla \Lambda_i - D_i \nabla^2 \Lambda_i = 0 \quad (13)$$

since

$$\vec{v} \cdot \nabla \Gamma' - (1 - k') D' \nabla^2 \Gamma' = 0 \quad (14)$$

(14) follows from (5b).

According to (8), at the wall of the channel

$$\mathcal{R}_i v_w c_i - \mathcal{D}_i (\nabla c_i)_\perp + a_i \mathcal{D}_i c_i (\nabla \Gamma')_\perp = 0 \quad (15)$$

where the subscript  $\perp$  denotes the vector component normal to the wall. To lowest order in  $\Gamma_i$  (15) becomes

$$\mathcal{R}_i v_w - \mathcal{D}_i (\nabla \Gamma_i)_\perp + a_i \mathcal{D}_i (\nabla \Gamma')_\perp = 0 \quad (16)$$

To lowest order in  $\Gamma'$ ,

$$\mathcal{R}' v_w - (1 - k') \mathcal{D}' (\nabla \Gamma')_\perp = 0 \quad (17)$$

so that

$$\mathcal{R}' v_w - \mathcal{D}_i (\nabla \Lambda_i)_\perp = 0 \quad (18)$$

At the center of the channel  $\nabla \Gamma' = \nabla \Gamma_i = 0$  by symmetry, and therefore  $\nabla \Lambda_i = 0$  there also. If we compare (14) and (17) with (13) and (18), respectively, we see that  $\Lambda_i$  and  $\Gamma'$  obey the same differential equation and boundary conditions except for the replacement of  $\mathcal{D}_i$  by  $(1 - k') \mathcal{D}'$ . Thus,

$$\Lambda_i = \Gamma' [\mathcal{D}_i] \quad (19)$$

where the notation means that to evaluate  $\Lambda_i$  one evaluates  $\Gamma'$  at the same point using  $\mathcal{D}_i$  as the diffusion coefficient. Hence,

$$\Gamma_i = \frac{a_i \mathcal{D}_i}{\mathcal{D}_i - (1 - k') \mathcal{D}' } \Gamma' [(1 - k') \mathcal{D}'] + \left( \frac{\mathcal{R}_i}{\mathcal{R}'} - \frac{a_i \mathcal{D}_i}{\mathcal{D}_i - (1 - k') \mathcal{D}' } \right) \Gamma' [\mathcal{D}_i] \quad (20)$$

It should be remembered that  $\Gamma'$  refers to a membrane whose rejection is  $\mathcal{R}'$ .

Equation (20) is valid when  $\Gamma' \ll 1$  irrespective of whether the concentration profile is developing or fully developed. When  $v_w \ell / \mathcal{D} \ll 1$ , as might happen in a hollow fine fiber,  $\Gamma' \ll 1$  everywhere in the channel.<sup>13</sup> Then (20) can be used everywhere to calculate  $\Gamma_i$ . When  $v_w \ell / \mathcal{D}$  is not  $\ll 1$ ,  $\Gamma'$  is still  $\ll 1$  in the early entrance region. In the early entrance region,<sup>13</sup>

$$\Gamma' [\mathcal{D}'] = 1.536 \mathcal{R}' (\zeta')^{1/3} \quad (21a)$$

where

$$\zeta' = \frac{1}{3} \left( \frac{v_w \ell}{D'} \right)^2 \frac{v_w x}{\bar{u} \ell} \quad (21b)$$

$x$  is the axial distance from the inlet, and  $\ell$  is the half-width for a slit channel and three-quarters of the radius for a cylindrical channel. Equation (21a) is an asymptotic formula whose accuracy improves when  $\zeta'$  becomes smaller. At  $\zeta = .02$ , for example, where (21a) gives  $\Gamma' = 0.417$  when  $R' = 1$ , the error in  $\Gamma'$  is about -15%. Using (21a) in (20), we find

$$\Gamma_1 = R' \left[ \frac{a_1 D_1}{D_1 - (1 - k') D'} (1 - k')^{-2/3} + \left( \frac{R_1}{R'} - \frac{a_1 D_1}{D_1 - (1 - k') D'} \left( \frac{D'}{D_1} \right)^{2/3} \right) \right] \cdot 1.536 (\zeta')^{1/3} \quad (22)$$

D. Fully developed concentration profile--laminar flow:

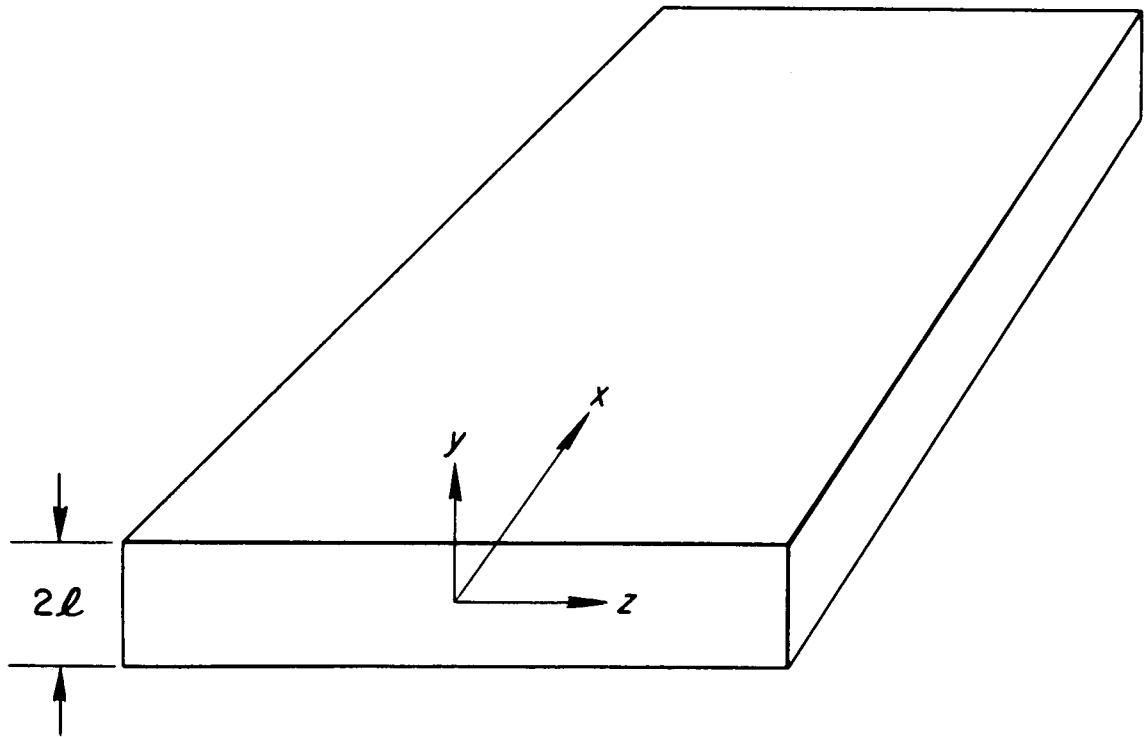
When the concentration profile is fully developed but  $\Gamma'$  is not  $\ll 1$ , we can solve for  $\Gamma_1$  if  $R' = R_1 = 1$  using the method outlined below. If  $R'$  and  $R_1 \neq 1$ , the computations become much more involved. For membranes for which salt rejections are close to 1, e.g., cellulose acetate, the added generality of not assuming  $R' = R_1 = 1$  is probably not worth the considerable increase in computational complexity, especially in view of the approximate nature of Equations (4) for the activity coefficients. These same remarks apply to the case of turbulent flow dealt with in sections E, F, and G.

Let us consider the flow to take place in a rectangular channel that is much wider than it is thick, and let us introduce the coordinates shown in Fig. 29. We take the components of the velocity  $\vec{v}$  to be

$$v_x = \bar{u}_0 \left( 1 - \frac{v_w x}{\bar{u}_0 \ell} \right) f'(\lambda) \quad (23a)$$

$$v_y = v_w f(\lambda) \quad (23b)$$

$$v_z = 0 \quad (23c)$$



HYPERFILTRATION CHANNEL BETWEEN PLANE  
PARALLEL MEMBRANES

- x - direction of brine flow (parallel to membranes)
- y - direction of product flow (perpendicular to membranes)
- $2l$  - width of channel (distance between membranes)

Fig. 29

and for the time being we drop the assumption that  $c_3, c_4 \ll c_1, c_2$ . Here

$\bar{u}_0$  is the mean stream velocity at the inlet ( $\text{m sec}^{-1}$ ),

$v_w$  is the (constant) permeation velocity at the wall ( $\text{m sec}^{-1}$ ),

$\ell$  is the half-thickness of the channel (m),

$\lambda = y/\ell$  (dimensionless), and

$f_\zeta$  is a dimensionless stream function which has the following properties:  $f_\zeta(0) = 0$ ,  $f_\zeta(1) = 1$ ,  $f'_\zeta(1) = 0$ . Berman<sup>14</sup> has determined  $f_\zeta(\lambda)$  for laminar flow.

Furthermore, we set  $\vec{\epsilon} = 0$  in laminar flow.

Since we are looking for a description of the fully developed concentration profiles, we try<sup>13,15</sup> solutions of the form

$$c_i = \left(1 - \frac{v_w x}{\bar{u}_0 \ell}\right)^{-1} Y_i(\lambda) \quad (24a)$$

$$E_x = 0 \quad (24b)$$

$$E_y = E_y(\lambda) \quad (24c)$$

Then

$$j_{ix} = \bar{u}_0 f'(\lambda) Y_i(\lambda) - \mathcal{D}_i \left(1 - \frac{v_w x}{\bar{u}_0 \ell}\right)^{-2} \frac{v_w}{\bar{u}_0 \ell} Y_i$$

$$- \mathcal{D}_i \left(1 - \frac{v_w x}{\bar{u}_0 \ell}\right)^{-1} Y_i \sum_j \frac{\partial \ln \gamma_i}{\partial \ln c_j} \left(1 - \frac{v_w x}{\bar{u}_0 \ell}\right)^{-1} \frac{v_w}{\bar{u}_0 \ell}$$
(25a)

The ratios of the second and third terms on the right to the first term are

of the order  $\frac{\mathcal{D}_i}{v_w \ell} \left(\frac{v_w}{\bar{u}_0}\right)^2$ . Now if  $\mathcal{D}_i/v_w \ell$  is, say  $> 10$ , there will be very

little concentration polarization.<sup>8,13</sup> On the other hand,  $v_w/\bar{u}_0 \sim 10^{-4}$  typically, so that the second and third terms on the right can be dropped.

Thus,

$$j_{ix} = \bar{u}_0 f'(\lambda) Y_i(\lambda) \quad (25b)$$

with good accuracy. From (25b) it follows at once that  $\frac{\partial j_{ix}}{\partial x} = 0$ , so that  $\frac{\partial j_{iy}}{\partial y} = 0$  since  $\text{div } \vec{j} = 0$ . Thus  $j_{iy} = j_{iy}(x)$ . But since  $j_{iy} = 0$  at  $y = \pm\ell$ ,  $j_{iy}$  must then vanish everywhere.

If we now insert (24a-c) into the y-component of (1), we get

$$\begin{aligned}
 0 = & v_{wc} f(\lambda) \left(1 - \frac{v_w x}{\bar{u}_o \ell}\right)^{-1} Y_i(\lambda) - \mathcal{D}_i \left(1 - \frac{v_w x}{\bar{u}_o \ell}\right)^{-1} \frac{1}{\ell} Y_i'(\lambda) \\
 & - \mathcal{D}_i \left(1 - \frac{v_w x}{\bar{u}_o \ell}\right)^{-1} Y_i \sum_j \frac{\partial \ln \gamma_i}{\partial \ln c_j} \frac{1}{\ell} \frac{Y_j'(\lambda)}{Y_j(\lambda)} \\
 & + z_i \left(1 - \frac{v_w x}{\bar{u}_o \ell}\right)^{-1} Y_i(\lambda) \mathcal{D}_i \frac{FE}{RT} Y
 \end{aligned} \tag{26a}$$

or

$$0 = \alpha_i f(\lambda) Y_i(\lambda) - Y_i'(\lambda) - Y_i(\lambda) \frac{d \ln \gamma_i}{d \lambda} + z_i \frac{FE}{RT} \ell Y_i(\lambda) \tag{27}$$

where  $\alpha_i$  is an abbreviation for the Péclet number  $\frac{v_w \ell}{\mathcal{D}_i}$ .

Equation (27) can then be written

$$\frac{Y_i'(\lambda)}{Y_i(\lambda)} = \alpha_i f(\lambda) - \frac{d \ln \gamma_i}{d \lambda} + z_i \frac{FE}{RT} \ell \tag{28}$$

which can be integrated to give

$$\frac{Y_i(\lambda)}{Y_i(0)} \cdot \frac{\gamma_i(\lambda)}{\gamma_i(0)} = \exp \left[ \alpha_i g(\lambda) - z_i \frac{F\phi(\lambda)}{RT} \right] \tag{29a}$$

where

$$\phi(\lambda) \equiv -\ell \int_0^\lambda E_y d\lambda \tag{29b}$$

and

$$g(\lambda) = \int_0^\lambda f(\lambda) d\lambda \tag{29c}$$

The unknown potential  $\phi$  can be eliminated from these equations in the following way. Suppose there is a molecule which upon dissociation gives  $v_i$  ions of type  $i$ . Then the integers  $v_i$  obey the relation

$$\sum_i v_i z_i = 0 \quad (30)$$

The mean activity  $a_{\pm}$  of the ions forming this molecule is proportional to

$$\prod_i (Y_i \gamma_i)^{v_i / \sum_i v_i} \quad (31)$$

Using (31), (30), and (29a) we see that

$$\frac{a_{\pm}(\lambda)}{a_{\pm}(0)} = \exp \left( \frac{\sum_i v_i \alpha_i}{\sum_i v_i} g(\lambda) \right) \quad (32)$$

When the component is a binary electrolyte

$$\frac{\sum_i v_i \alpha_i}{\sum_i v_i} \equiv \alpha = \frac{v_w \ell}{D_{\text{Nernst}}} \quad (33a)$$

where

$$D_{\text{Nernst}} = \left( \frac{\sum_i v_i / D_i}{\sum_i v_i} \right)^{-1} \quad (33b)$$

is Nernst's classical expression for the diffusion coefficient of a salt in terms of the diffusion coefficients of its constituent ions.

Equation (32) is quite general and does not depend on the assumption that any ions are present only in trace amounts. It says that the profile of mean ionic activity of any molecular component present in the solution depends only on the diffusion coefficient of that component, on  $\ell$ , and on  $v_w$ . The profiles of mean ionic activity are not complete information because we do not yet know how to normalize them. To proceed with this normalization, we now assume  $c_3, c_4 \ll c_1, c_2$ . Electroneutrality then requires that  $Y_1 = Y_2 \propto c'$ . Then for  $i=1$  or  $2$ ,  $\gamma_i(\lambda)/\gamma_i(0) = [c'(\lambda)/c'(0)]^{-k'} =$

$[Y_i(\lambda)/Y_i(0)]^{-k'}$ . Hence (29a) becomes

$$Y_i(\lambda) = Y_i(0) \exp \left[ (1 - k')^{-1} (\alpha_i g(\lambda) - z_i \frac{F \phi(\lambda)}{RT}) \right], \quad i = 1, 2 \quad (34)$$

Electroneutrality ( $Y_1 = Y_2$  for all  $\lambda$ ) requires that the exponents in (34) for  $i = 1$  and  $i = 2$  be equal. Thus

$$\frac{F\phi(\lambda)}{RT} = (1/2) (\alpha_1 - \alpha_2) g(\lambda) \quad (35)$$

Also since  $\gamma'_{\pm}(\lambda)/\gamma'_{\pm}(0) = [c'(\lambda)/c'(0)]^{-k'}$ , we have from (32)

$$c'(\lambda) = c'(0) \exp[(1 - k')^{-1} \alpha' g(\lambda)] \quad (36)$$

Now since  $\gamma_i(\lambda)/\gamma_i(0) = [c'(\lambda)/c'(0)]^{-k''}$  for  $i = 3, 4$  we have from (29a)

$$Y_i(\lambda) = Y_i(0) \exp[\beta_i g(\lambda)], \quad i = 3, 4 \quad (37a)$$

$$\beta_3 = \alpha_3 - \alpha_1 + \alpha_2 + k'' (1 - k')^{-1} \alpha' \quad (37b)$$

$$\beta_4 = \alpha_4 + \alpha_1 - \alpha_2 + k'' (1 - k')^{-1} \alpha' \quad (37c)$$

In the NaCl molality range, 0.1 - 1.0 molal  $k' (1 - k')^{-1} = 0.500$ .

The mixing-cup concentrations of  $\text{Ca(II)}$  and  $\text{SO}_4^{--}$  are given by

$$\bar{Y}_i = \int_0^1 \frac{f'(\lambda)}{\bar{c}} Y_i(\lambda) d\lambda, \quad i = 3, 4 \quad (38)$$

The quantity

$$\Gamma_i(\beta_i) \equiv \frac{Y_i(1)}{\bar{Y}_i} - 1 = \frac{\exp[\beta_i g(1)]}{\int_0^1 \frac{f'(\lambda)}{\bar{c}} \exp[\beta_i g(\lambda)] d\lambda} - 1 \quad (39)$$

has been calculated by the author<sup>13</sup> and Gill<sup>8</sup> when  $f(\lambda)$  is the stream function of Poiseuille flow in a slit, namely,  $f(\lambda) = (1/2)\lambda(3 - \lambda^2)$ . Gill gives his results in the two formulas

$$\Gamma(\alpha) = 0.485\alpha + 0.107\alpha^2 + 0.01335\alpha^3 \quad \alpha \leq 6.25 \quad (40a)$$

$$\Gamma(\alpha) = \frac{\alpha^2}{3} \left( 1 + \frac{1}{\alpha} - \frac{14}{\alpha^2} \right) \quad \alpha \geq 6.25 \quad (40b)$$

Berman<sup>14</sup> has shown that it is very accurate to take  $f(\lambda) = (1/2)\lambda(3 - \lambda^2)$  when the transverse Reynolds number  $v_w \ell / \mu_k \ll 1$ , a condition that is usually amply fulfilled in hyperfiltration. The symbol  $\mu_k$  indicates kinematic viscosity,  $\mu/\rho$ ,  $\mu$  being fluid viscosity ( $\text{kg m}^{-1} \text{sec}^{-1}$ ) and  $\rho$ , fluid density ( $\text{kg m}^{-3}$ ).

E. Turbulent flow:

In fully developed turbulent flow, the concentration profile develops fully in only a few channel thicknesses (about 5 at a Reynolds number of  $10^4$ ). We call this distance the entrance length. If we perturb the asymptotic concentration profile at any point, the perturbation dies out in about one entrance length. If the physical properties of the system which vary with  $x$ , namely  $\bar{u}$ , the mean stream velocity, and the  $\bar{c}_i$ , the mixing-cup ionic concentrations, vary little in one entrance length, then it is a good approximation to neglect their  $x$ -dependence in (1) and treat them as constants. After solving (1), we then replace  $\bar{u}$  and the  $\bar{c}_i$  by their actual  $x$ -dependent values. This is an excellent approximation here, since with  $v_w/\bar{u} = 10^4$ ,  $\bar{u}$  and the  $\bar{c}_i$  change by the order of only 0.1% in an entrance length. Then (1) becomes\*

$$0 = v_w c_i - D_i \frac{\partial c_i}{\partial y} - D_i c_i \frac{\partial \ln \gamma_i}{\partial y} - \epsilon_{yy} \frac{\partial c_i}{\partial y} + z_i c_i D_i \frac{FE}{RT} \quad (41)$$

In engineering practice, lengths and times appearing in the theory of turbulent flow are made dimensionless using the wall-shear velocity

$$u_* = (\tau_w/\rho)^{1/2} = \bar{u} (f/2)^{1/2} \quad (42a)$$

and the kinematic viscosity,  $\mu_k$ , where

$$\tau_w \text{ is the wall shear} = \frac{f}{2} \rho \bar{u}^2 \quad (\text{kg m}^{-1} \text{sec}^{-2}), \text{ and}$$

$f$  is Fanning's friction factor (dimensionless).

---

\* As before,  $j_{ix} = u c_i$  is taken independent of  $x$ ,  $\frac{\partial j_{ix}}{\partial x} = 0 = \frac{\partial j_{iy}}{\partial y}$ . Since  $j_{iy} = 0$  at the wall, it must vanish for all  $y$ . Also it is acceptable to replace  $v_y$  by  $v_w$  since the concentration boundary layer is thin compared with the thickness of the channel. We keep only the  $yy$ -component of  $\vec{\epsilon}$ , which is equivalent to ignoring the contribution to the  $y$ -component of  $\vec{j}_i$  due to  $\partial c_i / \partial x$ .

In terms of these parameters, (41) becomes

$$0 = \sigma_i v_+ + (1 + \sigma_i \frac{\epsilon_{yy}}{\mu_k}) \frac{d \ln c_i}{dy_+} + \frac{d \ln \gamma_i}{dy_+} + z_i \eta \quad (43)$$

where

$\sigma_i = \frac{\mu_k}{D_i}$  is the Schmidt number of ion  $i$ ,

$v_+ = v_w/u_*$  is the dimensionless permeation velocity,

$y_+ = u_*(\ell - y)/\mu_k$  is the dimensionless distance from the wall, and

$\eta = \mu_k F E_y / RT u_*$  is the dimensionless electric field.

Henceforth, we drop the subscript  $y$  on  $\epsilon$ .

F. Constant activity coefficients:

For the sake of simplicity, we first assume that the activity coefficients are constant over the range of concentrations being considered.

First, let us consider a solution containing only  $\text{NaCl}^*$ . Then the third term on the right hand side of (43) drops out. Then

$$c_1 = c' \quad (44a)$$

$$c_2 = c' \quad (44b)$$

$$z_1 + z_2 = 0 \quad (44c)$$

where primed quantities refer to the binary electrolyte (NaCl). Equation (43) now becomes for  $1$  and  $2$

$$0 = \sigma_1 v_+ + (1 + \sigma_1 \frac{\epsilon}{\mu_k}) \frac{d \ln c'}{dy_+} + z_1 \eta \quad (45a)$$

$$0 = \sigma_2 v_+ + (1 + \sigma_2 \frac{\epsilon}{\mu_k}) \frac{d \ln c'}{dy_+} + z_2 \eta \quad (45b)$$

---

\*The procedure outlined here can also be followed when the supporting electrolyte is unsymmetrical, but we do not need the results in these cases. The details are slightly different, and the formulas somewhat more cumbersome.

If we add (45a) and (45b), we get

$$0 = (\sigma_1 + \sigma_2)v_+ + [2 + (\sigma_1 + \sigma_2)\frac{\epsilon}{\mu_k}] \frac{d\ln c'}{dy_+} \quad (46)$$

or

$$\frac{d\ln c'}{dy_+} = - \frac{v_+}{\frac{2}{\sigma_1 + \sigma_2} + \frac{\epsilon}{\mu_k}} = - \frac{v_+}{\frac{1}{\sigma'} + \frac{\epsilon}{\mu_k}} \quad (47)$$

where  $\sigma$  is the Schmidt number of the binary electrolyte calculated using the Nernst value [Eq. (33b)] of the diffusion coefficient. Equation (47) can be integrated at once to give

$$\ln\left(\frac{c'(0)}{c'(y_+)}\right) = v_+ \int_0^{y_+} \frac{dy_+}{\frac{1}{\sigma'} + \frac{\epsilon}{\mu_k}} \quad (48)$$

Deissler<sup>16</sup> gives the dependence of  $\epsilon/\mu_k$  on distance  $y_+$  from the wall\* as

$$\frac{\epsilon}{\mu_k} = n^2 u_+ y_+ [1 - \exp(-n^2 u_+ y_+)], \quad n = 0.124 \quad (49a)$$

where

$$u_+ = y_+, \quad y_+ \leq 5 \quad (49b)$$

$$u_+ = -3.05 + 5.00 \ln y_+, \quad 5 \leq y_+ \leq 26 \quad (49c)$$

and

$$\frac{\epsilon}{\mu_k} = \frac{y_+}{2.777}, \quad y_+ \geq 26 \quad (49d)$$

Using these expressions, we can evaluate the integral in Eq. (48) and find

---

\* This is only one of many acceptable equations giving the eddy diffusivity as a function of distance from the wall. It is based on an impermeable wall. We assume here that the small permeation that occurs in hyperfiltration has no appreciable effect on the variation of  $\epsilon$  with distance from the wall.

the  $y_+$ -dependence of  $c$ . Deissler's work has shown that for Schmidt numbers  $\sigma$  greater than 100, the overwhelming bulk of the integral in Eq. (48) comes from points which  $y_+ < 10$ . Thus for  $y_+ > 10$ ,  $c$  is effectively constant. The constant value we denote by  $\bar{c}$ . Deissler also gives the value of the integral in Eq. (48) when the upper limit is  $> 10$  through the result<sup>17</sup>

$$\ell_+ = \int_0^{y_+ > 10} \frac{dy_+}{1 + \sigma \frac{\epsilon}{\mu_k}} = 8.95\sigma^{-1/4} \quad (50)$$

Then

$$\frac{c'(0)}{\bar{c}'} = \exp(v_+ \sigma' \ell_+') \quad (51)$$

Now that we know the  $y_+$ -dependence of  $c'$  (in principle at least), we can find  $\eta$ . If we subtract (45b) from (45a) and use (47) for  $d \ln c' / dy_+$ , we get

$$\eta = -v_+ \frac{\sigma_1 - \sigma_2}{z_1 - z_2} \cdot \frac{1}{1 + \sigma' \frac{\epsilon}{\mu_k}} \quad (52)$$

Using the value of  $\eta$  given in Eq. (52), we can solve (43) for any trace component  $i$ . The result turns out to be

$$\ln \left( \frac{c_i(0)}{c_i(y_+)} \right) = \sigma_i v_+ \int_0^{y_+} \frac{dy_+}{1 + \sigma_i \frac{\epsilon}{\mu_k}} - \frac{z_i v_+}{\sigma' - \sigma_i} \frac{\sigma_1 - \sigma_2}{z_1 - z_2} \left( \sigma' \int_0^{y_+} \frac{dy_+}{1 + \sigma' \frac{\epsilon}{\mu_k}} - \sigma_i \int_0^{y_+} \frac{dy_+}{1 + \sigma_i \frac{\epsilon}{\mu_k}} \right) \quad (53)$$

When  $y_+ > 10$ , we get

$$\frac{c_i(0)}{\bar{c}_i} = \exp \left[ v_+ \left( \sigma_i \ell_{+i} - z_i \frac{\sigma_1 - \sigma_2}{z_1 - z_2} \frac{\sigma_i \ell_{+i} - \sigma' \ell'_+}{\sigma_i - \sigma'} \right) \right] \quad (54)$$

Using (54) we can show easily that

$$\left[ \frac{c_3(0)c_4(0)}{\bar{c}_3\bar{c}_4} \right]^{1/2} = \exp(1710 v_+) \quad (55)$$

for trace  $\text{CaSO}_4$  in  $\text{NaCl}$ . Diffusion coefficients were obtained via the Nernst equation from limiting ionic conductances (see, for example, Ref. 18, p. 231).

G. Activity coefficients not constant:

If the activity coefficients in (43) are not constant, we may proceed as follows when  $\nu_1 = \nu_2 = 1$ . If we add (43) for  $i = 1$  and  $i = 2$  and divide by 2, we get

$$0 = \sigma' v_+ = \left( 1 + \sigma' \frac{\epsilon}{\mu_k} + \frac{d \ln \gamma'_\pm}{d \ln c'} \right) \frac{d \ln c'}{d y_+} \quad (56)$$

where  $\gamma'_\pm = (\gamma_1 \gamma_2)^{1/2}$  is the mean activity of the binary electrolyte formed from ions 1 and 2. If we can treat  $d \ln \gamma'_\pm / d \ln c'$  as a constant over the range of concentration involved, (56) becomes formally identical with (47)

if we replace  $\sigma'$  by  $\hat{\sigma} = \sigma' \left( 1 + \frac{d \ln \gamma'_\pm}{d \ln c'} \right)^{-1} = \sigma' / (1 - k')$ , i.e.,

$$0 = \hat{\sigma} v_+ + (1 + \hat{\sigma} \frac{\epsilon}{\mu_k}) \frac{d \ln c'}{d y_+} \quad (57)$$

from which it follows at once that

$$\frac{c'(0)}{\bar{c}'} = \exp (v_+ \hat{\sigma} \hat{\ell}_+) \quad (58)$$

If we subtract (43) for  $i = 2$  from (43) for  $i = 1$  and consider  $\ln(\gamma_1/\gamma_2)$  to be constant over the range of concentrations considered, then we get

$$\eta = - \frac{\sigma_1 - \sigma_2}{z_1 - z_2} \left( v_+ + \frac{\epsilon}{\mu_k} \frac{d \ln c'}{dy_+} \right) \quad (59a)$$

$$= - \frac{\sigma_1 - \sigma_2}{z_1 - z_2} \frac{v_+}{1 + \hat{\sigma} \frac{\epsilon}{\mu_k}} \quad (59b)$$

Inserting this in (43) we can solve for the trace ions

$$\frac{c_i(0)}{\bar{c}_i} = \exp \left[ v_+ \left( \sigma_i \ell_i - \left[ z_i \frac{\sigma_1 - \sigma_2}{z_1 - z_2} - \hat{\sigma} k'' \right] \frac{\sigma_i \ell_i - \hat{\sigma} \ell_+}{\sigma_i - \hat{\sigma}} \right) \right] \quad (60)$$

For trace  $\text{CaSO}_4$  in  $\text{NaCl}$ ,

$$\left[ \frac{c_3(0)c_4(0)}{\bar{c}_3 \bar{c}_4} \right]^{1/2} = \exp (2090 v_+) \quad (61)$$

H. Numerical results for trace  $\text{CaSO}_4$  in  $\text{NaCl}$  Solutions in laminar flow:

The concentration polarization  $\Gamma''$  of trace  $\text{CaSO}_4$  is defined by

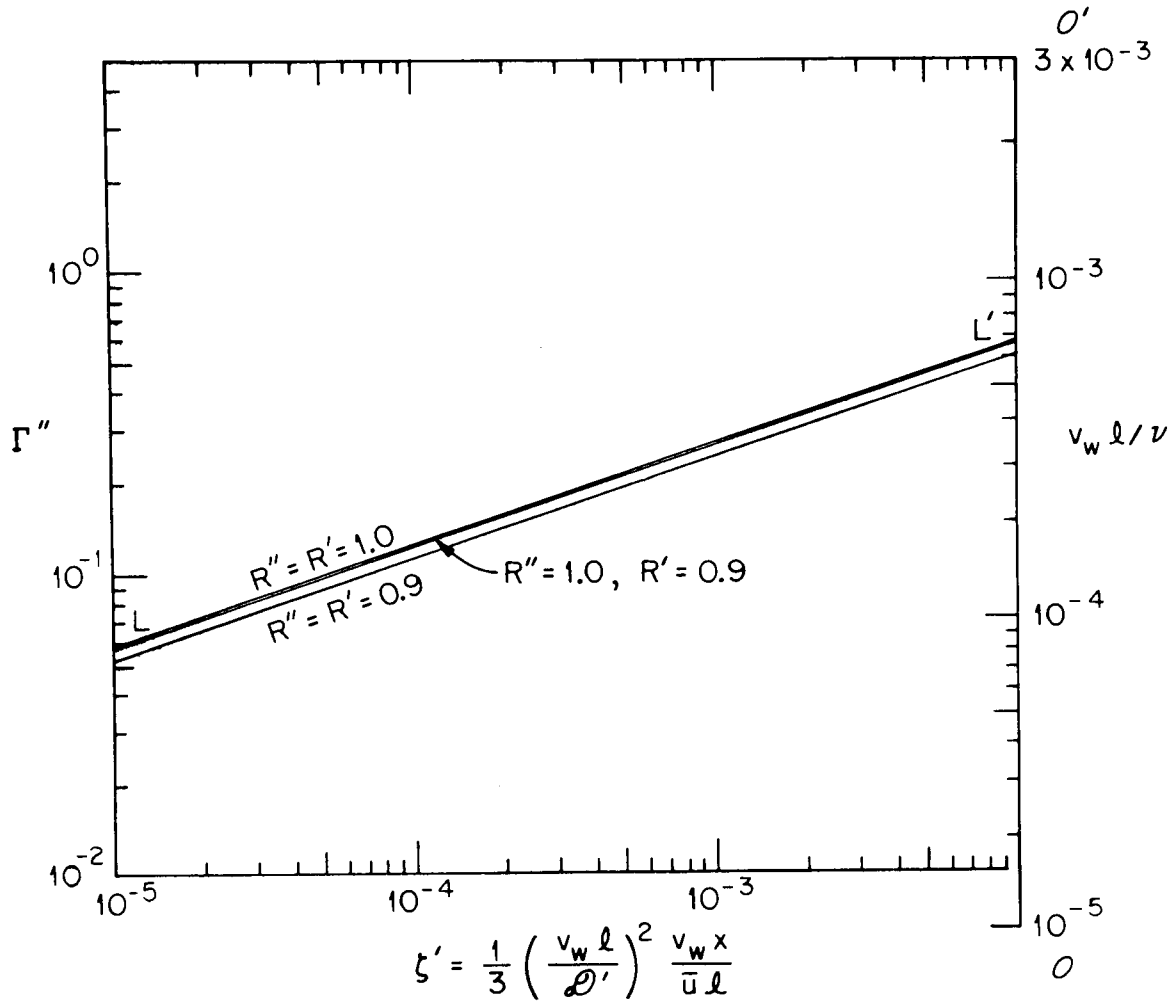
$$\Gamma'' = [(1 + \Gamma_3)(1 + \Gamma_4)]^{1/2} - 1 \quad (62)$$

so that  $(1 + \Gamma'')$  represents the ratio of the mean ionic concentration of  $\text{CaSO}_4$  at the membrane to the cup-mixing mean ionic concentration of  $\text{CaSO}_4$ . (The mean ionic concentration of  $\text{CaSO}_4$  is defined as  $\sqrt{[\text{Ca}^{++}][\text{SO}_4^{--}]}$ ).

Since solubility is a function of the product of the ion concentrations, concentration polarization in terms of the mean ionic concentration is appropriate for the present purposes.

When the membrane rejects all ions completely and the flow is laminar,  $\Gamma''$  can be obtained from the chart shown in Fig. 30. The chart is used as follows. The value of  $v_w \ell / \mu_k$  is located on the vertical scale  $00'$  at the right and a horizontal line is drawn through it. This line represents the asymptotic value of  $\Gamma''$  far downstream where the concentration profile is

ORNL-DWG. 72-10178



CONCENTRATION POLRIZATION OF TRACE  $\text{CaSO}_4$   
IN  $\text{NaCl}$  SOLUTIONS - LAMINAR FLOW

Fig. 30

fully developed. This value of  $\Gamma''$  is calculated from (62) using (39) to determine  $\Gamma_3$  and  $\Gamma_4$ .

The horizontal line should now be extended to the left until it intersects the oblique line  $LL'$  entering the chart from the left.  $LL'$  has been calculated from (62) and (22). The horizontal line and the oblique line  $LL'$  intersect in a point. The sharp corner at the point is now replaced by a smooth curve fairing one line into the other. The left-hand part of  $LL'$ , the right-hand part of the horizontal line, and the curved arc joining them now give  $\Gamma''$  for all values of  $\zeta'$ .

When the membrane does not reject all the ions completely, the line  $LL'$  must be shifted parallel to itself by an amount which is readily determined from (62) and (22). Shown in Fig. 30 are lines corresponding to the conditions  $\mathcal{R}_3 = \mathcal{R}_4 = 1$ , and  $\mathcal{R}' = 0.9$  and  $\mathcal{R}_3 = \mathcal{R}_4 = 0.9$ ,  $\mathcal{R}' = 0.9$ . (When  $\mathcal{R}_3 = \mathcal{R}_4$ , their common value is denoted by  $\mathcal{R}''$ .)

To correct the horizontal line for the effects of incomplete rejection, we use (20) when the asymptotic concentration polarization is small compared with one. When  $\Gamma'[\mathcal{D}'] \ll 1$ , it can be represented as\*

$$\Gamma[\mathcal{D}'] = 0.485 \frac{v \ell}{\mathcal{D}'} \cdot \exp[-0.634(1 - \mathcal{R}')] \quad (63)$$

for  $0.6 \leq \mathcal{R}' \leq 1$ . Substituting (63) into (20) and using (62) in the form  $\Gamma'' = (1/2)(\Gamma_3 + \Gamma_4)$ , we find, if  $\mathcal{R}_3 = \mathcal{R}_4 = \mathcal{R}''$ ,

$$\Gamma'' = [k''(1 - k')^{-1} + \mathcal{R}''\mathcal{D}'/\mathcal{R}'\mathcal{D}''] \exp[-0.634(1 - \mathcal{R}')] \cdot 0.485 \left( \frac{v \ell}{\mathcal{D}'} \right) \quad (64)$$

Here,  $\mathcal{D}'' = 2(\mathcal{D}_3^{-1} + \mathcal{D}_4^{-1})^{-1}$ . Comparing (64) for  $\mathcal{R}'' = \mathcal{R}' = 1$  with (64) for any  $\mathcal{R}''$  and  $\mathcal{R}'$ , we see that the horizontal line needs to be corrected by the factor

$$\begin{aligned} & (k''(1 - k')^{-1} + \mathcal{R}''\mathcal{D}'/\mathcal{R}'\mathcal{D}'') \exp[-0.634(1 - \mathcal{R}')] / (k''(1 - k')^{-1} + \mathcal{D}'/\mathcal{D}'') \\ &= \frac{1.78\mathcal{R}'' + 0.50\mathcal{R}'}{2.28\mathcal{R}'} \exp[-0.634(1 - \mathcal{R}')] \end{aligned} \quad (65)$$

\*Equation (63) is based on the first term of (40a) and the numerical calculations given in Fig. 32 of reference 10.

For illustrative purposes, let us consider a system in laminar flow wherein the following conditions prevail:

$$v_w = 7 \times 10^{-4} \text{ cm sec}^{-1}, \text{ (flux } \sim 15 \text{ gfd);}$$

$$\ell = 0.5 \text{ cm;}$$

$$\mu_k = 0.01 \text{ cm}^2 \text{ sec}^{-1};$$

$$D' = 0.913 \times 10^{-5} \text{ cm}^2 \text{ sec}^{-1};$$

and  $\bar{u} = 1 \times 10^2 \text{ cm sec}^{-1}$ .

Then,

$$\frac{v_w \ell}{\mu_k} = 3.5 \times 10^{-2},$$

which is far off-scale at the top of Fig. 30. This illustrates that for many practical systems,  $\Gamma''$  does not reach asymptotic values, i.e., the concentration profile is not fully developed, until far downstream. Either the flux or the dimensions of the channel, or their product, would have to be smaller by two orders of magnitude for asymptotic conditions to be reached within the confines of Fig. 30. Such channel dimensions would be more like those in hollow fiber and spiral wound configurations, but the flow patterns in the commercial units used in this work are too complicated for quantitative description. For the channels specified here, however, we can determine from Fig. 30 the concentration polarization in the first few millimeters of the channel. We have

$$\zeta' = \frac{v_w^3 \ell x}{3(D')^2 \bar{u}} = 0.00686 \times$$

Thus, at  $x = 0.1 \text{ cm}$ ,  $\zeta' = 6.86 \times 10^{-4}$ , and from Fig. 30, for  $R'' = R' = 1.0$

$$\Gamma'' \approx 0.23, \quad \text{or} \quad c_\alpha \approx 1.23 \bar{c}.$$

At  $x = 1.0 \text{ cm}$ ,  $\zeta' = 6.86 \times 10^{-3}$ , and, again for  $R'' = R' = 1.0$ ,

$$\Gamma'' \approx 0.51, \quad \text{or} \quad c_\alpha \approx 1.51 \bar{c}.$$

#### I. Effect of common ion and of non-ideality of solutions:

In this section we discuss the correction to the simple "two-component" theory introduced by the coupling between solutes with a common ion and the

non-ideality of NaCl solutions containing trace amounts of CaSO<sub>4</sub>. Perhaps the easiest place to begin is with the case of section D, fully developed concentration profile--laminar flow, with slit geometry. The concentration polarization for Ca(II) and SO<sub>4</sub><sup>2-</sup> is given by (39). When the concentration polarization is small so that we can use only the first term of (40a), it follows from (37b, c) that

$$\Gamma'' = 0.485\alpha'' + k''(1 - k')^{-1} \cdot 0.485\alpha' \quad (66)$$

where  $\alpha'' = (\alpha_3 + \alpha_4)/2 = v_w \ell / D''_{\text{Nernst}}$ . The term  $0.485\alpha''$  is the concentration polarization that one would calculate on the assumption that the feed solution contained only CaSO<sub>4</sub> and the solution was ideal; the term  $0.485\alpha'$  is the corresponding quantity for NaCl. The second term in (66) represents a correction to the simple "two-component" theory, and it is clearly substantial ( $\sim 28\%$  of the first term) since the concentration polarization for CaSO<sub>4</sub> and NaCl are comparable and  $k''(1 - k')^{-1} = 0.500$ . Interestingly, when the solution is ideal, the common-ion effect disappears for small concentration polarization (i.e., when we can confine ourselves to using the first term of (40a)).

While the disappearance of the common-ion effect for ideal solutions cannot be a general phenomenon, it is a good approximation for the system NaCl-trace CaSO<sub>4</sub> even when the concentration polarization is not small, as the figures in Table XII show. This table gives the concentration polarization of CaSO<sub>4</sub> for perfectly rejecting membranes in a slit channel for laminar flow with a fully developed concentration profile for several values of  $v_w \ell / \mu_k$ , for the three conditions: ideal CaSO<sub>4</sub> solutions; trace CaSO<sub>4</sub> in ideal NaCl solutions; and trace CaSO<sub>4</sub> in non-ideal NaCl solutions. A comparison of the values in the third column with those in the other two demonstrates that the common-ion effect and the non-ideality of NaCl solutions containing trace CaSO<sub>4</sub> increase the concentration polarization of the trace CaSO<sub>4</sub> by a substantial margin (about 30-50% over the range of the table) over what would be expected from the simple "two-component" theory.

TABLE XII. CONCENTRATION POLARIZATION IN LAMINAR FLOW WITH A FULLY DEVELOPED CONCENTRATION PROFILE

$\frac{v_w \ell}{\mu_k}$	$\Gamma$ for $\text{CaSO}_4$ in $\text{CaSO}_4$ Solns. (Constant $\gamma$ )	$\Gamma$ for Trace $\text{CaSO}_4$ in $\text{NaCl}$ Solns.	
		Constant $\gamma$	Variable $\gamma$
$3 \times 10^{-5}$	.01609	.01608	.02065
$10^{-4}$	.05454	.05453	.07035
$3 \times 10^{-4}$	.1718	.1717	.2246
$10^{-3}$	.6788	.6785	.9305
$3 \times 10^{-3}$	3.233	3.228	4.946

A similar situation prevails for laminar flow in the early entrance region, again assuming slit geometry. There the results are given by (22) and (62) and are most conveniently stated by giving  $\Gamma_{\text{CaSO}_4}$  as a multiple of  $1.536(\zeta')^{1/3}$ , which, for trace  $\text{CaSO}_4$  in  $\text{NaCl}$ , is equal to  $\Gamma_{\text{NaCl}}$  (see Section VII.B in Ref. 10). The ratio,  $\Gamma_{\text{CaSO}_4} / \Gamma_{\text{NaCl}}$ , is given in Table XIII for the same three cases as in Table XII assuming perfectly rejecting membranes.

TABLE XIII. CONCENTRATION POLARIZATION IN LAMINAR FLOW IN EARLY ENTRANCE REGION

$\Gamma_{\text{CaSO}_4} / \Gamma_{\text{NaCl}}$	$\text{CaSO}_4$ in $\text{CaSO}_4$ Solns. (Constant $\gamma$ )	Trace $\text{CaSO}_4$ in $\text{NaCl}$ Solns.	
		Constant $\gamma$	Variable $\gamma$
	1.46	1.47	1.76

The value 1.46 in the first column is derived from a value for  $\Gamma_{\text{NaCl}}$  which would be calculated if  $\text{NaCl}$  was present under the same conditions as the  $\text{CaSO}_4$ .

In turbulent flow, for any geometry, it is convenient to discuss the coefficient of  $v_+$ ,  $\zeta \equiv \sigma' \ell_+$ ; in the exponents in (51), (55), and (61).

For ideal solutions of  $\text{CaSO}_4$  (constant  $\gamma$ ),  $\zeta$  has the value 1700, which differs little from its value of 1710 for trace  $\text{CaSO}_4$  in ideal  $\text{NaCl}$  solutions. However, for trace  $\text{CaSO}_4$  in real  $\text{NaCl}$  solutions (variable  $\gamma$ ),  $\zeta$  has a value 2090. For small concentration polarizations, where a linear approximation to the exponentials in (51), (55), and (61) can be used, this corresponds to a 22% correction to concentration polarizations calculated by the "two component" theory. For large concentration polarizations, the correction is even larger.

The results in this section indicate that neglect of the common-ion effect on concentration polarization of  $\text{CaSO}_4$  is of relatively minor importance, but that failure to consider variation of activity coefficients has a much larger effect on  $\Gamma_{\text{CaSO}_4}$ . However, for practical purposes, the decrease in activity coefficient of calcium sulfate with increasing sodium chloride concentration, which causes the higher buildup at the interface, also implies an increase in calcium sulfate solubility. So far as prediction of occurrence of scale formation, therefore, the two effects are to some extent compensating.

It may be of interest to make a sample calculation of concentration polarization under turbulent flow conditions in which we take into account the common ion effect and the effect of non-ideality of solutions, and to compare the results with those obtained by the "two-component" theory for ideal solutions. Consider, then, a system in which the brine circulation velocity,  $\bar{u}$ , is 90 cm/sec ( $\sim 3$  fps), the permeation velocity,  $v_w$ , is  $7 \times 10^{-4}$  cm/sec (flux  $\sim 15$  gfd), and the geometry is such that the Reynold's number,  $N_{\text{Re}}$ , is 10,000.

We wish first to evaluate  $v_+ = v_w/u_*$ , using equation (42a) to find the wall-shear velocity,  $u_*$ . Values for  $f$ , Fanning's friction factor, may be obtained as a function of  $N_{\text{Re}}$  in a number of standard reference books.<sup>19</sup> For  $N_{\text{Re}} = 10,000$  in a smooth-walled system,  $f \sim 0.008$ , and  $v_+ = 1.23 \times 10^{-4}$ . Then, from  $\Gamma_{\text{CaSO}_4} = \exp(\zeta v_+) - 1 = \exp(2090 \times 1.23 \times 10^{-4}) - 1$ , we find that  $\Gamma_{\text{CaSO}_4} = 0.293$ .

Consider further a system that, at the membrane-feed interface, is saturated at 25°C in  $\text{CaSO}_4$  and 0.05 M in  $\text{NaCl}$ . Then, from Marshall and Slusher (Ref. 12, p. 4017),  $c_\alpha = 0.0194$ , and from  $\Gamma_{\text{CaSO}_4} + 1 = (c_\alpha/\bar{c}) = 1.293$ ,

we find  $\bar{c}$ , the concentration of  $\text{CaSO}_4$  in the bulk solution that will produce saturation at the wall under the conditions of this calculation, to be 0.015 M.

For the two-component, ideal solution case,  $v_+$  is the same as above,  $1.23 \times 10^{-4}$ , but  $\zeta$  is 1700 rather than 2090. Thus,  $\Gamma_{\text{CaSO}_4} = 0.233$ . The saturation concentration of  $\text{CaSO}_4$  in pure water is 0.0151 M, and consequently  $\bar{c} = 0.0151 \text{ M} / 1.233 = 0.0122 \text{ M}$ , which is the concentration of  $\text{CaSO}_4$  in the bulk feed that would produce saturation at the membrane-feed interface under the conditions of these calculations. This value is about 82% of that calculated above for multi-component, non-ideal solutions.

The results of this computation indicate that the increase in solubility of  $\text{CaSO}_4$  in the presence of  $\text{NaCl}$  overrides the increase of concentration polarization resulting from the  $\text{NaCl}$ . Insofar as precipitation of gypsum is the limiting factor in water recovery, one would thus underestimate the allowable recovery by using ideal two-component theory. We caution, however, that the computations are rather approximate, for example in the function used to represent activity coefficients (Equations 4a and 4b) and, perhaps more serious, the use of infinite dilution mobility data to supply diffusion coefficients.

REFERENCES

1. L. B. Yeatts, P. M. Lantz, and W. L. Marshall, "Solubilities of Calcium Sulfate Dihydrate at 25°C in Brackish Waters and their Concentrates; Effect of Calgon Additive and Predictions for Reverse Osmosis Processes," Part I of this report. (Issued as ORNL-4914 (1973)).
2. J. S. Johnson, Jr., R. E. Minturn, and P. H. Wadia, J. Electroanal. Chem., 37, 267 (1972).
3. For a description of these test sections, see the Water Research Program Biennial Progress Report for the Office of Saline Water for the period March 15, 1968 to March 15, 1970, ORNL-TM-4001 (1973), p. 7ff.
4. W. L. Marshall and R. Slusher, J. Phys. Chem., 70, 4015 (1966).
5. "Systems Analysis of Brine Disposal from Reverse Osmosis Plants," Office of Saline Water Research & Development Progress Report No. 587, 1970, by P. G. LeGros, et al.
6. D. G. Thomas, W. R. Mixon, and J. D. Sheppard, (1973) Final Report to the Office of Saline Water on "Engineering Development of Dynamic Membranes," (in preparation).
7. G. Scatchard, R. M. Rush, and J. S. Johnson, Jr., J. Phys. Chem., 74, 3786 (1970).
8. An excellent review can be found in "Convective Diffusion in Laminar and Turbulent Hyperfiltration (Reverse Osmosis) Systems," William N. Gill, Lewis J. Derzansky, and Mahendra R. Doshi, in Surface and Colloid Chemistry, Vol. IV, Egon Matijevic (Ed.), Wiley and Sons, 1971.
9. K. S. Spiegler, Trans. Faraday Soc., 54, 1408 (1958).
10. "Hyperfiltration (Reverse Osmosis)," by L. Dresner and J. S. Johnson, Jr., to be published in Principles of Desalination, 2nd Edition, K. S. Spiegler and A. D. K. Laird (Editors), Academic Press.
11. S. Srinivasan and C. Tien, Desalination, 5, 139 (1968).
12. W. L. Marshall and R. Slusher, J. Phys. Chem., 70, 4015 (1966); "The Physical Chemistry of Electrolytic Solutions," H. S. Harned and B. B. Owen, 3rd Edition, Reinhold Publishing Corp., New York, 1958, p. 731.
13. L. Dresner, Oak Ridge National Laboratory Report ORNL-3621, May, 1964.
14. A. S. Berman, J. Appl. Phys., 24, 1232 (1953).
15. T. K. Sherwood, P. L. T. Brian, R. E. Fisher, and L. Dresner, Ind. Eng. Chem. Fundam., 4, 113 (1965).
16. R. G. Deissler, NACA Report 1210 (1955).

17. T. K. Sherwood, "Mass, Heat, and Momentum Transfer Between Phases," Chem. Eng. Prog. Symp. Ser. No. 25, 55, p. 71, 1959.
18. H. S. Harned and B. B. Owen, "The Physical Chemistry of Electrolytic Solutions," 3rd Edition, Reinhold Publishing Corp., 1958.
19. See, for example, Transport Phenomena, by R. B. Bird, W. E. Stewart, and E. M. Lightfoot, Wiley and Sons, 1960, p. 186.

## APPENDIX

## EXPERIMENTAL RUNS MADE WITH MODULES DURING PRESENT INVESTIGATION

(400 psig)

Run #	Temp. °F	pH	Test <sup>a</sup> Solution	Run Duration (hours)	Calgon Conc. (ppm)	Module	Recovery <sup>b</sup> Rate (%)	Flux (gfd)	R <sub>obs</sub> (%) <sup>c</sup>	
									Ca(II)	Cl <sup>-</sup>
8A-2	66-73	4.8-6.6	Webster	64.25	0	DuPont	40-35	2.0-1.6	99.2	92-86
							GESCO	26-23	11.8-10.0	99.7
8A-3	67-76	5.8-6.2	Webster	29.25	20	DuPont	37-34	1.7-1.5	99.3	94-88
							GESCO	25-22	10.8-9.4	99.7
8A-4	74-75	5.9-6.1	Webster	25.5	0	DuPont	48-42	2.0-1.6	(99.4-98.8) <sup>d</sup>	---
							GESCO	27-23		12.1-9.9
8A-5	75-77	6.1-6.2	NaCl	25.0	0	DuPont	46-37	1.9-1.3	----	~85
							GESCO	29-23	11.2-8.1	----
8A-6	75-76	6-6.1	Webster	70.0	0	DuPont	46-40	1.9-1.4	(99.0) <sup>d</sup>	---
							GESCO	30-26		11.7-9.8
8A-7	74-76	6-6.7	Webster	506.75	0	DuPont	68-67	1.8-1.7	99.0	~91
							GESCO	69-64	11.8-10.8	99.9
8A-9	75-77	5.9-7.4	Webster	202.67	0	DuPont	67-71	1.7-1.6	~99.1	~81
							GESCO	69-73	11.2-10.8	99.9
8A-10A	75	7.0	Webster	66.5	0	DuPont	48-47	1.8-1.7	----	---
							GESCO	45-44	11.3-11.1	----
B	75	7.0	Recon.	2.0	0	DuPont	~20.0	~1.6	----	---
							GESCO	~68.0	~10.9	----
C	75	7.0	Recon.	5.4	0	DuPont	~70	~1.6	~96	~77
							GESCO	~68	~10.9	>99
D	75	7.0	Recon.	3.0	0	DuPont	~75.6	~1.6	~97	~73
							GESCO	~69	~11.0	>99
E	75	7.0	Recon.	3.0	0	DuPont	~90	~1.6	----	---
							GESCO	~88.4	~10.5	----
F	75	7.0	Recon.	4.8	0	DuPont	~90	~1.5	~86	~58
							GESCO	~90.4	11.2-10.3	>99

## APPENDIX - cont'd.

Run #	Temp. °F	pH	Test <sup>a</sup> Solution	Run Duration (hours)	Calgon Conc. (ppm)	Module	Recovery <sup>b</sup> Rate (%)	Flux (gfd)	R <sub>obs</sub> (%) <sup>c</sup>	
									Ca(II)	Cl <sup>-</sup>
G	75	7.0	Recon.	2.75	0	DuPont GESCO	88-79	~1.5	~91	~69
							~81	10.9-10.7	>99	~84
H	75	7.0	Recon.	3.0	0	DuPont GESCO	84-83	~1.5	----	----
							80.5	~10.7	----	----
I	75	7.0	Recon.	5.0	5	DuPont GESCO	~90	~1.5	~84	~58
							~90	10.9-10.5	>99	~78
J	75	7.0	Recon.	5.0	5	DuPont GESCO	~79	~1.5	~91	~71
							~80.3	11.2-10.7	>99	~84
K	75	7.0	Recon.	3.0	5	DuPont GESCO	69.6	~1.5	~93	~76
							68.2	11.1-11.0	>99	~88
8A-11A	75-76.5	6.0-7.0	Pre-treated Webster	166	0	DuPont GESCO	~84	~1.5	~88	~66
							~85	~11.0	~99	~76
B	75-76.5	7.0	Pre-treated Webster	140	0	DuPont GESCO	~89	~1.5	~82	~57
							~92	~10.7	~99	~66
8A-12	~76	5.3-6.6	Wellton- Mohawk	123.75	0	DuPont GESCO	55-49	~1.4	96	82
							50-49	10.6-10.3	>99	88
8A-13A	76-77	~5.8	2X Wellton- Mohawk	66	0	DuPont GESCO	~49	1.3-1.2	93	76
							~51	9.4-8.7	>99	86
B	76-77.5	5.4-5.5	Recon.	23	5	DuPont GESCO	51-50	~1.3	92	77
							49-50	9.5-9.4	99	86
C	76.5-78	5.4	Recon.	92	20	DuPont GESCO	52-60	1.3-1.2	92	77
							~50	9.5-9.3	>99	87
8A-15A	75.5-76.5	~7	Foss Reservoir	20.2	0	DuPont GESCO	51-58	1.5-1.4	93	78
							50-51	11.8-11.5	>99	90
B	73-75.5	7.4	Recon.	39.8	0	DuPont GESCO	51-48	~1.4	94	82
							49-58	11.3-10.8	>99	90
C	72.5-78.5	7.4	Recon.	45.7	5	DuPont GESCO	51-50	~1.4	94	81
							50-51	~11.2	>99	90

## APPENDIX - cont'd.

Run #	Temp. °F	pH	Test <sup>a</sup> Solution	Run Duration (hours)	Calgon Conc. (ppm)	Module	Recovery <sup>b</sup>		R <sub>obs</sub> (%) <sup>c</sup>	
							Rate (%)	Flux (gfd)	Ca(II)	Cl <sup>-</sup>
8A-19A	74.5-75	7.3-7.4	Recon. 2X Webster	24	0	DuPont	29.8-30.6	1.4	97	84
						GESCO	27.1-26.7	11.2-11.0	>99	88
B	74-76.5	7.4	Recon.	24	5	DuPont	29.0-30.2	1.4-1.5	96	83
						GESCO	26.7-27.2	11.0-11.3	>99	89
C	74.5-75.0	7.4-7.5	Recon.	24.5	20	DuPont	30.4-30.7	1.4	96	84
						GESCO	27.1-26.7	11.2-11.0	>99.6	91
8A-22A	73.0-74.5	6.1-6.4	2X Webster	25.0	0	DuPont	29.5-28.9	1.4-1.3	96	80
						GESCO	26.9-26.3	11.2-10.8	>99	84
B	74.0	7.9	Conc. <sup>e</sup> 2X Webster	29.2	0	DuPont	28.6-28.2	1.3	96	81
						GESCO	26.3-26.1	10.8-10.7	>99	83
C	71.5-75.0	6.3-6.8	2X Webster (fresh)	4.0	0	DuPont	26.0-31.5	1.2-0.9	82	28
						GESCO	25.6-26.1	10.4-10.7	99	81
8A-23	74.0-74.5	5.6-4.8	2X Webster	23.75	0	DuPont	29.6-26.5	1.4-1.1	76	82
						GESCO	26.7-26.2	11.0-10.7	98	87
8A-24A	74.0-75.0	5.6-5.3	2X Webster	6.0	0	GESCO	26.2-25.3	10.7-10.3	99	85
						DuPont	29.5-26.6	1.3-1.2	79	58
8A-26	74.0-74.5	5.4-6.1	2X Webster	24.0	0	DuPont	30.8-21.3	1.3-0.8	23	3
8A-27	73.0-77.0	5.2-5.6	2X Webster (no SiO <sub>2</sub> )	6.0	0	DuPont	27.1-21.6	0.9-0.6	50	4
8A-28	74.0-75.5	5.4-6.1	CaSO <sub>4</sub> in NaCl <sup>f</sup>	22.0	0	DuPont	25.8-19.8	1.0-0.7	5	2
8A-29A	73.5-74.5	5.3-6.3	2X Webster	20.0	0	GESCO	28.6-26.7	12.1-11.0	99	87
						DuPont	27.6-27.0	11.5-11.2	99	90
B	75.0-75.5	5.4-6.2	Recon.	19.3	0	GESCO	27.6-27.0	11.5-11.2	99	90
8A-30	73.5-75.0	5.5-6.2	2.5X Webster	24.0	0	GESCO	26.9-26.0	11.2-10.9	99	88
8A-31A	73.0-75.0	5.4-6.1	2.5X Webster	48.0	0	GESCO	26.9-26.1	11.0-10.4	99	88
						DuPont	26.7-26.1	11.0-10.7	99	88
B	74.0	6.0-5.2	Recon.	18.5	0	GESCO	26.7-26.1	11.0-10.7	99	88
8A-33	74.0-74.5	5.5-5.7	Recon.	19.0	20	GESCO	26.8-26.5	11.1-10.9	99	89

APPENDIX - cont'd.

- 
- a. Recon.  $\equiv$  reconstituted by adding  $\text{CaSO}_4$  to concentration at beginning of run.
  - b. Recovery rate equals 100X product rate divided by sum of product and reject rates. Actual simulated recovery depends on feed concentration.
  - c. Average rejection over period of run.
  - d.  $\text{Ca(II)} + \text{Mg(II)}$ .
  - e. 35% of water removed from feed of run 8A-22A.
  - f.  $\text{CaSO}_4$  at concentration in 2X Webster water,  $\text{NaCl}$  at concentration to give total ionic strength of 2X Webster water.
-